

**Hyperexcitability of Rat Thalamic and Hippocampal Neurons after
Exposure to General Anesthesia during Brain Development**

Michael Robert DiGruccio
Newport Beach, Ca

B.S. Biology, University of California Irvine, 1999

A Dissertation presented to the Graduate Faculty
of the University of Virginia in Candidacy for the Degree of
Doctor of Philosophy

Neuroscience Graduate Program

University of Virginia
December, 2014

ABSTRACT

i

The prevailing literature proves that common general anesthetics (GAs) cause long-term cognitive changes and neurodegeneration in the developing mammalian brain, especially in the thalamus and hippocampus. However, the possible role of GAs in modifying ion channels that control neuronal excitability has not been taken into consideration. Here in rats exposed to GAs at postnatal day 7, nucleus reticularis thalami (nRT) neurons display a lasting reduction in inhibitory synaptic transmission, an increase in excitatory synaptic transmission, and concomitant alterations of T-type calcium currents (T-currents). Collectively this plasticity of ionic currents leads to increased action potential firing in vitro and increased strength of pharmacologically-induced spike and wave discharges in vivo. Selective blockade of T-currents reversed neuronal hyperexcitability in vitro and in vivo. In the subiculum GA also alters T-current biophysical properties that likely contribute to observed increases in action potential firing. Utilizing another approach to ameliorate GA mediated neuronal function: administration of EUK-134 prior to GA exposure is also shown to attenuate GA mediated hyperexcitability. When considering the development of novel anesthetics, the T-channel antagonist B260 is also shown to preserve thalamocortical neuron function when used as an anesthetic during brain development. In conclusion, drugs that regulate T-channels may improve the safety of GAs used during brain development.

Table of Contents

ii

Abstract	i
Table of contents	ii
Acknowledgements	iv
List of abbreviations	v
I. Introduction	1
A. Anesthetics during brain development	2
B. Anesthetics mechanism of action and GA toxicity	5
C. Thalamus and cortex loop system and GA	5
D. Effects of ROS generation upon subiculum neuron action potential firing patterns	8
E. T-channels and GA	10
F. Figures 1-5	11-15
II. Early GA exposure leads to hyperexcitable nRT neurons	16
A. Introduction	17
B. Experimental design	17
1. Anesthesia	17
2. Electrophysiology	18
3. T-channels	19
C. Data analysis	20
D. Results	21
1. Exposure of rat pups at age P7 to GA leads to a lasting increase in intrinsic nRT neuron excitability	21
2. T-channel biophysical properties are altered after exposure to GA	23
E. Table 1	25
Figures 6-10	26-30
F. Discussion	31
III. Early GA exposure alters thalamic neuron synaptic plasticity	34
A. Introduction	34
B. Experimental design	36
1. Evoked synaptic transmission	36
2. Spontaneous synaptic currents	37
3. Cumulative distribution functions	38
C. Results	38
1. Plasticity of inhibitory synaptic transmission in the rat thalamus after a single exposure to GA	38
2. Plasticity of excitatory synaptic transmission in the rat thalamus after a single exposure to GA	40
3. T-channels modulate nRT neuron excitatory synapse properties	41
D. Figures 11-15	43-47

	iii
IV. Early exposure to GA alters thalamocortical EEG	53
A. Introduction	53
B. Experimental design	55
1. EEG	55
2. Operational amplifiers	55
3. Gamma Butyrolactone and TTA-P2	55
C. Results	56
1. Adolescent rats exposed to GAs at age P7 display hyperexcitability of intact thalamocortical networks	56
2. Selective antagonism of T-channels reversed hyperexcitability of nRT neurons in vitro and diminished cumulative duration of SWD in GA treated rats in vivo	57
3. B-260, a neuroactive steroid and selective T-channel antagonist with anesthetic properties, spares thalamocortical hyperactivity when used during brain development	59
D. Figures 16-19	61-64
E. Discussion	65
V. Early exposure to GA alters subiculum neuron firing patterns	68
A. Introduction	68
B. Experimental design	70
1. Anesthesia	70
2. Electrophysiology	70
3. Cell-attach	71
C. Results	71
1. Early GA exposure leads to hyper excitable pyramidal subicular neurons	71
2. In vivo co-administration of catalase super oxide dismutase mimetic EUK- 134 prior to early GA triple cocktail preserves pyramidal subicular neuron function	72
3. T channels contribute to subicular neuron AP firing	73
4. Subiculum T-channel biophysical properties are altered after exposure to GA	74
D. Figures 21-26	76-82
E. Discussion	83
VI Concluding remarks	86
VII References	91

Acknowledgements

iv

This thesis was a collaborative effort involving many supportive people. I would like to extend my gratitude to Dr. Srdjan Jocksimovic for his help with electrophysiology recordings in sections II, III, V, and statistical analysis. I would also like to thank Drs. Pavle Joksovic and Nadia Lunardi for their electrophysiology recording contributions in section III. For section III, custom software scripts used to construct cumulative distribution functions were authored by Dr. Mark Beenhakker and a significant contribution to the data analysis was made by Dr. Reza Salajegheh. Regarding the EEG experiments in section IV, the training and guidance of Dr. Howard Goodkin and John Williamson was invaluable. I would also like to thank Drs. Lyn wells, Paul De Marco and Samantha Adamson for advice and critical readings of all manuscript drafts. Tracy Mourton, Nadia Badir Cempre, Manoj Patel and the Neuroscience Graduate Program were also invaluable in supporting this work.

I will also extend my gratitude and appreciation for help and advice from my committee: Drs. Douglas Bayliss, Mark Beenhakker, Vesna Jevtovic-Todorovic, Howard Goodkin and Bettina Winkler. Lastly I am extremely grateful for the mentorship of Dr. Slobodan Todorovic whose guidance and resolve made these studies possible.

This research was supported by grants from National Institutes of Health GM 070726 and GM 075229 to SMT and NIH 2RO1 HD 044517 to VJT, and the Neuroscience Graduate Program training grant T32 GM08328.

List of Abbreviations

v

ACTH	adrenocorticotrophic hormone
AMPA	α -Amino-3-hydroxy-5-methyl-4-isoxazolepropionic acid
AP	action potential
BMI	bicuculline methiodide
B 260	3 β OH (3 β ,5 β ,17 β)-3-hydroxyandrostane-17-carbonitrile
CA1	cornus ammonis 1
CDF	cumulative distribution function
CT	corticothalamic: cortex to thalamus neuron projections
Ctx	cortex
D-APV	D-2-Amino-5-Phosphonovaleric acid
EC	entorhinal cortex
EEG	electroencephalography
eEPSC	evoked excitatory postsynaptic currents
eIPSC	evoked inhibitory post synaptic currents
EPSP	excitatory postsynaptic potentials
Etomidate	(ethyl 3-[(1R)-1-phenylethyl] imidazole-4-carboxylate)
EUK	chloro[[2,2'-[1,2-ethanediy]bis[(nitrilo- κ N)methylidyne]]bis[6- methoxyphenolato- κ O]]]-manganese
GABA	γ -Aminobutyric acid
HPA	hypothalamus pituitary adrenal axis
IC	internal capsule
IPSP	inhibitory postsynaptic potentials
ISO	isoflurane
nRT	nucleus reticularis thalami
LTCS	low threshold calcium spike
LTP	long term potentiation
LVA	low voltage activated T-type calcium channels
LMM	linear mixed model
mEPSC	miniature excitatory postsynaptic currents
mIPSC	spontaneous miniature inhibitory postsynaptic currents
NBQX	(2,3-dihydroxy-6-nitro-7-sulfamoyl-benzo[f]quinoxaline-2,3-dione)
NMDA	N-methyl-D-Aspartate
N2O	nitrous oxide
PPR	paired-pulse ratio
IEI	inter-event interval
GA	general anesthetics
GAERS	genetic absence epilepsy in rats from Strasbourg
GBL	γ -butyrolactone
REDOX	reduction and oxidation
Rin	input resistance
RMP	resting membrane potential
ROS	reactive oxygenated species
SEV	sevoflurane

List of Abbreviations

vi

SWD	spike and wave discharges
TC	thalamocortical: thalamus to cortex neuron projections
T-currents	T-type calcium current
TIVA	total intravenous anesthesia
TTA-P2	3,5-dichloro-N-[1-(2,2-dimethyl-tetrahydro-pyran-4-ylmethyl) -4-fluoro- piperidin-4-ylmethyl]-benzamide
TTX	tetrodotoxin
VB	ventral basal thalamus complex

I. Introduction

A. Anesthetics during brain development

This thesis is the first detailed functional study of GA exposed mammals during brain development that proves permanent thalamic neuron hyperexcitability is caused by the same GAs used in children. Worldwide, millions of neonates, infants, and young children are exposed to GA each year. Studies in rodents have shown that exposure to GA during synaptogenesis causes severe learning and memory deficits (Jevtovic-Todorovic et al., 2003). These studies demonstrated widespread neural apoptotic degeneration, and persistent learning and memory impairments induced by clinically relevant combinations of anesthetic drugs (Jevtovic-Todorovic et al., 2003). The effects of early GA exposure are not limited to the developing rodent brain. In studies utilizing rhesus monkeys, prolonged exposure to the NMDA antagonist ketamine resulted in long term cognitive deficits (Paule et al., 2009). These results have led to investigations regarding GA toxicity in humans. Recent retrospective studies have suggested an association between early exposure to GA and an increased incidence in learning disabilities. (Wilder et al., 2009) (figure1). Studies are now beginning to address the mechanisms of anesthetic mediated neuron loss and subsequent alterations in neuron function.

This study seeks to understand the alterations in action potential firing properties due to a single exposure to a clinically relevant triple anesthetic cocktail of 9 mg/kg midazolam, 80% nitrous oxide (N₂O), 0.75% Isoflurane (ISO) during synaptogenesis. Here, the functional effects of early GA exposure within thalamic and hippocampal formations are investigated. In the thalamus, the effects of early GA exposure within the neurons of the nucleus reticularis thalami (nRT) are characterized. GABAergic nRT neurons are key mediators of thalamocortical (TC) and corticothalamic (CT) circuits that are necessary for sensory perception, cognition, and consciousness (figure 2). The effects GA exposures during brain development upon the excitatory neurons of the subiculum were determined as well. Subiculum neurons are a key intermediary

between the hippocampus and the cortex, for it receives CA1 afferent axonal projections and subsequently sends axonal projections to the cortex (figure 3). Calcium channels, in particular the low voltage activated (LVA) T-type Ca^{2+} type, are critical for the formation of action potential patterns. Here, T-channels are investigated as mediators of neuronal hyperexcitability during early GA exposure. In order to expand this study, perioperative drug administration during GA is shown to attenuate GA mediated hyperexcitability. Finally, the idea that T-channel antagonism may be a novel and safe alternative target for anesthesia during brain development is also explored.

B. Anesthetic mechanisms of action and GA toxicity

The primary mechanism of action of anesthetics involves the potentiation of inhibitory GABA currents and the blockade of excitatory glutamate neural transmission (Franks, 2008). The effects of one of the oldest and widely used inhaled anesthetic N_2O are in part mediated by NMDA blockade (Jevtović-Todorović et al., 1998). Recent research has also shown that N_2O effects are mediated by interactions with the Cav3.2 isoform of low voltage activated (LVA) T type calcium channels (Orestes et al., 2005). Other volatile inhalation anesthetics, such as ISO and Sevoflurane (SEV), induce their neural inhibitory effects at least partly by acting as GABA_A agonists. Although SEV has surpassed ISO in the US as the volatile anesthetic of choice they share a common mechanism (Garcia et al., 2010). T channels are also modulated by the inhaled anesthetic ISO (Eckle et al., 2012). The anesthetic effects of ketamine are also partly mediated by NMDA blockade. At clinically relevant concentrations both N_2O and ketamine have very little effect on GABA_A -gated ionic currents (Kress 1997; Jevtović-Todorović et al., 1998). It is important to note that while GABA_A potentiation and NMDA blockade may account for anesthetic effects regarding hypnosis, analgesia, and immobility, they do not fully explain the differences in the clinical effects of various agents. Intravenous drugs with anesthetic properties

like Propofol, etomidate (ethyl 3-[(1R)-1-phenylethyl] imidazole-4-carboxylate) and various barbiturates also share this mechanism. Volatile anesthetics are also known K⁺ channel modulators (Sirois et al. 2000).

Both excitatory and inhibitory neurotransmitter systems play critical roles during brain development. Experimental evidence suggests that either GABA potentiation or NMDA blockade are sufficient to achieve long term structural and functional changes in brain structures. Pharmacological blockade of NMDA results in alterations of neuronal migration patterns, axon migration, dendrite structure, action potential firing patterns and synapse function (Kumoro et al. 1993, Reiprich et al., 2004). During development, GABA receptor subtypes can also mediate axon and dendrite morphology (Cancedda et al., 2007). In terms of GABA receptor subtypes, the selective blockade of the GABA_B receptors alters the migration and activity of cortical neurons whereas the selective pharmacological activation or blockade of GABA_A alters cortical neuron migration and attenuates transient intracellular Ca²⁺ (Lopez-Bendito et al., 2003, Heck et al., 2007).

Owing to the alterations in both excitatory and inhibitory neuron activity mediated by GA exposure, it is reasonable to surmise that exposure to GA during brain development leads to lasting alterations in both structure and function of the adult mammalian brain. There are common themes to anesthetic mediated neural toxicity such as direct activation of apoptotic pathways, disassembly of cytoskeleton proteins such as actin, and alterations in mitochondrial function, which in turn causes the production of reactive oxygenated species (ROS). These events may lead to changes in excitatory to inhibitory synapse ratios, loss of axon and dendritic arborization and changes in ion channel expression, as well as gating properties that lead to alterations in neuronal excitability.

There are a number of mechanisms that may lead to anesthetic induced neural degeneration. In neonatal rodents, ketamine exposure alters the expression of important proteins involved in hippocampal development such as CAMK II and GAP – 43. Long term behavioral alterations include changes in

locomotion and rearing (Viberg et al., 2008). GABA potentiation, as occurs in neonatal exposure to propofol, alters BDNF levels in neonatal rodent brains (Ponten et al., 2011). Studies of neonatal hippocampal slice cultures suggest that ISO directly activates Rho A, a small guanosine triphosphate actin depolymerization agent. Direct activation of Rho A in turn leads to cytoskeleton depolymerization and eventual apoptosis (Lemkuil et al., 2011). Neonatal rats exposed to SEV, a common inhaled GABA agonist, leads to neuronal apoptosis mediated by caspase 3, and long term alterations in behavior such as alterations in fear conditioning and social interactions (Satamoto et al., 2009). Extracellular Ca^{2+} influx and release from internal stores may also contribute to anesthetic induced neural toxicity. In primary neuronal cultures from rat and mouse, ISO exposure elevated intracellular Ca^{2+} levels. Subsequent pharmacological blockade of intracellular Ca^{2+} and siRNA knockdown of the Inositol 1,4,5 – triphosphate receptor ultimately reversed to some extent anesthetic induced toxicity (Zhao et al., 2010)

It is important to stress that these alterations are not limited to exposure to single anesthetic agents. Commonly, several anesthetic drugs are used in combination to lower the anesthetic requirements, such as ISO and N_2O . The clinically relevant triple cocktail results in widespread neuronal loss and learning and memory impairment in animal studies (Jevtovic-Todorovic et al., 2003). Long lasting structural disarray in the subicular neuropil, reduction in and scarcity of synaptic contacts, and distortions of mitochondrial morphology are also seen after neonatal exposure to the triple cocktail (Sanchez et al. 2011, Lunardi et al. 2010). Other anesthetic combinations also lead to alterations in behavior, learning, memory and cognition. Neonatal rodents exposed to both ketamine and thiopental had incidences of widespread neural apoptosis higher than that of controls (Fredriksson et al., 2007).

Recent studies also indicate that early GA exposure results in mitochondrial injury. The injured mitochondria are the source of subsequent increase in ROS which leads to lipid mediated subicular neuron loss and altered

function. In fact, these GA mediated damaging effects are reversed in the presence of synthetic free radical scavengers such as EUK-134 (Boscolo et al., 2012). GAs are also implicated in direct down regulation of anti-apoptotic proteins from the bcl-2 family, and up-regulation of pro – apoptotic factors caspase-9 and 3 mediated by increased permeability of mitochondrial membrane which causes cytochrome c release (Yon et al., 2005).

C. Thalamus and cortex loop system and GA

The thalamus cortex loop system and the hippocampal formation are the targets of many general anesthetic (GA) actions. GAs achieve analgesia, amnesia, sensory blockade, skeletal muscle relaxation, immobility, hypnosis and/or a sleep-like state by altering action potential firing patterns of thalamic and cortical brain structures. The mechanisms of volatile anesthetics such as ISO and SEV include the potentiation of GABA channels, which causes chloride ion influx, and subsequent hyperpolarization of the neuronal membrane (Ito et al., 1998). Anesthetics such as N₂O may also exhibit their effects by the blockade of fast excitatory glutamatergic pathways (Jevtović-Todorović et al., 1998). Typically, anesthetics are administered in combinations in order to achieve the desired clinical effects. Benzodiazepines such as midazolam are administered before induction to relieve to anxiety and to interfere with memory acquisition by blocking long term potentiation (LTP) (Tokuda et al., 2010). Powerful GABA_A agonists such as propofol are used to induce sleep and to maintain sedation. A triple anesthetic cocktail of midazolam, ISO and N₂O has been used for many decades as a typical GA combination. N₂O is used in combination with other inhaled anesthetics such as ISO in order to lower anesthetic dosage requirements.

Within the central nervous system, GAs alter the function of thalamic and cortical neurons. Functional imaging studies in mammals suggest that direct and indirect depression of TC relay neuron activity may account for the clinical effects

of GAs (Lin et al. 2012). Centrally, sensory perception is blocked at thalamic relay nuclei by inducing a switch from tonic action potential firing to rhythmic oscillatory firing that is characteristic of sleep. These patterns are characterized by low frequency delta electroencephalographic (EEG) waves that are induced by GABAergic activation of the reticular thalamic nucleus. Thalamocortical (TC) and corticothalamic (CT) neurons and projections are necessary for sensory perception, cognition, consciousness, sleep and wake patterns. Typically, alterations in the normal balance of excitation and inhibition within the thalamocortical loops results in absence epilepsy-like EEG patterns (Paz et al. 2011) and altered thalamic neuron firing patterns (McCormick., 2002). T-type calcium channels (T-channels) are crucially involved in the control of both excitatory TC neurons and the inhibitory neurons of nRT. The neural networks formed by the interconnections of TC, cortical and nRT neurons establish tonic and burst action potential formations that are important for normal sensory processing, attention, transitions from sleep and awake states, and anesthesia; in pathological conditions this network contributes to brain disorders including epilepsy (Steriade et al., 2005; Llinas et al., 2005; Sherman, 2005). At the molecular level, alterations in T-channel gating and or expression within the nRT are strongly associated with absence epilepsy (Talley et al., 2000; Chen Y et al., 2003; Heron et al., 2007; Vitko et al., 2005). In fact, the T-channel Cav 3.1 isoform KO demonstrates remarkable resistances to both hyperpolarization induced burst firing and to drug-induced absence epilepsy patterns (Kim et al., 2001). However, the chronic effects of exposure to GAs during critical periods of brain development on the function of the major groups of ion channels that control excitability in thalamocortical networks are not well characterized. Our previous study has established that a single exposure to the common volatile anesthetic ISO during brain development causes a dose dependent and widespread neurodegeneration in rats, and that thalamic nuclei are among the most severely affected (Jevtovic-Todorovic et al., 2003). When a triple cocktail of anesthetics was utilized, such as a mildly toxic dose of ISO (0.75 vol%), mixed

with nontoxic doses of N₂O of 75 vol%, and midazolam (9 mg/kg, i.p.) widespread neurodegeneration of cortical and thalamic neurons was also observed (Jevtovic-Todorovic et al., 2003).

The hypothesis that exposure of rat pups to the anesthetic triple cocktail may cause permanent functional alterations in thalamocortical circuitry is explored in this thesis. Here, it is shown that exposure of postnatal day 7 rats (P7) to a clinically relevant anesthetic cocktail consisting of midazolam, ISO and N₂O triggers plasticity of synaptic and intrinsic ion channels in nRT neurons. This, in turn, contributes to lasting hyperexcitability in thalamocortical and subiculum neurons. Furthermore, thalamocortical neuron hyperexcitability can be curtailed by selectively inhibiting T-channel function. Hence, drugs that regulate neuronal excitability may be useful as novel therapeutic agents to reverse lasting effects of GAs on the function of thalamocortical circuitry.

Gabaergic nRT thalamic neurons receive cortical inputs that modulate feed forward inhibition of TC neurons whereas glutamatergic excitatory systems mediate the communication of the reciprocally connected TC and CT pathways. During states of oscillations such as slow wave sleep and absence seizure, a stronger synaptic strength is present between CT pathways than the TC pathway, which allows feed-forward inhibition of TC cells to overcome direct TC excitation. Network oscillations are initiated if this inhibition is followed by post-inhibitory rebound bursts of action potentials in TC neurons that in turn re-excite nRT neurons. Iterations of this cycle maintain oscillatory states. Alterations in the strength of the TC and cortex- nRT pathway or over activity of nRT neurons may lead to pathological conditions such as absence seizure.

There is debate regarding equivalent periods of brain development when comparing humans and rodents. In humans this occurs from the third trimester of pregnancy lasting until the 4th year of life. In rodents this period is considered to be from the late embryonic stage to postnatal day 10 (Dobbing et al., 1979). Regarding experimental treatments, rats were given the GA triple cocktail at P7

and electrophysiology experiments in live nRT brain slices were performed between P10 and until P21 (figure 4). For experiments within the subiculum, electrophysiology experiments were continued into adulthood. *In vivo*, any aberrations to EEG patterns that are relevant to oscillatory thalamocortical activity such as low frequency oscillations ranging from 4-16 Hz, sleep spindles and spike and wave discharges (SWD) associated with absence seizure activity will be characterized.

Exposure to GAs during synaptogenesis may lead to alterations in TC and CT neurons and projections that are necessary for normal thalamic loop function. Thus, alterations in sensory perception, cognition, wakefulness and consciousness may be a consequence of early GA exposure. Alterations in TC neuron circuit properties such as the action potential firing properties of the nRT, and possibly the ventral basal thalamic complex (VB), may lead to abnormal brain function. These functions may manifest in EEG patterns indicative of abnormal sensory perception, modified sleep patterns and/or absence seizure. Thus, the active/passive properties of nRT neurons and alterations in TC and CT synapse properties are characterized. The mechanisms of GA mediated alterations in other brain circuits such as the hippocampal formation are also explored. Recent findings suggest that elevations in ROS during GA may be a key mediator of GA induced alterations of hippocampal neuron activity (section V).

D. Effects of ROS generation upon subiculum neuron action potential firing patterns

Many neurotransmitter systems are sensitive to ROS. Hydrogen peroxide (H_2O_2), the superoxide anion ($O_2^{\cdot-}$) and the hydroxyl radical (OH^{\cdot}) are generated as byproducts of oxidative metabolism in neurons and are the products of certain inhaled anesthetics (Kann et al., 2007; Orestes et al., 2010). In this study, the effects of free radicals on membrane excitability and synaptic transmission within the pyramidal neurons of the subiculum were evaluated. To date there is little

functional data regarding the activity of pyramidal subicular neurons during elevated ROS levels. The hippocampus is located within both medial temporal lobes of the brain and is primarily devoted to memory formation and storage (Squire et al., 1991). The hippocampus may be divided into three regions: the dentate gyrus (DG), Ammon's Horn or Cornu Ammonis fields 1-3 (CA1-3), and the subiculum. The subiculum is highly intertwined with the hippocampal CA1 region, anterior thalamic nuclei, entorhinal cortex (EC), and cingulate cortices, and serves as the main input from CA1 to cerebral cortex (Witter et al., 1990, 2006) (figure 3). Most studies regarding early exposure to GA have sought to characterize ultra-structural changes at the level of the synapse (Lunardi et al., 2009), the production of ROS (Sanchez et al., 2011) and peroxidative species that promote neuron death (Boscolo et al., 2012). In this study, the active and passive membrane properties of pyramidal subicular neurons in rats exposed to GA at P7 were investigated. Alterations in pyramidal subicular neuron membrane activity may contribute to the well characterized deficiencies in memory acquisition in GA treated rats. Furthermore, in order to potentially reverse the effects of GA, the active membrane properties of rats that were pretreated with a catalase and superoxide dismutase mimetic EUK 134 are also characterized.

E. T-channels and GA

Current research investigating the mechanisms of anesthetic action centers upon the hypothesis that anesthetics interact and change the biophysical properties of ion channels and receptors that are expressed throughout the nervous system. One mechanism of action of the commonly used volatile anesthetic ISO involves binding to the GABA_A receptor and altering the resulting currents (Franks and Leib 2008). In order to further investigate the mechanisms of its action, the effects of ISO upon action potential formations in TC neurons in live brain slices were determined. Findings included alterations in T-channel mediated properties such as decreases in thalamic neuron burst AP firing, and a prolonged latency for bursting of TC neurons in response to hyperpolarizing stimuli. The end effects of ISO could include reducing the fidelity of neurotransmission in TC neurons which in turn contributes to the clinical aspects of the drug such as analgesia and amnesia.

T-channels may also be a suitable target for the development of novel GA's. In order to understand how T-channel antagonism contributes to anesthesia, utilizing a novel high affinity T-channel specific neuroactive steroid B260, the effects of T-channel antagonism upon synaptic properties were characterized. Finally, in order to propose that T-channels may be a suitable and safe target for use during brain development, P7 rats were subjected to 6 hours of B260 anesthesia. Utilizing EEG, the function of TC neurons in rats that received the GA and sham treatments is also compared.

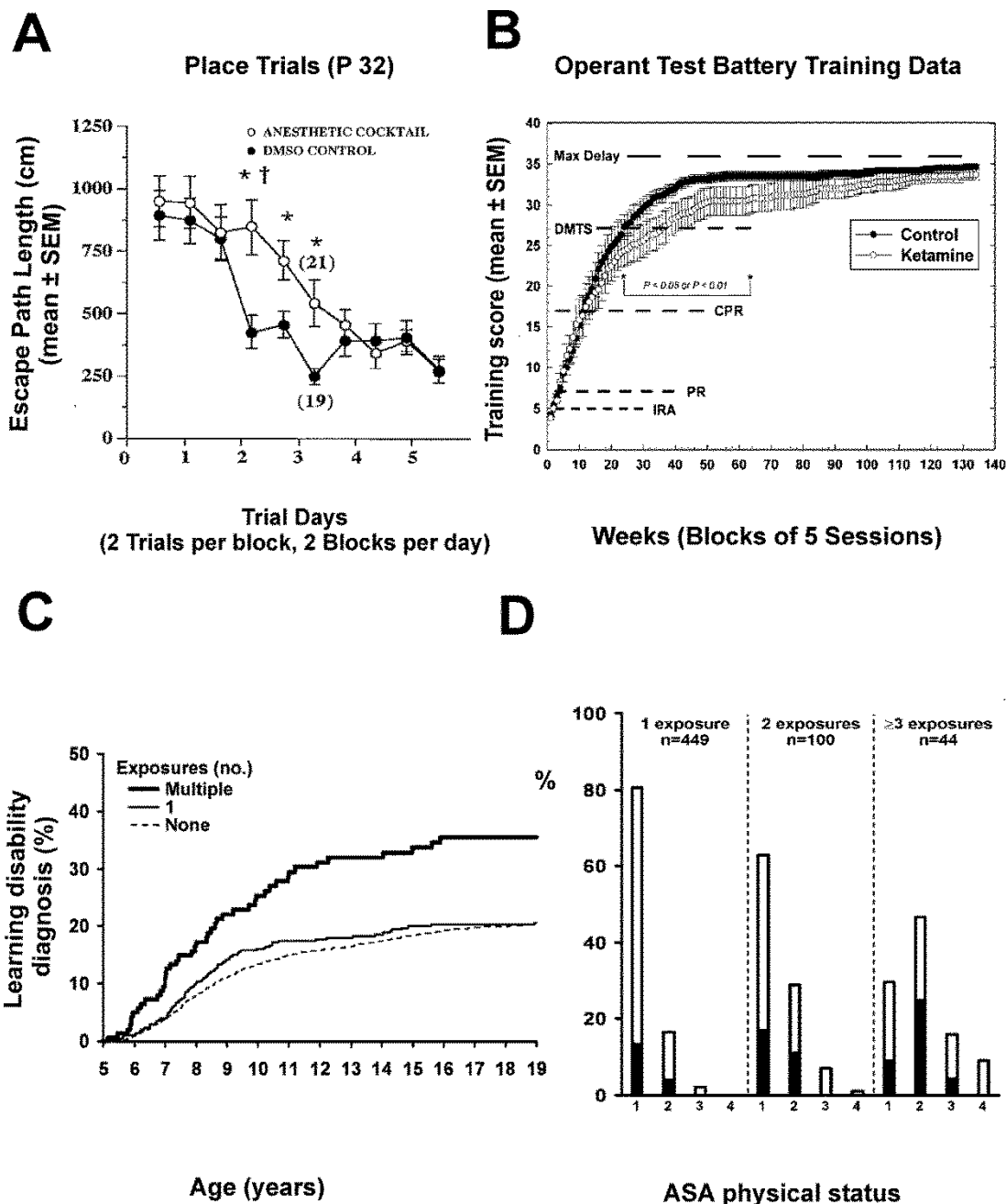


Figure 1. Exposure to GA during brain development causes learning disabilities in mammals. (Panel A: data are from rats exposure to the anesthetic triple cocktail, Panel B: data is from Rhesus monkeys exposed to Ketamine, Panels C and D data are from a retrospective study in humans.) **A:** Adapted from Jevtovic Todorovic et al., 2003 Effects of neonatal triple anesthetic cocktail treatment on spatial learning. a, Rats were tested at P32 for their ability to learn the location of a submerged (not visible) platform. An ANOVA of the escape path length data yielded a significant main effect of treatment ($p = 0.032$) and a significant treatment by blocks of trials interaction ($p = 0.024$), indicating that the performance of the rats that received the anesthetic cocktail was significantly inferior to that of control rats during place training. Subsequent pairwise comparisons indicated that differences were greatest during blocks 4, 5, and 6 ($p = 0.003$, 0.012 , and 0.019 , respectively). However, the rats receiving the anesthetic cocktail improved their performance to control-like levels during the last four blocks of trials.

Figure 1. Exposure to GA during brain development causes learning disabilities in mammals continued. B: Adapted from Paule et al., 2009 Training scores for OTB task performance. Data are raw means +/- SEMs for 5 test sessions (one week's worth of data). Dotted lines indicate the scores at which animals began performing under the final rules of reinforcement for the indicated tasks: IRA = incremental repeated acquisition (learning) task; PR = progressive ratio (motivation) task; CPR = conditioned position responding (color and position discrimination) task; DMTS = delayed matching-to-sample (short-term memory) task with no recall delays in place; Max Delay = point at which all DMTS delay sets are attained. Note that the separation between the groups began during the time subjects had to learn the concept associated with correct performance of the DMTS task. Bracket indicates sessions over which training scores for control subjects were significantly higher than those for ketamine-exposed subjects. **C:** adapted from Wilder et al., 2009 Cumulative percentage of learning disabilities diagnosis by the age at exposure shown separately for those that have zero, one, or multiple anesthetic exposures before the age 4 yr. **D:** Distribution of American Society of Anesthesiologists (ASA) physical status across patients with one, two and three anesthetic exposures with learning disability under age 19. For this presentation, individuals who had incomplete follow-up are categorized based on information available through last follow-up before age 19 yr. ASA Physical Status 1 - A normal healthy patient, ASA Physical Status 2 - A patient with mild systemic disease, ASA Physical Status 3 - A patient with severe systemic disease, ASA Physical Status 4 - A patient with severe systemic disease that is a constant threat to life, ASA Physical Status 5 - A moribund patient who is not expected to survive without the operation, ASA Physical Status 6 - A declared brain-dead patient whose organs are being removed for donor purposes. For panels C and D: Adapted with permission from Lippincott Williams and Wilkins/Wolters Kluwer Health: Wilder RT, Flick RP, Sprung J, Katusic SK, Barbaresi WJ, Mickelson C, Gleich SJ, Schroeder DR, Weaver AL, Warner DO. Early exposure to anesthesia and learning disabilities in a population-based birth cohort. *Anesthesiology*. 2009 Apr;110(4):796-804. license number 3547150029293

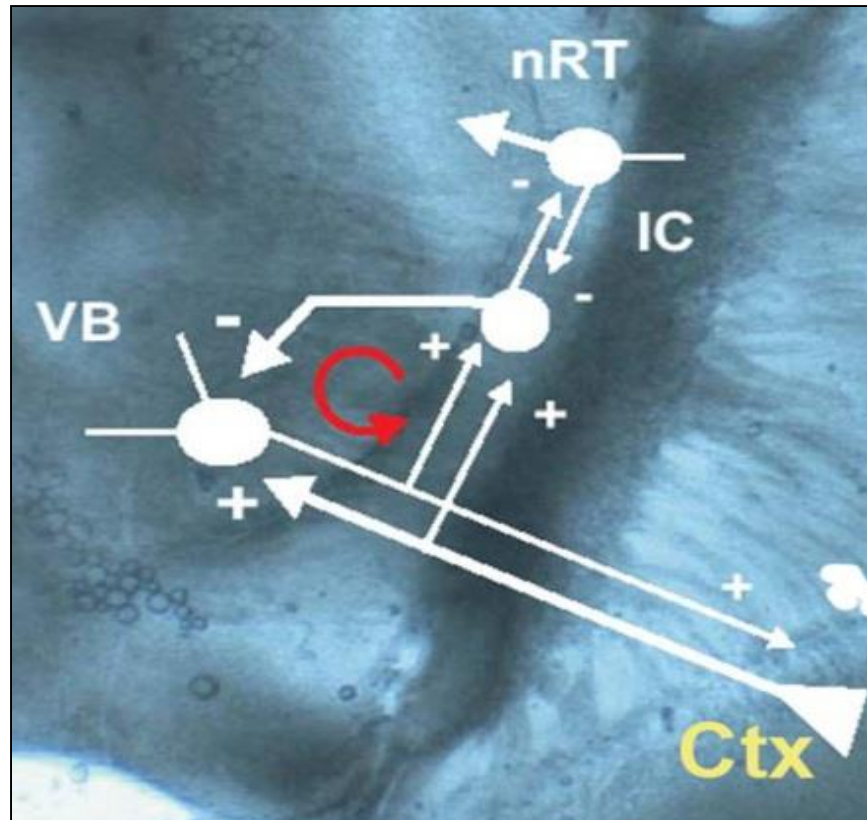


Figure 2. Schematic of sensory thalamic pathways. The ventral basal complex (VB) thalamus is the second synapse of the peripheral sensory pathway that receives afferent sensory projections from the dorsal horn lamina of the spinal cord and projections of the visual system. These neurons are Glutamatergic and send projections to both the somatosensory cortex (Ctx) and to the nucleus reticularis thalami (nRT), forming the first of two inhibitory feedback loops. In turn, the nRT is heavily innervated by excitatory efferent projections stemming from the somatosensory cortex thus forming a second inhibitory feedback loop. Finally, neurons of the nRT share gap junctions and form a labyrinth of reciprocally interconnected inhibitory GABAergic synapses that in turn further regulate action potential firing patterns of this nucleus.

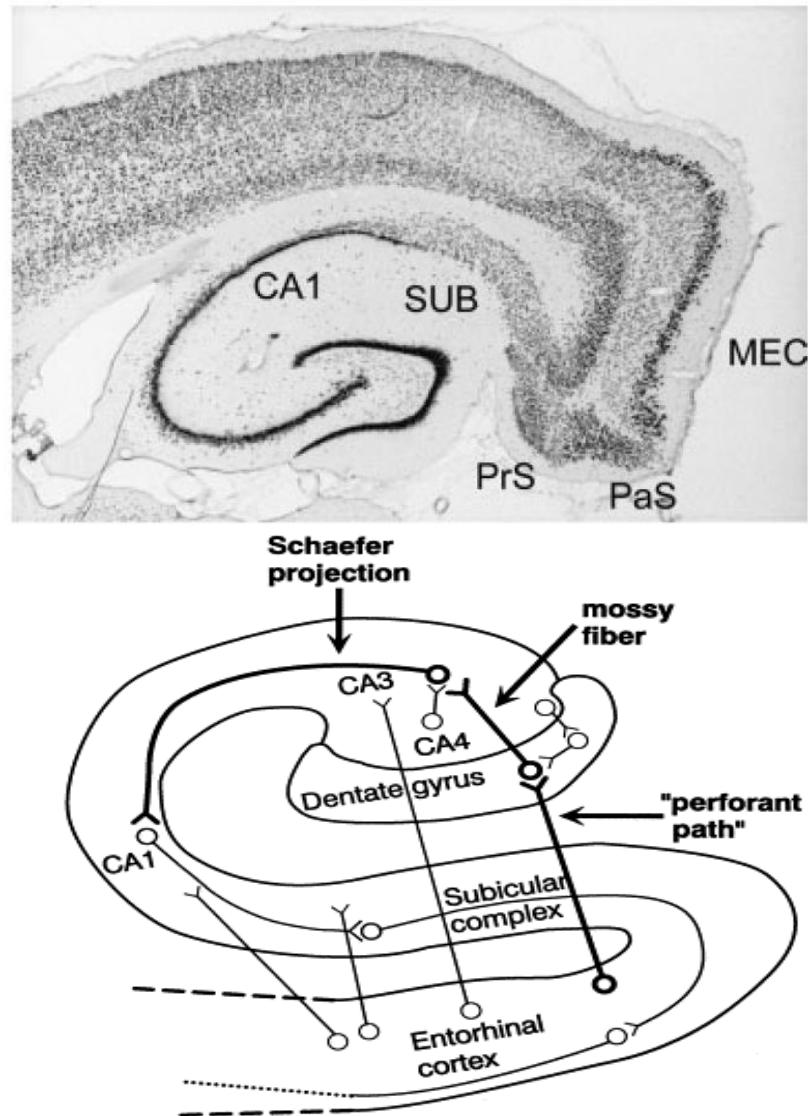


Figure 3. The hippocampal formation and the subiculum. The subiculum forms a highly intertwined network with both thalamic and cortical structures. The subiculum receives primary projections from the CA 1 region of the hippocampus, projections from the layer III of the entorhinal cortex, the parahippocampal cortex and the frontal cortex. In turn, the subiculum also returns projections to the previously mentioned cortical structures. Other projections included those to the forebrain limbic system that are associated with the hypothalamus pituitary adrenal axis (HPA). (Adapted from O'Mara, 2005 with permission Wiley and Sons license number 3564470026160; de la Prida et al., 2006 with permission Elsevier Limited license number 3564480286965; Weinberger 1999 with permission Elsevier Limited license number 3564480286965)

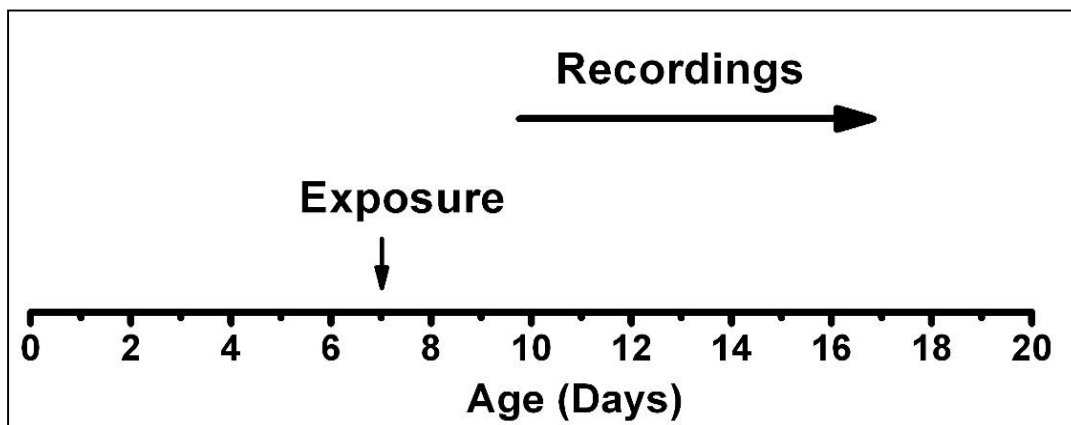


Figure 4. Timeline for performing all experiments. Exposure to the anesthetic triple cocktail of 9 mg/kg midazolam, 0.75% isoflurane and 80% N₂O is performed at post natal day 7. Subsequent electrophysiology experiments are performed during post natal day 10 and beyond.

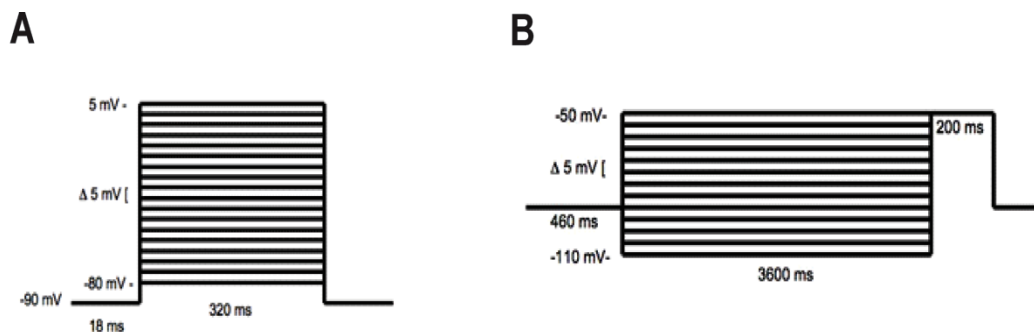


Figure 5. Voltage clamp protocols used for the interrogation of T-channel biophysical properties. **A:** Depiction of activation the voltage clamp protocol used to evoke T-currents within nRT neurons **B:** Voltage clamp protocol used to discern the inactivation properties of T-channels expressed in nRT neurons

II. Early GA exposure leads to hyperexcitable nRT neurons

A. Introduction

In order to determine the long term alterations mediated by early anesthetic exposure upon the action potential firing patterns of nRT neurons, both tonic and hyperpolarization induced rebound firing properties, such as burst pattern formations, number of firing events and burst frequency, were investigated. The firing properties of these neurons were also assessed with and without pharmacological blockade of excitatory and inhibitory potentials in order to investigate the firing properties within the context of intact TC-CT circuits, and in isolation from other excitatory and inhibitory currents. The long term modifications of the underlying Ca^{2+} conductance or T-channel mediated low threshold calcium spikes (LTCS) that are in part responsible for the switch from tonic to burst action potential firing in nRT neurons were also investigated.

Neurons of the thalamus have two distinct modes of action potential firing: tonic and burst. Tonic action potentials are present during wake periods and are integral for sensory perception, while burst action potentials are present during sleep, and also underlie oscillatory and low frequency EEG patterns. Therefore, early GA exposure mediated alterations in both tonic and burst nRT neuron action potential firing patterns were characterized.

Changes in nRT neuron action potential properties may alter critical physiological processes such as faithful transfer of somatosensory information, TC oscillations that are integral to sleep and wakefulness, and possibly induce absence epilepsy. Previous studies have shown that alterations in both excitatory thalamic relay nuclei neuron firing properties and the inhibitory nRT neuron firing properties, leads to a higher incidence of thalamic neuron burst firing, and manifests behaviorally as absence seizure (Paz et al., 2010). It is important to note that alterations in nRT firing patterns may also lead to disturbances in sleep rhythms and sleep and wake cycles (Lee et al., 2004). Burst or LTCS crowning

action potentials (figure 7 and 9) are present during sleep and more specifically are associated with slow wave sleep. These action potential formations also underlie the low frequency high amplitude SWD EEG patterns present during sleep and pathological conditions such as absence seizure. Utilizing patch clamp electrophysiology, GA mediated alterations in tonic and burst firing action potential patterns are characterized. In this section our data will demonstrate GA mediated increases in tonic action potential frequencies, rebound action potential frequencies and LTCS mediated burst firing.

Owing to an increase in tonic and rebound action potential frequencies, as well as LTCS mediated burst firing, alterations in ion channel properties are explored. LVA T-type Ca^{2+} channels are well-established mediators of nRT neuron action potential firing (Steriade et al., 1990). It is also well established that deinactivation of T-type calcium channels causes a switch from tonic to burst action potential firing. Thus, activation and inactivation properties of T-currents present in both GA and Sham animals are determined. The properties of T-channel conductance and current density are also investigated.

B. Experimental design

Anesthesia At postnatal day 7 (P7) both male and female Sprague Dawley rats were exposed to 6 hours of a clinically relevant triple anesthetic cocktail consisting of 9 mg/kg midazolam, 80% N_2O , and 0.75% ISO. Sham controls were exposed to 6 hours of mock anesthesia consisting of a vehicle injection of 0.1 % DMSO H_2O and separation from their mother. Midazolam (Sigma-Aldrich) was dissolved in 0.1 % DMSO and was given via an i.p. injection prior to exposure to volatile anesthetics. Exposure involving N_2O , O_2 and ISO utilized a dedicated pre mixer of N_2O and O_2 followed by an agent-specific ISO vaporizer that delivered a set percentage of anesthetic into a temperature controlled chamber preset to maintain 33-34 °C. The composition of the gas chamber was analyzed by real time feedback (Datex Capnomac Ultima) for N_2O , ISO, CO_2 , and O_2 percentages. For

EEG experiments performed in section IV, B260 was dissolved to 1 mg/ml in 15% β -cyclodextran. In order to achieve anesthesia, rats were repeatedly administered B260 i.p. at a final dose of 50 mg/kg.

Electrophysiology The external solution for current clamp electrophysiology experiments consisted of in (mM) NaCl 125, D-Glucose 25, NaHCO₃ 25, NaH₂PO₄ 1.25, KCl 2.5, MgCl₂ 1, CaCl₂ 2 mM. For current clamp experiments the internal solution consisted of in (mM) Potassium-D-Gluconate 130, EGTA 5 mM, NaCl 4 mM, CaCl₂ 0.5 HEPES 10, Mg ATP 2 mM, Tris GTP pH 7.2. The internal solution for experiments involving the isolation of T-currents in (mM) TMA-OH 130, EGTA 4, MgCl₂ 2 mM HEPES 40 mM pH 7.2. The external solution consisted of the current clamp external solution supplemented with 1 μ M TTX (Tocris). Glass micro electrodes, Sutter instruments O.D. 1.2 mm, were fabricated to maintain an initial resistance of 4-9 M Ω . Glass electrodes were pulled by using a Sutter instruments model P97. Neuron membrane responses were recorded using an Axopatch 200 B amplifier (Molecular Devices, Foster City, CA).

Patch clamp recordings in live adolescent (P9-30) horizontal 300 μ m rat brain slices in the presence or absence of synaptic blockers (20 μ M picrotoxin, 5 μ M APV and 5 μ M NBQX) were used in order to study the alterations in action potential firing patterns induced by early GA exposure. It is well established that nRT neurons exhibit tonic firing patterns at depolarized membrane potentials (Steriade et al., 1990). In order to evoke tonic firing action potentials an initial depolarizing pulse of 0.05 nA was injected followed by a stepping sequence from 10 to 190 pA by 10 pA for a 500-ms duration per step. Utilizing a multi-step protocol both tonic and burst firing properties of nRT neurons were determined. Neurons of the nRT were patched in whole cell configuration and resting membrane potentials were recorded for 100 ms. After this, neurons were injected with a single depolarizing step 0.2 nA for 400 ms, and allowed to rest for 400 ms. Then, hyperpolarizing currents in 0.05 nA intervals stepping from -0.2 to -0.5 nA were

injected. Subsequent resting membrane potentials, tonic action potential frequencies, rebound action potentials, input resistances and LTCS events were characterized.

T-channels T-channel activation was measured by stepping the neuron from an initial holding potential of -90 mV for 18 ms from -80 mV to 5 mV in 5 mV increments over a period of 320 ms. Subsequent I–V curves were generated and peak current amplitudes and inactivation properties were established and compared. Current densities were calculated by measuring average peak current divided by the capacitance of the neuron. Steady-state inactivation curves will be assessed using a standard double-pulse protocol with 3.6 s-long prepulses to variable voltages (from -110 to -50 mV in 5 mV increments) and test potentials to -50 mV (figure 5). The voltage dependencies of activation and steady-state inactivation will be described with single Boltzmann distributions of the following forms:

Activation: $G(V) = G_{\max} / (1 + \exp [-(V - V_{50}) / k])$

Inactivation: $I(V) = I_{\max} / (1 + \exp [(V - V_{50}) / k])$

In these forms, I_{\max} is the maximal amplitude of current; G_{\max} is the maximal conductance (calculated by dividing current amplitude with estimated driving force); V_{50} is the voltage at which half of the current is activated or inactivated; and k represents the voltage dependence (slope) of the distribution. The time courses of macroscopic T-current inactivation were fitted using either a single-exponential equation. For double-exponential fits the resulting inactivation tau values were weighted using the equation $\tau_w = [(\tau_1 * A_1) + (\tau_2 * A_2)] / (A_1 + A_2)$ (A_1 is amplitude 1 and τ_1 is decay constant 1; A_2 is amplitude 2 and τ_2 is decay constant 2) the resulting value was averaged with cells where single-exponential fits were used.

C. Data analysis

In every *in vitro* experiment, an attempt was made to obtain as many neurons as possible from each animal in order to minimize number of animals used. Statistical analysis for all electrophysiology studies were clustered according to animal. For pairwise and repeated measures experiments, linear mixed models (LMM) were applied in order to account for intracluster correlation effects, and to avoid reducing the data to means per animal (Galbraith *et al.*, 2010). Statistical analysis was also performed using One-way and Two-way ANOVA, Mann-Whitney rank sum test, as well as Student T-test and paired T-test where appropriate; significance was accepted with p values < 0.05. All p values are reported in Table 1, thus providing a comprehensive overview and comparison between results originating from different analysis (per neuron, per animal and LMM). Issues of normality and heterogeneity of variation were evaluated to determine the adequacy of the ANOVA models and whether additional manipulations were warranted. Voltage current/commands and digitization of the resulting voltages and currents were performed with Clampex 8.3 software (Molecular Devices) running on an IBM compatible computer. Resulting current and voltage traces were analyzed using Clampfit 10.3 (Molecular Devices). Statistical and graphical analysis was performed using GraphPad Prism 5.01 software (GraphPad Software, La Jolla CA) or Origin 6.1 (OriginLab, North Hampton MA). Linear mixed model statistical analyses for pairwise and repeated measures factors were conducted using PASW Statistics 18 (SPSS Inc., Chicago, IL, USA).

D. Results

1. Exposure of rat pups at age P7 to GA leads to lasting increases in nRT neuronal excitability

Here, the possible alterations in intrinsic excitability of nRT neurons in GA-treated rats were examined by utilizing the current-clamp experiments and investigating action potential firing patterns of nRT neurons. Original traces from representative neurons (figure 6A) indicate that at current injections of 20, 70 and 150 pA, the GA group neuron (top gray traces) responded with relatively uniform APs at a higher firing frequency than the neuron from the Sham group (bottom black traces). Similarly, Fig. 6B shows that the average GA group response (■) had a higher average firing frequency across all current pulses (overall significance $p < 0.01$, LMM), as compared with neurons from the Sham group (○).

Thalamic neurons exhibit a characteristic oscillatory burst firing mode after periods of membrane hyperpolarization that may occur during inhibitory synaptic potentials *in vivo* (Steriade *et al.*, 1990). Thus, the differences between the rebound firing frequencies in GA-treated vs. Sham groups were investigated by progressively hyperpolarizing the neuron membrane. Fig. 7A shows typical membrane responses to the series of hyperpolarizing current injections in representative nRT neurons from the Sham-treated group (middle black traces) and GA-treated group (bottom gray traces). Input resistances (R_{in}) and resting membrane potentials (RMP) were derived from the protocol depicted in panel 7A. After injection of a hyperpolarizing current of sufficient amplitude to remove inactivation of T-current, the same neurons exhibited rebound low-threshold-calcium spikes (LTCSs) and burst firing mode (see gray arrows on Fig. 7A). The burst firing mode was more readily evoked in the neuron from the GA group than in that from the Sham.

The average R_{in} of these neurons did not significantly vary between the two groups over the range of tested current injections (Fig. 7B). Similarly, there was no significant difference in RMPs between the two groups (GA -54 ± 3 mV; Sham -56 ± 1 mV; data not shown). In contrast, figure 7C shows that the same amplitudes of hyperpolarizing current injections induced significantly (about 3-fold, overall $p < 0.001$, LMM) higher AP firing frequency in the GA-treated group (■, $n = 16$ rats, 25 neurons) than in the Sham-treated group (○, $n = 10$ rats, 24 neurons). The frequencies of APs per LTCSs were compared over the range of the same current injections and found to be increased by 2.5-fold (overall $p < 0.01$, LMM) in the GA group as compared with the Sham (Fig. 7D and 7E). Hence, increased excitability of nRT neurons in GA-treated animals cannot be attributed to alteration of passive membrane properties.

Initial current clamp experiments performed in the absence of synaptic blockers revealed elevated average tonic firing frequencies for GA versus Sham neurons, 25.1 ± 1.4 Hz ($n=11$) for GA, 19.5 ± 1.0 Hz ($n=11$) for Sham, $p < 0.01$ t-test (figure 8D). Rebound AP frequencies were also found to be elevated in GA (■) versus Sham (○) animals (figure 9C). At higher amplitude hyperpolarizations early GA exposure significantly increased rebound action potential firing frequency. The effects of anesthetic exposures upon associated burst firing of APs were also analyzed. In experiments without synaptic blockers, for the GA group there was an increase in average number of APs per burst (4.2 ± 0.2 for GA ($n=11$) and 2.8 ± 0.1 ($n=11$) for Sham $p < 0.01$ t-test) (figure 9D). There were also no significant differences in T-channel mediated LTCS amplitudes and durations between Sham and GA groups in all experiments (data not shown). Resting membrane potentials were found to be slightly more depolarized in the Sham versus that of GA group (-52.2 ± 1.4 mV for Sham and -55.6 ± 1.4 mV for GA $p < 0.05$ t-test) (figure 9E). Input resistance was not different between Sham and GA groups in all experiments (figure 9B).

2. T-channel biophysical properties are altered after exposure to GA

Since T-channels are crucially involved in burst firing of thalamic neurons, the hypothesis that alterations in T-current density and/or biophysical properties could have contributed to increased intrinsic excitability of nRT neurons in the GA group was tested. The amplitudes of T-currents were measured in voltage-clamp experiments with V_h at -90 mV and with a series of V_t from -80 to -35 mV given in 5 mV increments. T-current waveforms in representative nRT neurons from the Sham and GA groups are depicted in Figs. 10A and 10B, respectively. Using I-V relationships, it was found that, on average, peak T-current densities were increased two-fold in the GA group (■) as compared with the Sham group (○) over the range of test potentials (Fig. 10C, overall $p < 0.01$, LMM). Fig. 10D shows that V_{50} for the voltage-dependence of activation in the GA group demonstrated a significant depolarizing shift ($p < 0.01$, LMM) of about 8 mV (■, -58 ± 2 mV) as compared with that in the Sham group (○, -66 ± 1 mV). The time constant of T-current inactivation in these neurons was assessed by fitting the decaying portions of the current waveforms in the I-V relationships with a single exponential function; these values were not statistically different between GA (57 ± 3 msec, 13 rats, 36 neurons) and Sham (55 ± 4 msec, 17 rats, 52 neurons) groups. In order to assess the voltage dependence of inactivation and to compare current densities in GA and Sham groups an independent test was used by evoking T-currents at a V_t of -50 mV after preconditioning potentials from -110 mV to -55 mV in 5 mV increments. Average data points presented in Fig. 10E demonstrate that current densities were increased about two-fold in the GA group (■) as compared with those in the Sham group (○) over the range of membrane potentials (overall $p < 0.001$, LMM). The voltage-dependence of inactivation using Boltzmann fits was also calculated. Similar to the voltage dependence of activation, Fig. 10F shows that V_{50} for the voltage dependence of inactivation in the GA group also demonstrated a small but

significant depolarizing shift of about 4 mV (■, -84 ± 1 mV) in comparison with that in the Sham group (○, -88 ± 2 mV, $p < 0.05$, LMM).

	eIPSC	mIPSC	eEPSC	mEPSC	Input-Output	Rebound AP	APL/TCS	Input resistance	Current density - activation	V50 - activation	Current density - inactivation	V50 - inactivation	EEG	T-channel antagonism	
t-test (per neuron)	Tau: p<0.001* PPR: p=0.001	A: p=0.039 HW: p=0.334* Tau: p=0.430* F: 0.031*	AMPA: p=0.002* NMDA: p=0.327* TOTAL: p=0.054*	A: p<0.001* HW: p=0.348* Tau: p=0.072* F: 0.002* CT: p=0.088*	/	/	/	/	/	p<0.001	/	p=0.018	/	/	/
t-test (per animal)	Tau: p=0.030* PPR: p=0.003*	A: p=0.083 HW: p=0.268* Tau: p=0.392 F: 0.131*	AMPA: p=0.032* NMDA: p=0.246* TOTAL: p=0.072*	A: p=0.010* HW: p=0.204 Tau: p=0.155 F: p=0.032 CT: p=0.047	/	/	/	/	/	p=0.003	/	p=0.002	EL: p=0.443 CD: p=0.005	%TAP: p=0.008 %BAP: p<0.001 %GR: p=0.003	
2-way RM ANOVA (per neuron)	T: p<0.001 I/O: p<0.001 T x I/O: p<0.001	/	/	/	T: p=0.002 CI: p<0.001 T x CI: p<0.001	T: p<0.001 CI: p<0.001 T x CI: p=0.105	T: p=0.002 CI: p<0.001 T x CI: p=0.116	T: p=0.599 CI: p=0.514 T x CI: p=0.750	T: p=0.004 VS: p<0.001 T x VS: p<0.001	/	T: p<0.001 VS: p<0.001 T x VS: p<0.001	/	/	/	
2-way RM ANOVA (per animal)	T: p=0.002 I/O: p<0.001 T x I/O: p<0.001	/	/	/	T: p=0.010 CI: p<0.001 T x CI: p<0.001	T: p=0.016 CI: p=0.131 T x CI: p=0.965	T: p=0.012 CI: p<0.001 T x CI: p=0.272	T: p=0.613 CI: p=0.871 T x CI: p=0.705	T: p=0.037 CI: p<0.001 T x CI: p=0.095	/	T: p=0.012 VS: p<0.001 T x VS: p<0.001	/	/	/	
LMM	Tau: pPR: p=0.007 I/O: p<0.001 T x I/O: p<0.001	A: p=0.257 HW: p=0.611 Tau: p=0.944 F: p=0.311	AMPA: p=0.022 NMDA: p=0.993 TOTAL: p=0.243	A: p=0.024 HW: p=0.324 Tau: p=0.867 F: p=0.083 CT: p=0.167	T: p=0.005 CI: p<0.001 T x CI: p=0.325	T: p<0.001 CI: p=0.006 T x CI: p=0.050	T: p=0.003 CI: p<0.001 T x CI: p=0.367	T: p=0.603 CI: p=0.427 T x CI: p=0.050	T: p=0.004 VS: p<0.001 T x VS: p=0.002	p=0.004	T: p<0.001 VS: p<0.001 T x VS: p=0.001	p=0.043	(ED) T: p=0.026 Time: p<0.001 T x Time: p=0.063	%TAP: p=0.016 %BAP: p<0.001 %GR: p=0.006	

Table 1. Statistical comparisons (GA vs. SHAM) across all *in vitro* and *in vivo* analysis using t-test or 2-way RM ANOVA (per neuron and per animal), and linear mixed model. *Mann-Whitney U test; T = treatment; CI = current injection; VS = voltage step; A = amplitude; HW = half-width; F = frequency; CT = charge transfer; I/O = input output; EL = SWD event latency; CD = cumulative duration of SWD events; ED = SWD event duration; %TAP = the percent of predrug tonic action potential firing; %BAP = the percent of predrug burst action potential firing; %GR = the percent of GBL response.

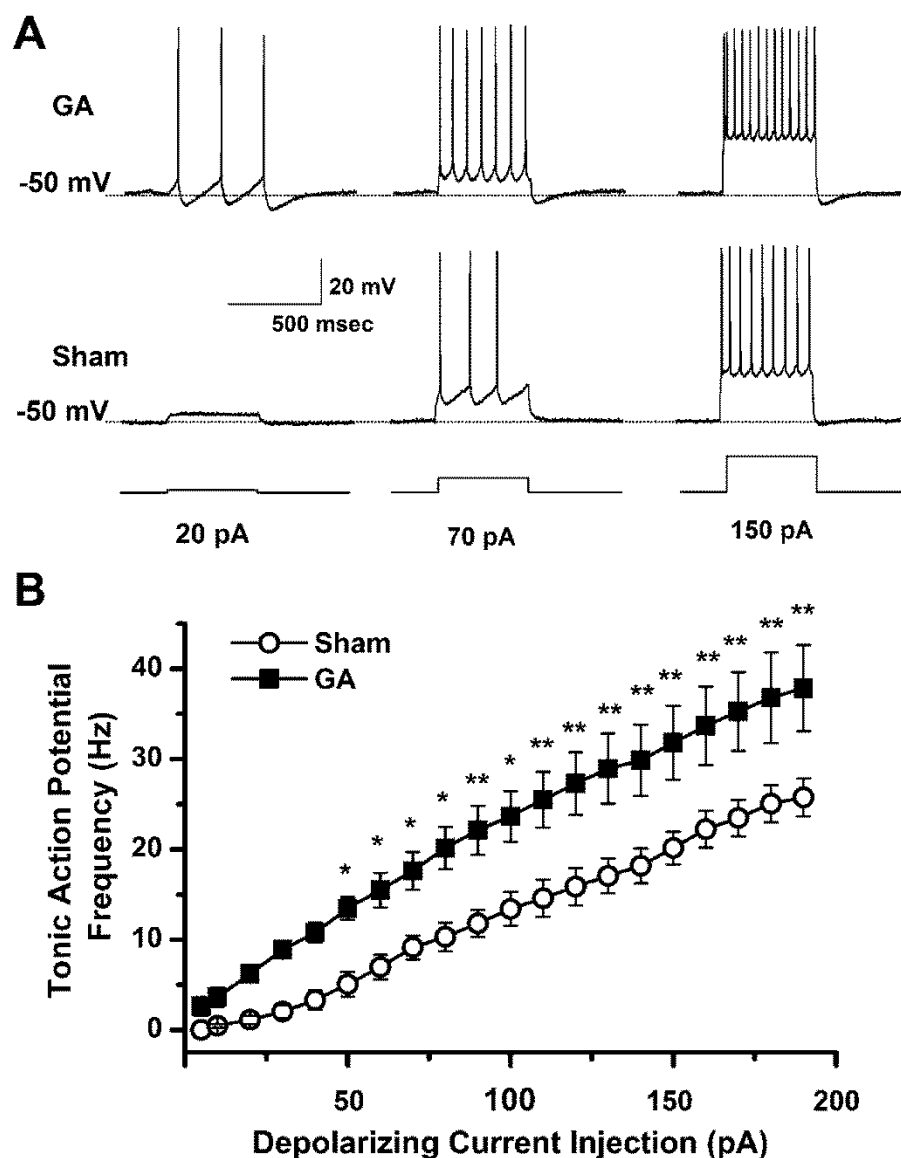


Figure 6. Depolarization-induced tonic firing pattern of nRT neurons is altered in GA-exposed rats. **A:** Original traces from representative nRT neurons from GA-treated (top gray traces) and Sham-treated (middle black traces) rats show active membrane responses to escalating depolarizing current injections of 0.02 nA, 0.07 nA and 0.15 nA via the recording electrode. Bottom traces indicate our current injection protocols. At all current injections, neurons from GA-treated rats fired more APs as compared with nRT neurons from Sham-treated rats. Note that at the smallest current injection of 0.02 nA, the Sham-treated neuron did not fire at all, while the GA-treated neuron fired 3 APs. Dotted lines represent RMP of -50 mV. **B:** A graph of average values shows that a family of escalating current injections induced more firing APs in the GA-treated group (■, n = 17 neurons from 6 rats) as compared with nRT neurons from Sham-treated group (○, n = 18 neurons from 8 rats * indicates significance of $p < 0.05$, ** indicates significance of < 0.01 , *** indicates significance $p < 0.001$ by Repeated measures Two-way ANOVA). All symbols on panel B of this figure indicate mean values from multiple animals and vertical lines are SEM.

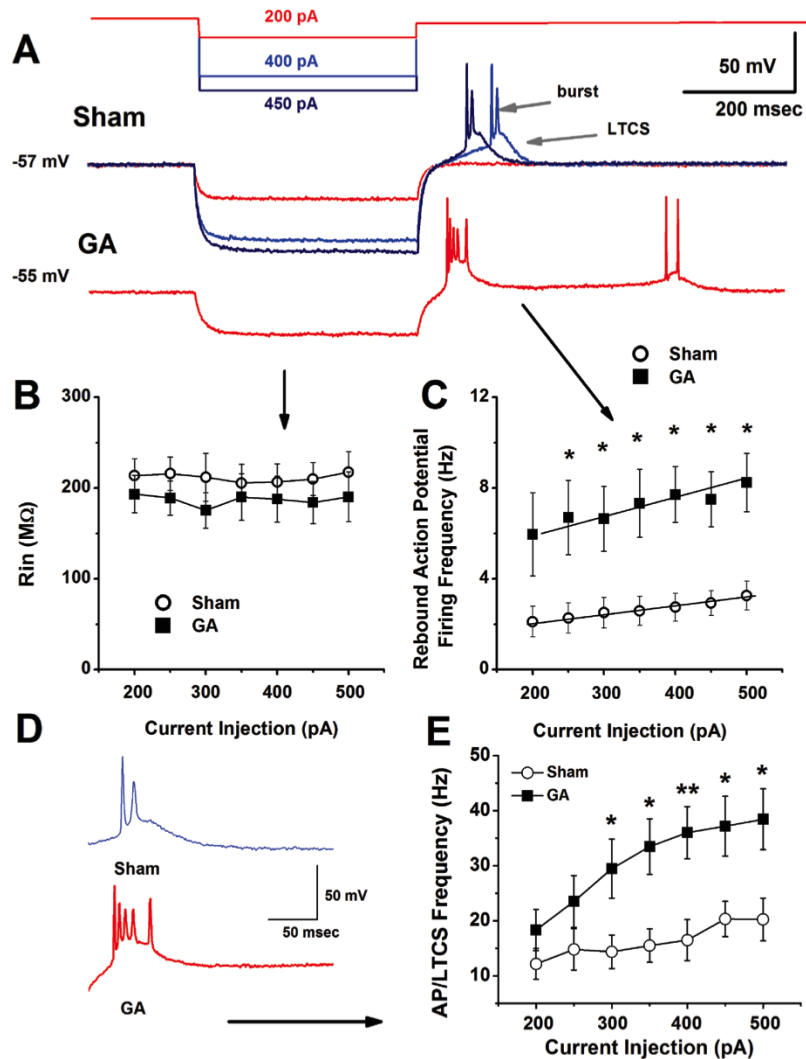


Figure 7. Hyperpolarization-induced burst spike firing pattern of nRT neurons is altered in GA-exposed rats. **A:** Hyperpolarization-induced burst spike firing pattern of nRT neurons is altered in GA-exposed rats. **A:** Top: drawing illustrates the current injection protocol used in our experiments, in which neurons are hyperpolarized with a series of -200 pA, -400 pA, and -450 pA current injections. The middle traces indicate the passive membrane response of an nRT neuron from the Sham group followed by rebound LTCS and burst firing resulting from current injections of -200 pA (red trace), -400 pA (blue trace) and -450 pA (green trace). The bottom red trace indicates the passive membrane responses and rebound burst firing pattern of an nRT neuron from the GA group treated with a current injection of -200 pA. Note that the current injection of -200 pA evoked burst firing in an nRT neuron from a GA-treated rat (bottom red trace), while the same current injection failed to evoke rebound burst firing in an nRT neuron from a Sham-treated rat (middle red trace). Two fold stronger current injections (-400 and -450 pA) were needed to evoke rebound burst firing in this nRT neuron from the Sham-treated rat (blue and green traces on middle panel respectively). **B:** There was no significant difference between Sham and GA groups in R_{in} for nRT neurons subjected to hyperpolarized current injections. **C:** Average data points on this graph show that the rebound firing frequency, measured during the 1.2 sec-long period following the hyperpolarizing pulses, was about 5-10-fold increase in the GA-treated group (■) as compared with the Sham group (○). Numbers in parenthesis in all panels indicate number of different neurons (* indicates $p < 0.05$ repeated measures 2 way ANOVA). **D:** Original traces show LTCS and burst of AP evoked by current injections of -0.4 nA in nRT neurons from the Sham group (top trace), and -0.2 nA in nRT neurons from GA group (bottom trace), respectively. The traces are from the same nRT neurons presented in panel A of this figure. **E:** Graph bars show the average number of APs per first evoked burst from multiple neurons in the Sham (○) and GA-treated (■) groups. Vertical bars indicate \pm SEM from multiple ($n=11-12$) determinations. Note that the number of APs per first burst is significantly increased in the GA group by about two-fold. ** indicates significance of $p < 0.01$ (Student's t-test). All data presented in this figure were obtained from 16 GA-treated animals (25 neurons) and 10 Sham-treated animals (24 neurons).

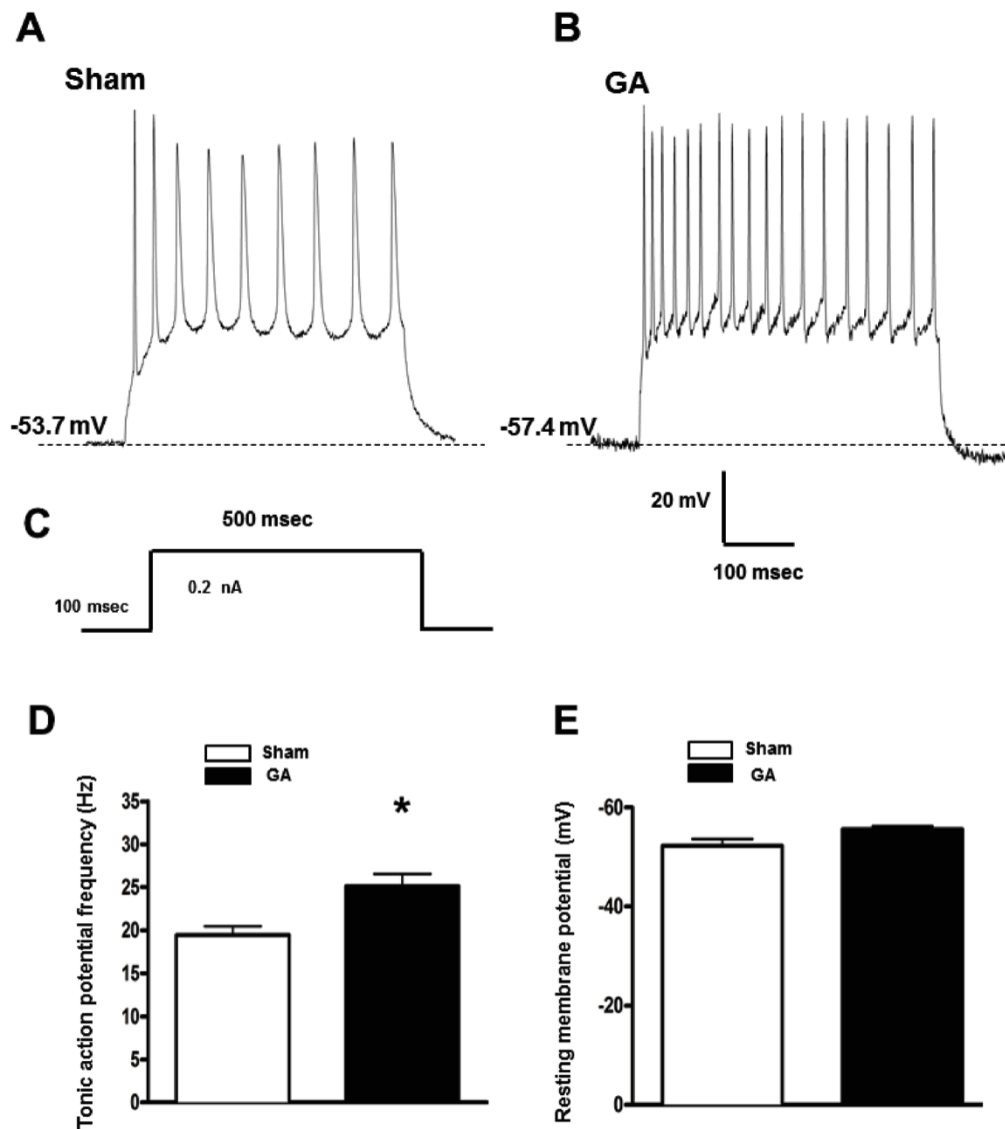


Figure 8. Tonic action potentials are increased in GA –exposed rat nRT neurons. **A:** Representative trace from a Sham nRT neuron firing tonic APs. **B:** Representative trace from a GA- exposed nRT neuron firing tonic APs. **C:** Portion of the dual step current clamp protocol used to illicit tonic AP firing of nRT neurons. **D:** Tonic action potential frequency is elevated in GA versus Sham treated nRT neurons (n=11 for GA and n= 11 for Sham student's T-test * indicates significance $p < 0.05$) **E:** There was no significant difference between the resting membrane potential of GA and Sham treated nRT neurons.

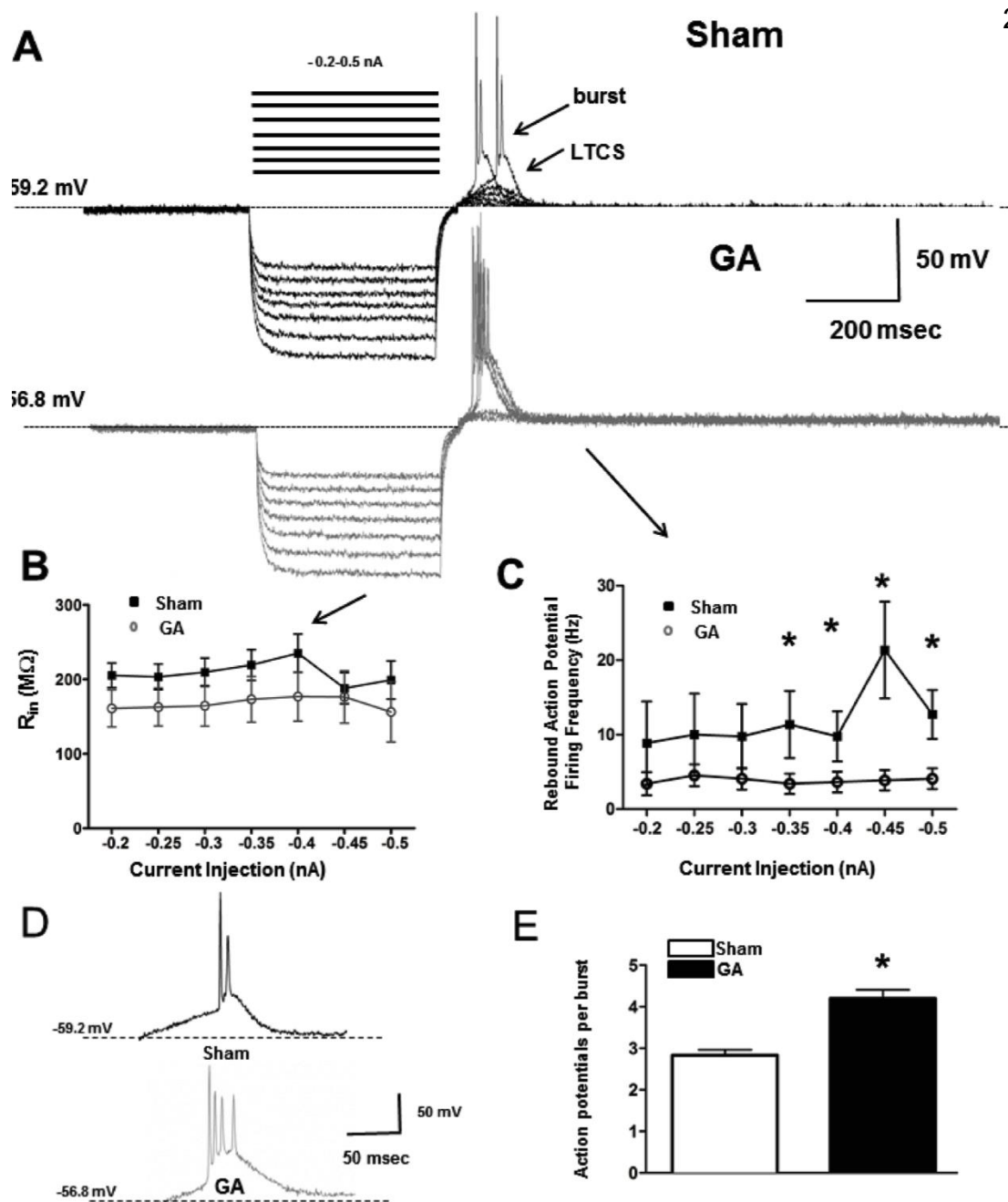


Figure 9. Hyperpolarization-induced burst spike firing pattern of nRT neurons is altered in GA-exposed rats with intact inhibitory and excitatory synaptic drive. **A:** Top: drawing illustrates the current injection protocol used in our experiments when neurons are hyperpolarized with a series of -0.2 nA to -0.5 nA current injection in 0.05 nA incremental steps. Middle black traces indicate passive membrane response of an nRT neuron from the Sham group followed by rebound LTCSs and burst firing of APs. Bottom gray traces indicate passive membrane responses and rebound burst firing pattern of another nRT cell from the GA group with the same current injection protocol. The dotted line represents RMP. **B:** There was very little difference between Sham and GA groups in R_{in} in the nRT cells subjected to hyperpolarized current injections (*, $p < 0.05$). **C:** Average data points on this graph show that rebound firing frequency, measured during 1.2 sec-long period following preceding hyperpolarized pre-pulses, was about 5-10-fold increase in the GA-treated group (■) as compared with the Sham group (○). Numbers in parenthesis in all panels of this figure indicate different cells, * denotes $p < 0.05$ SNK. **D:** Original traces show LTCS and burst of AP evoked by current injections of -0.4 nA in nRT cells from Sham group (top trace), and -0.2 nA in nRT cell from GA group (bottom trace), respectively. The traces are from the same nRT cells presented on panel A of this figure. **E:** Graph bars show the average number of APs per first evoked burst from multiple cells in the Sham (○) and GA-treated (■) groups. Vertical bars indicate \pm SEM from multiple ($n=11-12$) determinations. Note that number of APs per first burst is significantly increased in the GA group by about two-fold. ** indicates significance of $p < 0.01$ (Student's t-test). All data presented in this figure are obtained from 7 GA-treated animals and 3 Sham-treated animals.

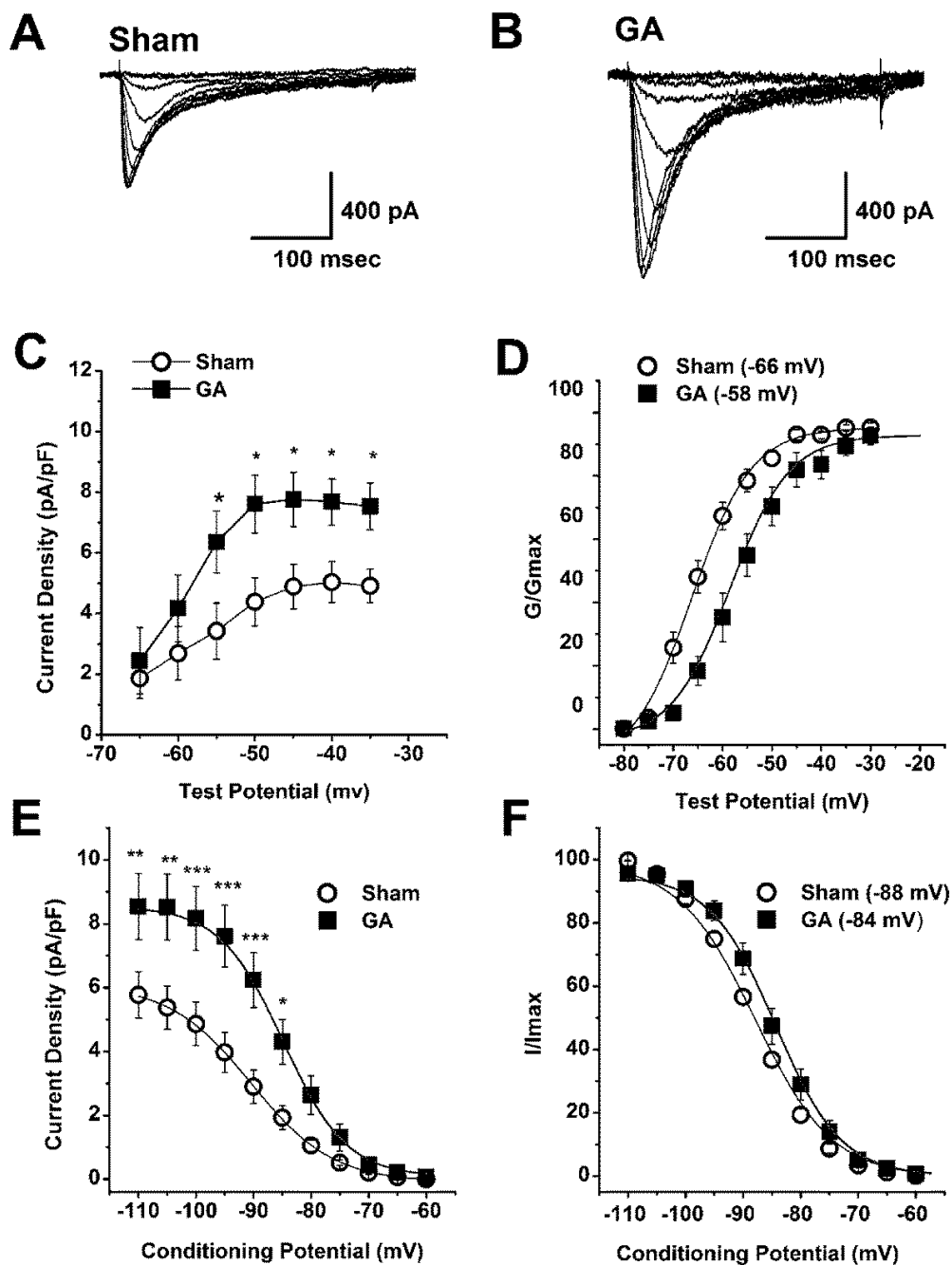


Figure 10. T-current properties of nRT neurons are altered by exposure to GA. **A-B:** Representative families of original T-current traces from both Sham (A) and GA (B) nRT neurons in the range of V_i from -80 to -35 mV from V_h of -90 mV. Bars indicate calibration. **C:** T-channel current density as calculated from the voltage dependence of activation is increased about 2-fold across a broad range of test potentials in the GA-treated group ($n = 14$ rats, 40 neurons) when compared to the Sham group ($n = 12$ rats, 49 neurons) (symbol *, $p < 0.05$, SNK). **D:** The V_{50} for the voltage-dependence of activation (noted in parentheses) for the GA (■, $n = 14$ rats, 43 neurons) group demonstrated a significant depolarizing shift of 8 mV as compared with that in the Sham (○, $n = 18$ rats, 55 neurons) group ($p < 0.01$, LMM). **E:** T-channel current density as calculated from the voltage-dependence of inactivation is increased nearly 2-fold in the GA group ($n = 13$ rats, 31 neurons) when compared to the Sham group ($n = 9$ rats, 22 neurons) across a broad range of conditioning potentials (symbol *, $p < 0.05$; ** $p < 0.01$; *** $p < 0.001$, SNK). **F:** The V_{50} of the voltage-dependence of inactivation of the GA group ($n = 12$ rats, 30 neurons) also demonstrated a small but significant depolarizing shift (as noted in parentheses) when compared with that in the Sham group ($n = 14$ rats, 45 neurons; $p < 0.05$ LMM). All symbols on panels C-F of this figure indicate mean values from multiple animals and vertical lines are SEM.

F. Discussion

In this section it is clearly shown that early GA exposure leads to hyperexcitable nRT neurons. In experiments where nRT neurons are within the circuit context, both tonic and hyperpolarization induced firing frequencies are increased. LTCS crowning action potential frequencies are increased in the GA group as well. Such increases may be attributed to alterations in input resistance, a decrease in intra nRT negative feedback properties and/ or ion channel characteristics that lead to alterations in nRT neuron firing properties. Our data indicates that the hyperexcitable state is not attributed to an increased input resistance. Application of glutamate receptor antagonists APV and NBQX allows for the isolation of nRT from excitatory inputs from the Ctx and VB thalamus, whereas the GABA antagonist picrotoxin should abolish intra nRT negative feedback properties. Co-administration of all three antagonists should theoretically isolate nRT neurons from intra nRT inhibition and excitatory inputs from both the Ctx and the VB thalamus. Once again, in a circuit independent context, nRT neurons are clearly more excitatory than Sham counterparts, in a non-input resistance dependent manner. In the presence of synaptic blockers, GA nRT neuron tonic action potentials frequency, rebound action potentials and LTCS crowning action potentials are also increased as compared to Sham. This suggests that alterations in nRT neuron firing properties may be in part attributed to changes in ion channel properties. Furthermore, alterations in T-channel window currents may also alter tonic action potential frequencies (Dryfus et al., 2010). Surprisingly, there is no significant difference in LTCS amplitude and/or duration between GA and Sham (data not shown). This may be in part due to large Na⁺ conductance masking the contribution of Ca²⁺ mediated LTCS events. Differences in LTCS amplitudes in GA versus Sham animals may be resolved by the addition of sodium channel blockers, such as TTX, during the same current clamp protocol. Differences in resting membrane potentials may be attributed to

the presence of synaptic blockers. Furthermore, changes in synapse properties and/or synaptic plasticity that allow for increases in excitatory strength between glutamatergic VB-nRT or Ctx-nRT pathways need to be addressed (section III experiments). There may also be a reduction of inhibitory GABA tone within the nRT proper (also to be addressed in section III). It is important to consider the possibility that an increase in sodium conductance may also contribute to these findings.

In order to further validate the contribution of T-channels to GA exposed nRT neuron firing properties, blockade by Ni^{2+} or other high affinity T-channel antagonists such as TTA-P2 should return hyperexcitable nRT neurons to Sham nRT neuron firing frequencies. Ni^{2+} is a well-established traditional T-channel blocker (Lee et al., 1991) whereas TTA-P2 is a novel highly specific and well characterized T-channel antagonist (Choe et al., 2011).

This study has shown that a single exposure to GAs at P7 leads to alterations in the T-channel properties of nRT neurons. GA-mediated alterations of T-channel biophysical properties and current density of nRT neurons may account for the increases in both tonic and burst action potential firing properties. Biophysical studies were performed in order to discern GA mediated alterations in T-channel properties that may contribute and underlie the changes fundamental to the alterations in rebound burst firing observed in early GA exposed rats. It is also proposed that alterations in T-channel window current properties may allow for T-channel participation in tonic nRT neuron firing. Taken together, these shifts in gating kinetics would cause a larger 'window current' or voltage range where channels are available to open but do not inactivate completely. This increase in window current promotes hyperexcitability and or increased neuron firing. In future experiments a faster recovery from inactivation in nRT neurons from GA as compared to Sham controls may be revealed. A faster recovery from inactivation would allow the channels to cycle through the open→closed→inactive cycle, thus returning them to become available to open

and pass more current. Correct operation of T-channels is normally important for the modulation of burst firing which underlies low-frequency oscillations in thalamocortical networks, whereas aberrant activity may contribute to pathological conditions of hyperexcitable neurons such as epilepsy.

Furthermore, depolarizing shifts of T-current activation and inactivation in the GA group allows T-channels to participate in tonic firing of nRT neurons. These alterations in T-channel properties contribute to the observed hyperexcitability of nRT neurons and that selective T-channel blockade may be used to reverse nRT neuron hyperexcitability following exposure to GAs during brain development. This idea is addressed in section IV. Based on these findings, the *in vitro* effects of a specific T-channel antagonist TTA-P2, upon tonic and burst nRT action potentials were also investigated. The *in vivo* effects of T-channel antagonism upon pharmacologically induced absence seizure like SWD are also investigated in section IV.

III. Early GA exposure alters thalamic neuron synaptic plasticity

Introduction

The balance between inhibitory and excitatory synapse drive is critical for shaping the action potential firing properties of nRT neurons. Inhibitory nRT neurons participate in rhythmic neuronal activities such as sleep spindles, and spike and wave activity as measured by EEG. These oscillations arise during deep sleep and possibly during waking, and manifest as absence seizure in pathological conditions. These patterns can also be generated *in vitro* (Jacobsen et al., 2001; McCormick 2002; von Krosigk et al., 1993). Spindle-like activity in ferret and rat thalamic brain slices can be transformed into highly synchronous, 2- to 4-Hz epileptiform oscillations by bath application of bicuculline methiodide (BMI), a GABA_A receptor antagonist that increases thalamic dependence on GABA_B-mediated currents (Huguenard and Prince, 1994; Kleinman-Weiner et al., 2009; McCormick et al., 2002; von Krosigk et al., 1993). The ion conducting channels that form currents essential for oscillations consist of T-currents (I_T), I_h and fast and slow inactivating potassium channels. It has been well documented that oscillations primarily occur due to interactions between I_T and I_h . Activation of I_T leads to LTCS, which leads to inactivation of I_h . Following each LTCS I_h reactivates and subsequent membrane depolarization leads to another LTCS and the cycle repeats. In section II, it is reported that there are alterations in T-channel biophysical properties that contribute to nRT neuron hyperexcitability. In order to further understand the effects of GA upon the oscillatory nature of thalamic circuits, changes in GA-mediated synaptic transmission within thalamic networks will be explored in this section.

Neurons of the nRT express multiple NMDA receptor subtypes, namely NR2A and NR2B, however, the biophysical characteristics such as decay times and rectification, match closely with those of the NR2C receptor (Zhang et al., 2009). In terms of GABA_A receptors, as measured by RT PCR, the predominate

subunits are α_3 and α_5 , γ_2 , γ_3 and δ . Regarding mIPSC properties, nRT decay times are much slower as compared to those of the VB (Zhang et al., 1997; Browne et al., 2001). The propensity of nRT neurons to oscillate may also impact the function of this circuit. Specifically, in this section, the functions of both excitatory and inhibitory nRT neuron synapses are explored in GA treated rats. Changes that allow for a greater duration of oscillation may include behavioral outcomes such as absence seizure, alterations in sleep patterns or changes in somatosensory reception.

Recent studies have demonstrated that a reduction in Ctx- nRT pathway strength by AMPA receptor knockout results in a strengthening of T-Ctx pathways resulting in hyperexcitable VB neurons and subsequent absence seizures (Paz et al., 2011). In order to assess any possible alterations of GA exposed nRT neuron synapse properties, both spontaneous and evoked inhibitory/excitatory post synaptic currents were studied. Cortical-thalamic neuron firing leads to bursts of excitatory postsynaptic potentials (EPSPs) in the target nRT neurons. Excitatory TC neuron projection firing also leads to bursts of EPSPs. Alterations in glutamate receptor function and/or glutamate release may very well lead to alterations in neuronal activity within the nRT which in turn leads to altered circuit activity. Thus, an experimental strategy that characterizes both evoked and spontaneous (action potential independent) synapse activity was utilized.

Neurons within the nRT form a labyrinth of reciprocally interconnected GABAergic synapses. Modifications in GABA quantal release at nRT synapses and/or alterations in GABA channel expression within the nRT synaptic terminals may also lead to alterations in circuit activities. Thus, it is of great importance to detect GA-mediated alterations in inhibitory synapse properties within nRT. In order to further validate any GA-mediated changes in inhibitory synapse properties, evoked inhibitory postsynaptic currents will be studied by electrode stimulation within the IC. Differences between GA and Sham inhibitory synapse properties are also studied by using a paired-pulse ratio (PPR) stimulation

protocol. Spontaneous miniature inhibitory postsynaptic currents (mIPSC) are evaluated as well. GA-mediated changes in nRT neuron excitatory synapse properties will be detected by recording evoked excitatory postsynaptic currents (eEPSCs) within the nRT by electrode stimulation within the IC. Finally, GA mediated alterations in spontaneous miniature excitatory postsynaptic currents (mEPSCs) are also investigated.

T-type calcium channel antagonists have been utilized therapeutically in order to treat epilepsy (Browne et al., 1975, Beenhakker and Huguenard, 2009). Recently, within the peripheral nervous system, this role has been expanded to treat painful diabetic neuropathies and neuropathic pain (Latham et al., 2009; Messinger et al., 2009). In this section the novel effects of a neuroactive steroid and fairly selective T-channel antagonist B260 are presented (Todorovic et al., 2004). The contribution that T-channels make to the excitatory nRT synapses will be investigated by characterizing the effects of B260 upon pre and post synaptic mEPSC properties.

B. Experimental design

Evoked synaptic transmission In order to investigate evoked synaptic transmission, neurons of the IC were electrically stimulated, and the responses were recorded within patch-clamped nRT neurons. Synaptic stimulation was achieved using a constant current isolated stimulator DS3 (Digitimeter Ltd., Welwyn Garden City, Hertfordshire, England). For each evoked response, the threshold current stimulus, 50% maximum, and maximal EPSC current amplitude were determined. All nRT eEPSCs were recorded at a holding potential of -70 mV in the presence of 20 μ M picrotoxin. All excitatory synaptic currents were eliminated when 5 μ M NBQX and 50 μ M D-APV were included in the external solution. The external solution for experiments with synaptic currents included the following (in mM) NaCl 130, CaCl₂ 2, KCl 2, MgCl₂ 1, NaHCO₃ 26, NaH₂PO₄ 1.25 and D-Glucose 10. This solution was equilibrated with a mixture of 95 vol%

O₂ and 5 vol% CO₂ for at least 30 minutes with a resulting pH of about 7.4. For recording of inhibitory postsynaptic currents, an internal solution containing, in mM, KCl 130, NaCl 4, CaCl₂ 0.5, EGTA 5, HEPES 10, MgATP₂ 2, Tris-GTP 0.5, and lidocaine N-ethyl bromide 5. pH was adjusted with KOH to 7.25 was used. For recordings of evoked excitatory postsynaptic currents, the external solution was modified by lowering MgCl₂ concentration to 0.5 mM, whereas internal solution contained K-gluconate 130, NaCl 5, CaCl₂ 1, EGTA 11, HEPES 10, MgCl₂ 1, MgATP₂ 4, and lidocaine N-ethyl bromide 5. pH was adjusted with KOH to 7.25.

Properties of eIPSCs were explored using a paired pulse response (PPR) stimulus protocol. After the determination of the 50% maximum current stimulus, this stimulus was applied within the IC at an interval of 0.01-10 s. GABA_A-mediated currents were isolated in the presence of 50 μM D-APV and 5 μM NBQX, which blocked NMDA and AMPA-mediated excitatory synaptic currents, respectively. The ratio of the maximum amplitude of the first peak to the maximum amplitude of the second was calculated and compared. The time course of eIPSCs decay usually was described using a single exponential function. In some cells, decay of eIPSCs was better described using a double exponential function, in which case a weighted average for our analyses was used. In each group, rat pup recordings were from at least 3 different litters.

Spontaneous synaptic currents Regarding spontaneous synaptic currents, recordings in patch clamp configuration were made from nRT neurons within live horizontal rat brain sections from P11-23 rats. Miniature excitatory postsynaptic currents (mEPSCs) were isolated from nRT neurons utilizing a holding potential of -70 mV in the presence of 1 μM tetrodotoxin (TTX) in order to block voltage-gated sodium channels and 20 μM picrotoxin in order to block γ-aminobutyric acid (GABA) inhibitory currents. In experiments measuring miniature inhibitory postsynaptic currents (mIPSCs), GABA_A-mediated currents were isolated in the presence of the N-methyl-D-Aspartate (NMDA) channel antagonist 50 μM D-APV and the α-Amino-3-hydroxy-5-methyl-4-

isoxazolepropionic acid (AMPA) channel antagonist 5 μ M NBQX. All data were analyzed using MiniAnalysis software (Synaptasoft). The limits for mEPSCs and mIPSCs were set in most of recordings at three times the root mean square of baseline noise. All events selected by the detection criteria were verified by eye and only included in the analysis if they displayed decay kinetics consistent with previously characterized nRT neuron mIPSC and mEPSC events (Browne et al., 2001, Zhang et al., 2009) In our analysis of kinetics of spontaneous synaptic currents only isolated (i.e. non-overlapping) events were included. All spontaneous inhibitory currents (mIPSCs) were analyzed with respect to peak amplitude and 10-90% rise time and fastest events (rise times < 3 ms) were chosen for further analysis of decay time course and half-width. The decay time course of these experiments was fit utilizing a single exponential function.

Cumulative distribution functions Cumulative Distribution Functions: plots describing the cumulative distribution functions (CDFs) of mEPSC and mIPSC properties [i.e. amplitude, inter-event interval (IEI) and half-width] were empirically-derived using custom scripts written in Matlab (Mathworks, Natick MA). In brief, the CDF describes the probability that an event amplitude (or IEI, half-width) will be found that is less than or equal to that event. CDFs were derived for individual neurons, and data pooled from all neurons.

C. Results

1. Plasticity of inhibitory synaptic transmission in the rat thalamus after a single exposure to GA

Stimulation of fibers in close proximity to the IC (approximately 200 μ m from the patched nRT neurons) evokes picrotoxin-sensitive GABA_A-mediated eIPSCs as previously described (Joksovic et al., 2009). Figure 11 (panel A on the left) shows an average of 20 traces of eIPSCs in the population of nRT neurons from the control group (black trace) and an average of 22 traces of eIPSCs in the

population of nRT neurons from the group exposed to GA (gray trace). eIPSCs from GA-exposed animals showed about a 50% decrease in peak amplitudes (average $48 \pm 10\%$, $p < 0.001$, t-test) as compared with those from the Sham group. Normalized traces depicted in the right panel of figure 11A and the bar graphs in figure 11B show that the decay τ for eIPSCs in GA-treated pups (■, 86 ± 5 ms) was significantly decreased as compared with that from Sham-treated animals (■, 115 ± 13 ms, $p = 0.001$, LMM). It was also found that stimulus-output curves (I-O curves) after exposure to GA (■) were significantly ($p < 0.001$, LMM) reduced to about 40-60% of curves from the Sham group (○) across most stimulus intensities (figure 11C).

Next, the mechanisms of synaptic plasticity were investigated using paired-pulse analysis. In nRT neurons, stimulation with a paired-pulse stimulus interval of 1 second usually results in depression of the second (test) IPSC as compared with the first (conditioning) IPSC (Joksovic *et al.*, 2009). This depression of PPR of test IPSCs relative to conditioning IPSCs has been proposed to be due to depletion of a fraction of readily available synaptic vesicles by the conditioning pulse (Zucker and Regehr, 2002). Representative traces from paired-pulse experiments in nRT neurons from the Sham- (black trace) and GA-treated rats (gray trace) are depicted in figure 11D. In summary, the bar graphs in Figure 11E show that the average PPR was decreased significantly in the GA group (■, 0.77 ± 0.03) as compared with that from the Sham group (■, 0.90 ± 0.03 , $p < 0.01$, LMM), strongly suggesting involvement of presynaptic mechanisms of synaptic plasticity.

Subsequently, mIPSCs were recorded in order to discern independently any possible presynaptic and postsynaptic effects of GAs on inhibitory synapses. Typically in studies of spontaneous synaptic events, any changes in frequency reflect presynaptic mechanisms while alterations of event amplitudes and/or kinetics reflect postsynaptic mechanisms. Original traces of mIPSCs from representative nRT neurons in Sham (top black trace) and GA (bottom red trace) groups are depicted in panel 12A. Cumulative probabilities of mIPSCs

amplitudes, decay times estimated by measuring half-widths, and frequency measured by IELs from all recordings in the Sham group (black lines) and the GA group (red lines) are depicted in figures 12 panels B-E. In contrast to the effects on eIPSCs, a small but non-significant difference was detected between amplitudes (figure. 12B and 12C) of mIPSCs between the Sham (35.8 ± 4.0 pA) and GA group (29.1 ± 2.8 pA). Similar values for half-width (figure 12D) and frequency (figure 12E) of spontaneous mIPSCs between neurons from the animals in Sham group and the GA group ($p > 0.05$, LMM) were found. There was also a minimal difference in mIPSCs decay τ values between the GA (73 ± 8 msec) and Sham groups (76 ± 10 msec) (data not shown).

2. Plasticity of excitatory synaptic transmission in the rat thalamus after a single exposure to GA

It was observed that in most of the nRT neurons, eEPSCs consisted of two components based on different decay τ s; the faster decaying component of eEPSCs was blocked completely by 5 μ M NBQX, an AMPA receptor antagonist, whereas the slower decaying component of eEPSCs was completely blocked by 50 μ M D-APV, an NMDA receptor antagonist (figure 13A). Neurons from the nRT were then challenged with 50 μ M D-APV, and the isolated eEPSCs amplitudes between the Sham group (\square) and the GA group (\blacksquare) were compared in Fig. 13B. The apparent difference between the Sham group (648 ± 90 pA) and the GA group (1094 ± 226 pA) in the maximal amplitude of eEPSCs did not reach significance, as assessed with LMM ($p > 0.05$).

However, when the D-APV-insensitive components were compared, the GA group amplitudes (536 ± 83 pA) were increased approximately two-fold, as compared with Sham (295 ± 71 pA, $p < 0.05$, LMM). In contrast, the amplitudes of D-APV-sensitive components in the GA group (550 ± 182 pA) were not significantly different from those in the Sham group (381 ± 126 pA, $p > 0.05$,

LMM). Regarding PPR, a slight difference was observed for the D-APV-insensitive eEPSC component between the Sham group (0.73 ± 0.06) and the GA group (0.81 ± 0.05 , $p > 0.05$, data not shown). Therefore in conclusion the AMPA component of eEPSCs is increased in GA-exposed rats, while the NMDA component is seemingly preserved.

In order to further study the potential mechanisms for GA-induced plasticity of excitatory synaptic transmission mEPSCs properties were determined (figure 14). Panel 14A shows representative original traces from the nRT neurons in the Sham group (top black trace) and the GA group (bottom red trace). Cumulative probabilities of mEPSCs amplitudes, decay times estimated by measuring half-widths, and frequency measured by IELs from all recordings in the Sham group (black lines) and the GA group (red lines) are depicted in figure 14 panels B-E. Regarding mEPSCs, the average amplitudes of events were significantly increased in the GA (14.1 ± 2.2 pA), as compared with the Sham group (9.5 ± 1.2 pA, $p < 0.05$ LMM; figure 14B). However, when the half-width durations were analyzed it was shown that this parameter, related to postsynaptic properties, was similar for both groups (Fig. 14D). Regarding presynaptic properties, it was observed that the GA group had a higher mean mEPSCs frequency (9.5 ± 2.5 Hz) as compared to the Sham group (3.6 ± 1.5 Hz), nonetheless this effect was of borderline significance (Table 1; figure 14E). Overall, our data with mEPSCs independently confirms that the GA-induced increase in AMPA-mediated excitatory synaptic transmission is mostly mediated by postsynaptic mechanisms.

3. T-channels modulate nRT neuron excitatory synapse properties

The modulatory effects that T-channels have upon excitatory nRT neuron synapses are poorly understood. Here, it is shown, that the specific T-channel antagonist B 260 modulates both pre and post synaptic properties of excitatory nRT synapses. Figure 15 panel A depicts representative traces showing control

and the response after application of 3 μ M B 260. Regarding presynaptic properties, application of 3 μ M B 260 during experiments sampling mEPSC events resulted in a significant decrease in average mEPSC frequency (figure 15B). Analysis of post synaptic properties revealed that there was also a decrease in the average amplitude after the application of B 260 (figure 15C). In panel D, a significant decrease in charge transfer was observed as well. However, in panel E, application of B 260 had no effects upon mEPSC decay properties. There were no significant differences in mEPSC half widths post B 260 application (data not shown). Although there is a robust characterization of T-channel mediated burst action potential formation, the functional contribution of T-channels to post and pre synaptic properties of excitatory nRT synapses is just beginning to be understood. Alterations in nRT neuron excitatory synaptic drive can readily influence both sleep and wake states and faithful transmission of somatosensory information.

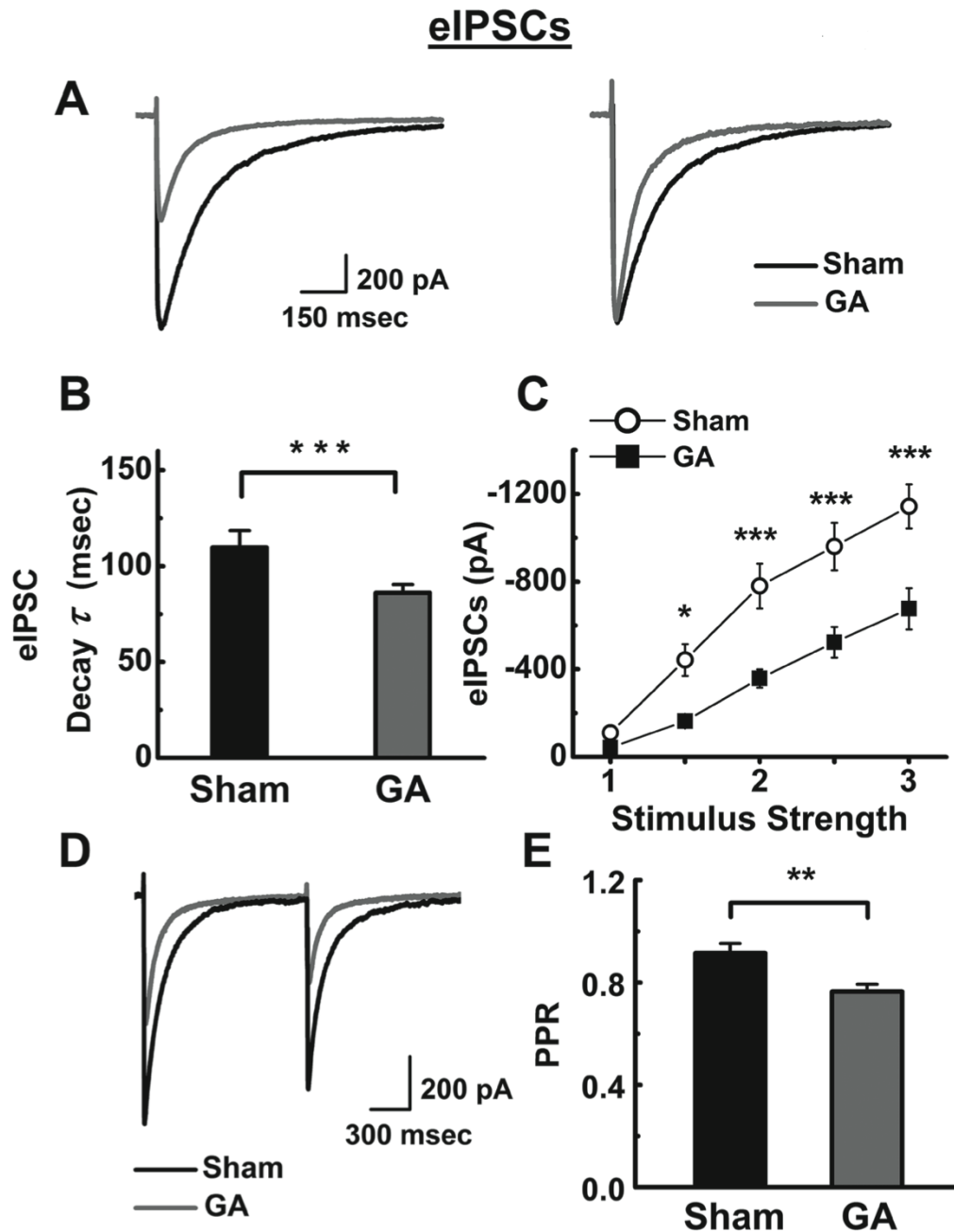


Figure 11. Alterations in eIPSCs of nRT neurons mediated by GA exposure. **A:** Left panel depicts averaged traces from nRT neurons from the Sham group (black trace) and the GA-exposed group (gray trace). The right panel shows the same traces of eIPSCs as in panel A that are scaled for easier comparison. Note faster decay of current in the GA group. **B:** Decay time constants are decreased in the GA ($n = 13$ rats, 45 neurons) versus the Sham ($n = 23$ rats, 63 neurons) group ($p < 0.001$, LMM). **C:** The averaged data of I-O curves show decreased synaptic strength of eIPSCs in the GA group (\blacksquare , $n = 12$ rats, 41 neurons) versus the Sham group (\circ , $n = 15$ rats, 52 neurons; *, $p < 0.05$; ***, $p < 0.001$ Two-way ANOVA). We first determined threshold stimulus (denoted as 1) in each experiment, then we used progressively stronger stimuli 1.5-, 2-, 2.5-, and 3-fold higher than the threshold stimulus. **D:** Averaged traces of paired-pulse stimulus protocol separated by 1 sec show eIPSCs in Sham group (black trace) and GA group (gray trace). **E:** Bar graph shows that in GA-treated animals ($n = 13$ rats, 37 neurons), the average PPR ratio is significantly decreased as compared with that in Sham-treated animals ($n = 19$ rats, 56 neurons) (**, $p < 0.01$, LMM). All symbols on panels B, C and E of this figure indicate mean values by animal and vertical lines are SEM.

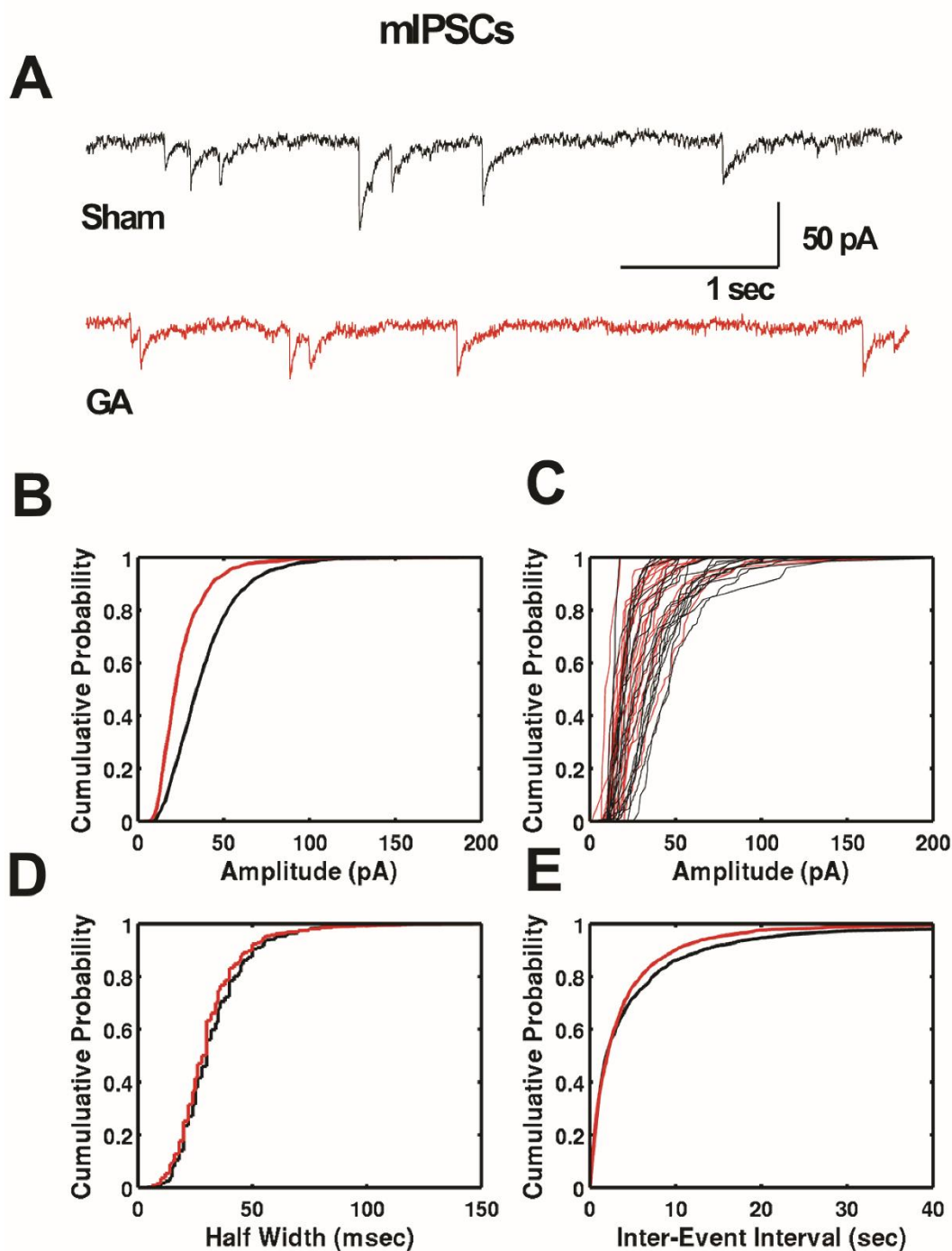


Figure 12. Effects of GA exposure on mIPSCs of nRT neurons. **A:** Sample of original mIPSC traces from Sham- (black) and GA-treated (red) nRT neurons. **B-E:** Plots describing CDFs of isolated mIPSC events in the Sham group ($n = 1971$ events) and the GA group ($n = 1659$ events) demonstrate very little change in the amplitude (B-C), kinetics (D) and frequency (E) of events. Solid lines on graphs B, D and E represent averages of all events for Sham (black lines) and GA (red lines) groups. Panel C depicts CDFs for the amplitudes of mIPSCs in all nRT neurons used for this analyses in Sham (black lines, $n = 21$ neurons) and GA (red lines, $n = 21$ neurons) groups. All data presented in this figure were obtained from 10 GA-treated animals and 7 Sham-treated animals.

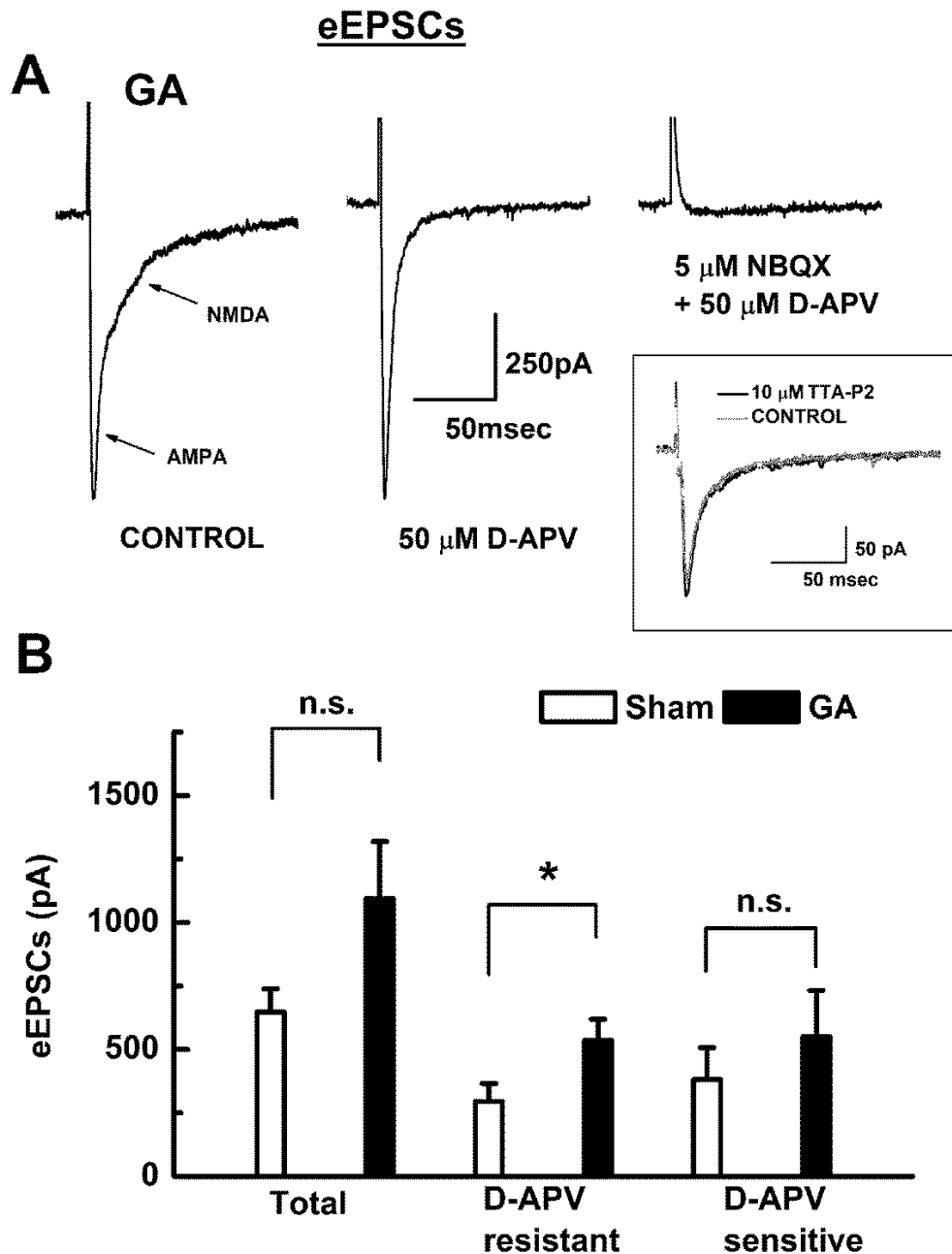


Figure 13. GA exposure increases the AMPA component of nRT neuron eEPSCs. **A:** Progressive eEPSC current blockade in a representative nRT neuron from the GA-treated group. Bath application of 50 μ M D-APV blocks the slower component of eEPSCs and isolates AMPA currents. A subsequent application of 5 μ M NBQX induced almost complete blockade of the remaining current. Inset, traces from a representative neuron from the GA group in the control condition (gray trace) and after addition of 10 μ M TTA-P2 for 10 min (black trace). **B:** Bar graphs of average values show that there is no significant difference between the total eEPSC amplitudes in GA (■, $n = 7$ rats, 18 neurons) and Sham (□, $n = 5$ rats, 17 neurons) groups. However, pharmacological isolation AMPA currents by blockade of NMDA with 50 μ M D-APV reveals a significant increase in D-APV-resistant (AMPA component) current amplitudes (* $p < 0.05$, LMM) while the D-APV-sensitive component of eEPSCs in nRT neurons is similar in both groups. All bar graphs on panels of this figure indicate mean values from multiple animals and vertical lines are SEM.

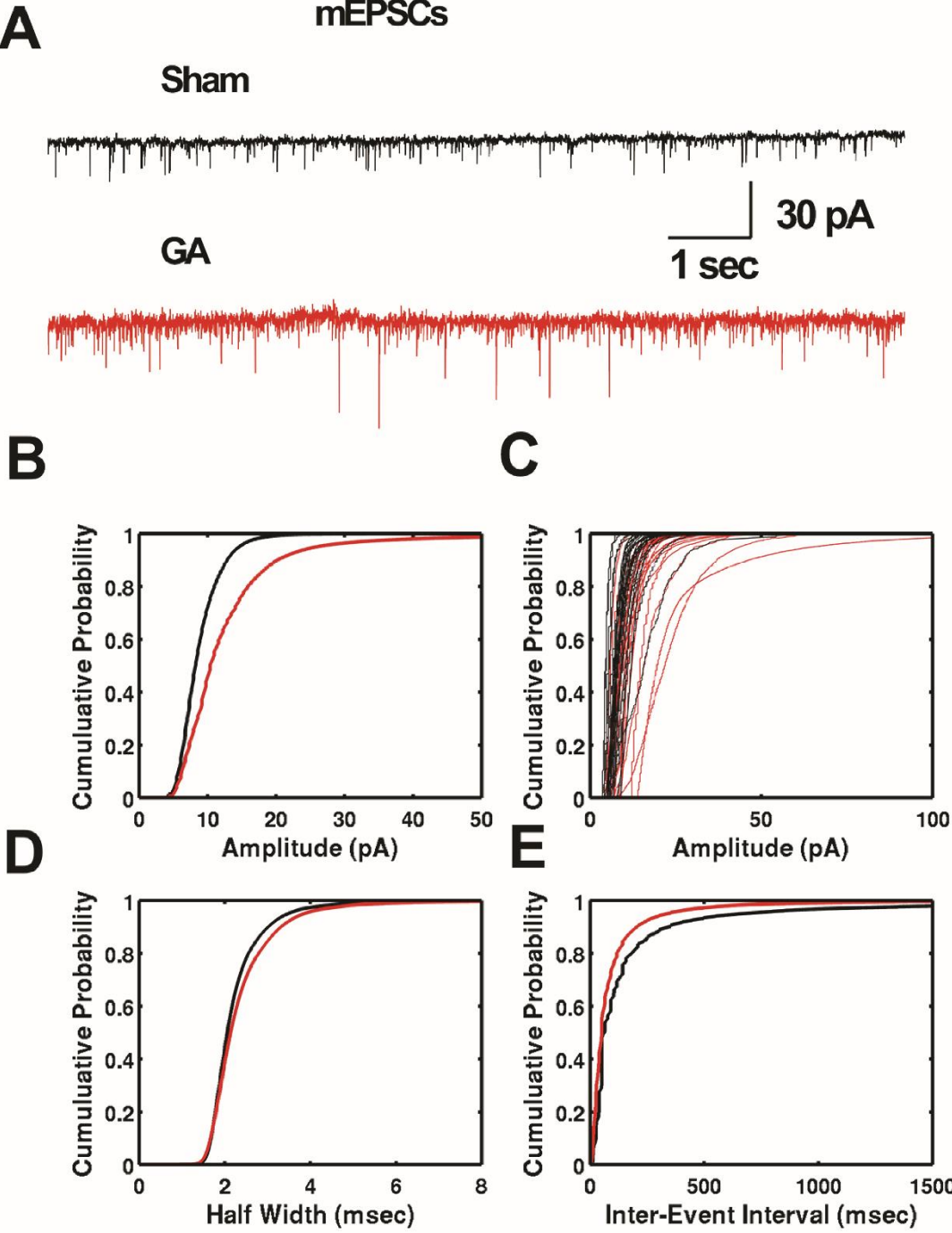


Figure 14. GA exposure alters nRT neuron mEPSC properties. **A:** Sample of original mEPSC traces from Sham- (black) and GA-treated (red) nRT neurons. **B-E:** Plots describing CDFs of isolated mEPSC events in the Sham group (n = 78,987 events) and the GA group (n=154,951 events) demonstrate a significant ($p < 0.05$, LMM) increase in the amplitude (B-C) and no significant change ($p > 0.05$, LMM) in kinetics (D) and frequency (E) of events. Solid lines on graphs B, D and E represent averages of all events for the Sham (black lines) and GA (red lines) groups. Panel C depicts CDFs for the amplitudes of mEPSCs in all nRT neurons used for this analyses in Sham (black lines, n = 29 neurons) and GA (red lines, n = 24 neurons) groups. All data presented were obtained from 8 GA-treated animals and 8 Sham-treated animals.

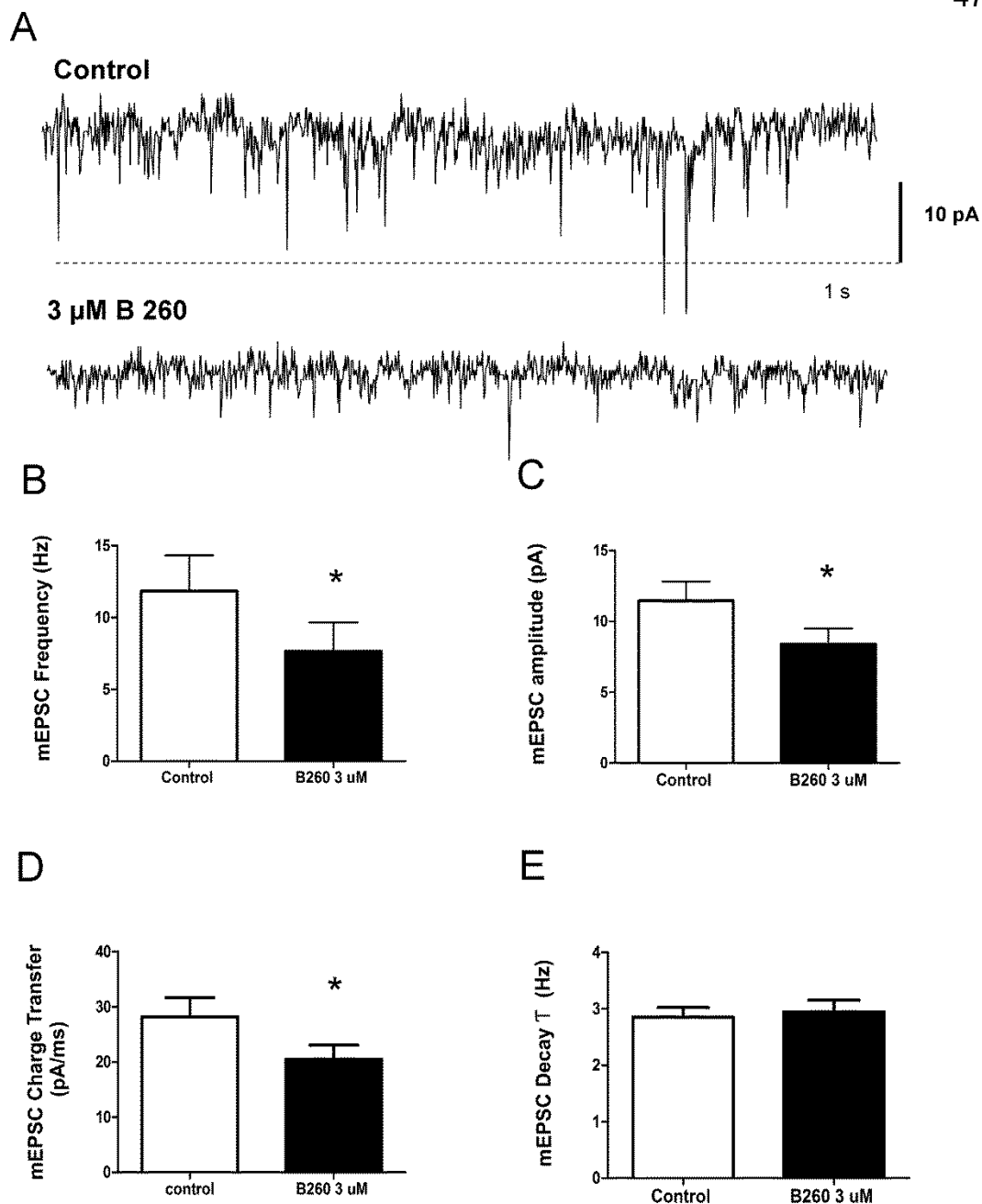


Figure 15. B 260 decreases both mEPSC amplitude and frequency. **A:** Representative traces from control, top trace, and after application of 3 μ M B 260, bottom trace. **B:** B 260 decreases average mEPSC amplitudes: 11.4 ± 1.3 pA for control vs. 8.4 ± 1.1 pA after B 260 bath application (\pm SEM n=6 rats and 6 neurons for both groups, * $p < 0.05$ repeated measures T-test). **C:** Bath application of B 260 reduces mEPSC average frequency: 11.8 ± 2.5 Hz for control vs. 7.6 ± 2.0 Hz after B 260 treatment (\pm SEM n=6 rats and 6 neurons for both groups, * $p < 0.05$ repeated measures T-test). **D:** Charge transfer is also decreased after B260 application: 28.2 ± 3.5 pA/ms for control vs. 20.5 ± 2.6 pA/ms for B 260 treated (\pm SEM n=6 rats and 6 neurons for both groups, * $p < 0.05$ repeated measures T-test). **E** There is no difference in mEPSC decay properties after application of B 260.

E. Discussion

Combined, this data suggests that early exposure to GAs causes alterations in the balance between excitatory glutamate and inhibitory GABA synapse drive. Alterations in glutamate receptor function and/or glutamate release may very well lead to alterations in neuronal activity within the nRT. A greater excitatory synaptic drive, or EPSP, stemming from either projections from the Ctx or VB thalamus, may set the tone for increased inhibitory potentials from already intrinsically hyperexcitable nRT neurons (see section II). This in turn may lead to more robust depolarizations within VB neurons that in turn may lead to more robust action potential burst firing. Coupled with possibly decreased intra nRT inhibitory tone may lead to a greater propensity for increased nRT neuron firing upon VB neurons that lead to stronger iterations of burst firing cycles owing to a weaker ability to self-inhibit. The greater propensity for burst iterations may lead to a greater propensity towards oscillations. This increased oscillation propensity may manifest in behavior as alterations in sleep cycles, alterations in somatosensory perception and possible absence seizure (see section IV). Decreased I-O curves indicate that axonal recruitment is diminished in nRT neurons from GA-treated rats. It also is possible that GAs decrease spillover inhibitory transmission via presynaptic mechanisms as suggested by alterations in PPR of eIPSCs. Alterations in the PPR may be facilitated by a change in the probability of transmitter release from presynaptic terminals. Typically, presynaptic depressants will cause a smaller fraction of vesicles to be released, thus decreasing the PPR. If a fraction of the vesicle pool is eliminated from availability the PPR should remain unchanged. If the amplitudes and/or decay τ s of evoked synaptic currents are altered, postsynaptic sites may be affected. Strong synaptic stimulation and resulting multiquantal vesicular release may result in recruitment of many synaptic and extra-synaptic GABA_A receptors in nRT neurons. This, in turn, may generate a slow tail (decay) of the eIPSCs.

Thus, any decrease in action potential-dependent presynaptic release of GABA may diminish probability of spillover and consequently decrease eIPSCs decay τ in the postsynaptic membrane while mIPSCs would not be affected. This possibility is supported by our previous finding showing that decreasing extracellular $[Ca^{2+}]$ in healthy rats decreases amplitudes of eIPSCs and decreases decay τ in nRT neurons, effectively mimicking effects of exposure to GAs (Joksovic et al., 2009). However, inhibitory spillover transmission in the thalamus is well documented in TC relay neurons with slowly decaying eIPSCs τ s attributed to the expression of δ -subunits of extra-synaptic GABA_A receptors (Herd et al., 2013). It remains to be determined in future investigations if similar mechanisms may operate in nRT neurons as well.

Our data with eEPSCs in Sham animals are different from those of one other study, which showed a smaller NMDA component of eEPSCs in nRT neurons from healthy rats (Gentet and Ulrich, 2004). Some possibilities include lower concentrations of $MgCl_2$ in external solution in our study (0.5 mM vs. 1 mM), different strains of animals, (our study used Sprague Dawley rats, whereas the cited study used Wistar rats); different temperature of recordings (our study was done at room temperature; the other was done at 34-36^o C); and/or different stimulation protocols (our study used internal capsule stimulation; the other used local stimulation of layer VI cortical neurons by application of K^+).

Both human and animal studies have pointed to the potential role of GABA_A receptor dysfunction and/or hyperactivity of thalamic T-channels in absence seizures (reviewed in Beenhakker and Huguenard, 2009; Crunelli *et al.*, 2012). It is of particular interest for this study that intra-nRT connections mediated by long-lasting eIPSCs are critical for regulating inhibitory output and phasic bursting activity. Thus, during thalamocortical oscillations, GABA_A-mediated inhibition of nRT neurons may prevent the pathological hypersynchrony of absence epilepsy, although intracortical mechanisms also may contribute (Steriade *et al.*, 1990). Based on our findings that exposure of young rats to common GAs caused lasting loss of inhibitory function of nRT, as well as up-

regulation of T-currents and AMPA-mediated excitatory transmission, it is reasonable to conclude that these animals may display increased propensity for absence seizures. Indeed our experiments with *in vivo* measurements of GBL-induced SWD strongly support this idea (section IV). Exposure to GA modulates both postsynaptic and presynaptic mechanisms in inhibitory synapses within nRT. It is important to note that a decrease in inhibitory PPR of eIPSCs is consistent for what is observed in GAERS rats which display spontaneous absence seizure (Bessaïh et al, 2004).

It is possible that other variables during exposure to GAs may contribute to the plasticity of synaptic transmission (e.g. hypoxia, hypoglycemia). However, alterations in these variables are extremely unlikely to explain the plasticity given that extensive previous studies have not demonstrated such events using exactly the same protocols (Jevtovic et al., 2003; Lu et al., 2006; Rizzi et al., 2008; Loepke et al., 2009).

In order to understand GA mediated alterations in cortex and thalamus circuits it is necessary to pinpoint where possible alterations in activity balance occur. Thus it may be necessary to separate thalamus to cortex and cortex to thalamus projections and to study neuronal excitability within these circuits in order to understand where and how excitatory and inhibitory imbalances occur. A selective stimulation of CT or TC axons is impossible with electrical stimulation. However, this difficulty can be overcome by expressing channelrhodopsin-2 (ChR2), a light-sensitive cation channel, in either CT or TC neurons. ChR2 expression enables somata and axons to be activated by blue light with a high temporal precision. Injection of virus based ChR2 into the VB allows for the selective study of TC projections whereas injection into the somatosensory cortex allows for the selective study CT projections.

The VB thalamus is functionally connected to the somatosensory cortex (Cruikshank et al. 2010, Bernardo et al. 1987, Agmon et al., 1993, Pinault et al., 1995). Injection into VB thalamus with a virus carrying a transgene encoding a ChR2-enhanced yellow fluorescent protein (EYFP) fusion protein driven by the

Camk2a promoter (Dittgen et al., 2004) should lead to intense ChR2-EYFP expression (Cruikshank et al. 2010) in TC relay nuclei and their projections in nRT. In contrast, injection of a ChR2- EYFP virus into the deep layers of the somatosensory cortex will lead to EYFP labeling and ChR2 expression within the injection site, the deep layers of the cortex and the axons projecting to the nRT (Paz et al., 2011). Action potentials can be evoked by a blue laser aimed at the area of interest and recorded within the VB and nRT. Evoked action potential frequencies in burst and tonic firing modes could also be characterized as well. Laser evoked excitatory post synaptic current amplitude and frequency could also be measured. In conclusion, in order to fully understand the effects of GA upon excitatory nRT neuron synaptic plasticity, it is necessary to separate thalamic excitatory inputs from cortical using optogenetics.

Regarding the synaptic roles of T-channels, in the spinal cord, pharmacological antagonism of T-channels inhibited spontaneous synaptic release of glutamate in the dorsal neurons, while GABA release was unaffected (Jacus et al., 2012). Within the nRT, both pre and post synaptic properties of mEPSCs are affected during T-channel blockade. In summary, during nRT neuron T-channel blockade the presynaptic property of frequency was observed with a concomitant decrease in the post synaptic properties of amplitude and charge transfer. Thus, it is reasonable to envision that T-channels may regulate both neurotransmitter release and nRT neuron synapse plasticity. Regarding T-channels and neurotransmitter release, Cav 3.2 channels have been shown to interact with synaptic vesicle proteins such as syntaxin 1A and SNAP-25, suggesting that T-channels may regulate secretory vesicles at more hyperpolarized membrane potentials (Weiss et al., 2011). Cav 3.3 channels that are critical for burst LTCS AP firing, are present within dendrites and are also implicated in dendritic $[Ca^{2+}]_i$ increases (Cueni., et al 2008; Astori et al., 2013). NMDA receptors expressed throughout the thalamus (Gentet and Ulrich 2003, 2004) contribute to synaptic plasticity in a Ca^{2+} influx regulated manner. While the interplay between T type calcium channels and NMDA receptors has been

explored in the spinal cord dorsal horn (Ikeda et al., 2003), this concept has only been recently explored in nRT neuron synapses. In mice lacking Cav 3.3 channels, LTP within the nRT was severely diminished (Astori et al., 2013). However, further study is needed in order to determine the mechanism of T-channel mediated reduction of NMDA mediated synaptic plasticity. Moreover, this may also be extended into the realm regarding what effects T-channel antagonism may have upon AMPA receptor function. It also remains to be determined what role T-channels may play in dendritic Ca²⁺ influx and how this may affect synaptic plasticity. In order to further validate these studies, a highly specific T-channel antagonist, such as TTA-P2, may be utilized.

IV. Early exposure to GA alters thalamocortical EEG

A. Introduction

Alterations in thalamic oscillatory networks drive seizure activity in absence epilepsy (Paz et al. 2011, Zaman et al. 2011, Bessaïh T et al. 2006). Characteristic oscillatory activity of inter-connected, nRT, TC and Ctx neurons may underlay many physiological and pathological processes, including absence epilepsy. Typical absence seizures of idiopathic generalized epilepsies occur in childhood or adolescence and are characterized by brief loss of consciousness and EEG with SWDs (Panayiotopoulos 2008). In rodents, absence seizure-like activity may manifest in behaviors such as behavioral arrest, facial myoclonis and vibrissal twitching (Snead et al. 1993).

Electrophysiology studies of nRT neurons demonstrate states of hyperexcitable nRT neurons (see section I). Ionic mediators of neuronal excitability are also altered by early GA exposure (e.g. T-channel current densities are found to be increased along with depolarizing shift in gating properties). Pre and post synaptic nRT neuron properties are altered as well. Evoked GABA vesicular release is diminished, whereas excitatory post synaptic AMPA currents are increased (see section III). The roles of GABA_A (Beenhakker and Huguenard, 2009), AMPA (Lacey et al., 2012; Beyer et al., 2008) and T-channels (Khosravani and Zamponi, 2006) in absence seizures are well established. Typical absence seizures are characterized by a brief loss of consciousness and the appearance of 3-5 Hz SWDs in the EEG that result from paroxysmal and synchronized firing in thalamic and cortical networks.

Our findings of decreased eIPSCs amplitudes in nRT neurons from GA-treated rats are similar to those from a genetic rat model of absence seizures (Bessaïh et al., 2006). Hence, hyperexcitability of nRT neurons resulting from plasticity of AMPA, GABA_A and T-channels in concert could increase the

propensity for absence seizures in GA-treated rats. It may be safe to assume that GA exposure alters the balance of inhibitory and excitatory synapse drive towards a state that may promote an increased propensity of thalamocortical networks to oscillate within a low frequency range. When coupled with nRT neurons that are inherently hyperexcitable, the observed increase in excitatory synaptic tone may drive the thalamocortical networks to favor lower frequency EEG patterns.

The current hypothesis regarding absence seizure genesis is in due in part to the increased activity of nRT neurons (Crunelli et al. 2002) although intracortical mechanisms may also contribute (Steriade et al., 1990, 1994). Early GA-exposed rats were assessed for absence seizure-like activity such as appearance of 3-5 Hz SWDs in the EEG that results from paroxysmal firing in thalamic and cortical networks. Pharmacologically induced seizures in P20 and older GA and Sham treated rats was studied using γ -butyrolactone (GBL). This compound is known to induce behaviors and EEG patterns consistent with absence seizure (Snead et al., 1991). In mammals, GBL produces behaviors and EEG patterns reminiscent of absence seizures (Snead et al. 1991, Zaman et al. 2011). It is well established that systemic administration of T-channel blockers in animals and humans can correct excessive excitability of thalamocortical networks and consequently will abolish GBL-induced SWDs and absence seizures (Beenhakker and Huguenard, 2009). Thus, T-channel blockade may reverse chronic hyperexcitability of nRT neurons, which, in turn, may diminish hyperexcitability of intact thalamocortical circuits in vivo, as determined by the intensity of GBL-induced SWDs. To address this issue, TTA-P2, a recently discovered selective and potent antagonist of T-channels was utilized (Dreyfus et al. 2010).

T-type calcium channel antagonists have been utilized therapeutically in order to treat absence seizure. Recently, within the peripheral nervous system, this role has been expanded to treat diabetic neuropathies and neuropathic pain (Latham et al., 2009; Messinger et al., 2009). In this section, the novel effects of

a neuroactive steroid and T-channel antagonist B260 are presented. In terms of potential clinical applications, centrally acting neuroactive steroids may be used to ameliorate a variety conditions such as stress and depression (Zorumski et al., 2013). Regarding the mechanism of action, research concerning the development of neuroactive steroids has primarily focused upon steroid analogs designed to modulate GABA_A channels (Lambert et al., 2005). In this section pharmacologically induced absence seizure is explored when a T-channel specific neuroactive steroid B260 is used as a general anesthetic during brain development. Importantly, B260 has no significant direct effect on GABA_A and NMDA receptors.

B. Experimental design

EEG EEG recordings were obtained from the somatosensory cortex with bilateral stainless steel electrodes accompanied by an operational amplifier (Texas Instruments TL2274x) in both GA and Sham rats. Reference electrodes were placed within the cerebellum (Zaman et al., 2011). The following coordinates were utilized to place bilateral somatosensory cortex electrodes: from bregma (mm) - 2.2 rostral caudal, \pm 5.5 medial lateral, 1.5 dorsal ventral.

Operational amplifiers Operational amplifiers were surgically implanted utilizing ISO anesthesia during P19. EEG recordings coupled with video were acquired from P19 to P25. Recordings were obtained utilizing tethered wires coupled to a freely moving commutator. EEG video and signal were analyzed utilizing Harmonie Stellate software and EEG signals were acquired utilizing a Grass instruments signal processor.

Gamma Butyrolactone and TTA-P2 Gamma Butyrolactone (Sigma) was dissolved in sterile saline in stock solutions of 50 mg/ml for 70 mg/kg injections. All injections were given i.p. in a sterile fashion. Animals were then monitored for absence seizure activity such as behavioral arrest with open eyes and vibrissal twitching (Snead., 1991). TTA-P2 (Merck) was dissolved in DMSO at a

concentration of 5 mg/ml for i.p. injection. For electrophysiology experiments, TTA-P2 was initially dissolved at a concentration of 300 mM and subsequently serially diluted in the appropriate electrophysiology external solution. For *in vivo* studies involving the use of TTA-P2, rats were pretreated with an i.p. injection of 5 mg/ml TTA-P2 at a final dose of 5 mg/kg. GBL was first administered at an average time of 2.5 hours post TTA-P2 injection and the resulting EEG was analyzed. A second injection of GBL was administered at a minimum of 4 hours post the first GBL treatment and the resulting GBL mediated EEG response was then characterized.

C. Results

1. Adolescent rats exposed to GAs at age P7 display hyperexcitability of intact thalamocortical networks

In order to study the effects of P7 GA exposure upon thalamocortical circuits *in vivo* EEG recordings in freely moving animals were used in concert with pharmacological activation of thalamocortical circuits by GBL. Figure 16 shows representative traces of original EEG recordings from a rat that received GAs (panel A) and from a rat that received sham anesthesia (panel B). The top trace in each panel (line a) shows baseline awake EEG activity characterized by a mixture of low frequency and high frequency waveforms. In contrast, middle traces in lines b-d and the traces on expanded time scale (panels 1 and 2) show periods of characteristic high amplitude 3-5 Hz activity consistent with GBL-induced SWDs. Bottom lines (line e) show final SWD events and return of EEG to the awake patterns. The time course of SWD events is summarized in figure 16C and shows that administration of GBL to GA-treated (●, n=6 rats) and sham-treated (□, n=6 rats) animals induced typical paroxysmal SWDs in both groups with an increase in the duration of SWDs in the GA group during each 1 minute-segment ($p < 0.05$, LMM), with the most robust effect being observed during

minutes seven through eleven. The total duration of SWD events was 30 minutes after GBL injections in the GA group and only 18 minutes in Sham group. Figure 16D demonstrates that latency to onset of first SWDs after GBL injections was not statistically different between the two groups (Sham: 97 ± 17 sec; GA: 101 ± 24 sec, $n=6$, $p>0.05$, t-test). On the other hand, the cumulative SWD duration over all events during the 30 min observation period was significantly increased in GA-treated group by about 40% (figure 16E; Sham: 733 ± 86 sec; GA: 1267 ± 143 sec, $n = 6$, $p<0.01$, t-test).

2. Selective antagonism of T-channels reversed hyperexcitability of nRT neurons in vitro and diminished cumulative duration of SWD in GA-treated rats in vivo

It has been shown previously that TTA-P2 blocks T-currents and LTCs with very little effect on tonic firing mode in nRT and TC neurons in brain slices from healthy rats (Dreyfus et al., 2010). However, its effects on T-currents and two firing modes in nRT neurons in vitro and on SWD *in vivo* from GA-treated rats warranted investigation. First, the ability of TTA-P2 to influence *in vitro* action potential firing of nRT neurons in thalamic slices from the GA-treated group, using the same protocol as in figure 17 was tested. Original traces in figure 17A depict AP tonic firing (left traces) and burst firing (right traces) in a representative nRT neuron from the GA group before (top trace) and 1-5 minutes after addition of $10 \mu\text{M}$ TTA-P2 to the external solution (left black bar indicates time course of events). Dotted lines on this graph indicate original RMP of -60 mV. After application of TTA-P2 the baseline RMP was hyperpolarized by about 8 mV, during tonic firing mode the number of APs was progressively decreased from 14 to 10, and finally, in burst firing mode, TTA-P2 completely inhibited AP firing after 5 minutes of incubation. Burst firing in two other nRT neurons was also abolished, whereas only partial inhibition was observed in another five neurons (data not shown). Bar graphs in figure 17B show that on average, TTA-P2 decreased tonic firing frequency in the GA-treated neurons by $24 \pm 9\%$ (■, $n = 11$

neurons, $p < 0.05$, paired t-test). Figure 17B also indicates that TTA-P2 decreased the frequency of rebound burst firing (\square) by about $70 \pm 10\%$ as compared with the baseline predrug values ($n = 7$ neurons, $p < 0.001$, paired t-test). In the same nRT neurons, TTA-P2 significantly hyperpolarized RMP from a control of -55 ± 2 mV to -58 ± 2 mV ($p < 0.01$, paired t-test) without significantly affecting R_{in} (data not shown). It was also found that $10 \mu\text{M}$ TTA-P2 after 10 minutes of incubation within the external bath solution did not significantly affect the decay or amplitude of eEPSCs in nRT neurons from GA-treated rats ($6 \pm 14\%$ change $n=3$ $p > 0.05$, data not shown).

The small hyperpolarizing effect of TTA-P2 is likely consistent with the effect of TTA-P2 on baseline T-type “window” current, which represents a small number of channels that are available for activation at physiological membrane potentials (Dreyfus et al., 2010). In contrast to a previous study by Dreyfus and colleagues (2010) which found complete inhibition of burst firing with TTA-P2 in healthy rats, only partial inhibition of burst firing with TTA-P2 in GA-treated rats was found. This could be related to the slow on/off kinetics of TTA-P2 blockade of T-channels in GA-treated animals, slow diffusion of drug through the slice tissues, and/or shorter drug applications in our study. Inhibitory effects of TTA-P2 on the tonic firing mode in our study but not in healthy rats (Dreyfus et al., 2010) could be related to our findings of up-regulated T-currents in nRT neurons from GA-treated rats (section II). Towards this end, TTA-P2 strongly inhibited APs in the beginning of depolarizing pulse when T-channels are still operational, while the later part of the tonic firing mode was minimally affected (figure 17A). Furthermore, TTA-P2-induced hyperpolarization of membrane potential could have also contributed to the reduced frequency APs in tonic firing mode.

Based on the ability of TTA-P2 to reduce nRT frequency of AP firing in vitro, it was reasoned that i.p. injections of 5 mg/kg TTA-P2 may lead to reduced nRT activity in thalamocortical circuits of GA-treated rats and diminished responses to GBL in vivo, as measured by EEG. Indeed, this expectation was confirmed in representative EEG traces as shown in Fig. 17C, which reveals

diminished SWD discharges following injections of 5 mg/kg of TTA-P2 prior to administration of 70 mg/kg GBL i.p. in a rat exposed to GA at P7 (traces a-c). In the same animal, the same GBL injection was repeated 5 hours later and an increased cumulative duration of SWDs was found (traces d-e). Black short arrows on Fig. 17C indicate initial SWD events and black long arrows indicate final SWD events after GBL injections. With a pretreatment of TTA-P2, the overall cumulative duration of the GBL response was decreased by $24 \pm 5\%$ on average ($n = 6$ rats, $p < 0.01$, paired t-test), as depicted in the bar graph in figure 17D.

3. B-260, a neuroactive steroid and selective T-channel antagonist with anesthetic properties, spares thalamocortical hyperactivity when used during brain development

In order to assess if T-channel mediated anesthesia causes thalamocortical hyperactivity, P7 rats were exposed to 6 hours of B260 anesthesia and thalamocortical activity was measured using GBL. Figure 18 shows representative traces of original EEG recordings from a rat that received GAs (panel A) and from a rat that received sham anesthesia (panel B) and B260 (panel C). The top trace in each panel (line a) shows baseline awake EEG activity characterized by a mixture of low frequency and high frequency waveforms. In contrast, middle traces in lines b-d and the traces on expanded time scale (panels 1-3) show periods of characteristic high amplitude 3-5 Hz activity consistent with GBL-induced SWDs. Bottom lines (line e) show final SWD events and return of EEG to the awake patterns. The time course of SWD events is summarized in figure 18D and shows that administration of GBL to GA-treated (\bullet , $n=6$ rats), sham-treated (\square , $n=6$ rats) and B260 treated rats (Δ , $n=2$ rats) animals induced typical paroxysmal SWDs in both groups with an increase in the duration of SWDs in the GA group during each 1 minute-segment with the most robust effect being observed during minutes seven through eleven. The total

duration of SWD events was 30 minutes after GBL injections in the GA group and only 18 minutes in Sham group. The latency of onset for GBL was increased in the B260 treated group as compared to Sham and GA: 210.5 ± 4.5 ms for the B260 group vs. 97.3 ± 17.0 and 101.7 ± 24.0 for Sham and GA respectively. Cumulative SWD duration over all events during the 30 min observation period was significantly increased in GA-treated group by about 40% (figure 18E; Sham: 733 ± 86 sec; GA: 1267 ± 143 sec, $n = 6$, $p < 0.01$, t-test) whereas the B260 treated group was similar to that of Sham 644 ± 44 ms ($n = 2$ rats).

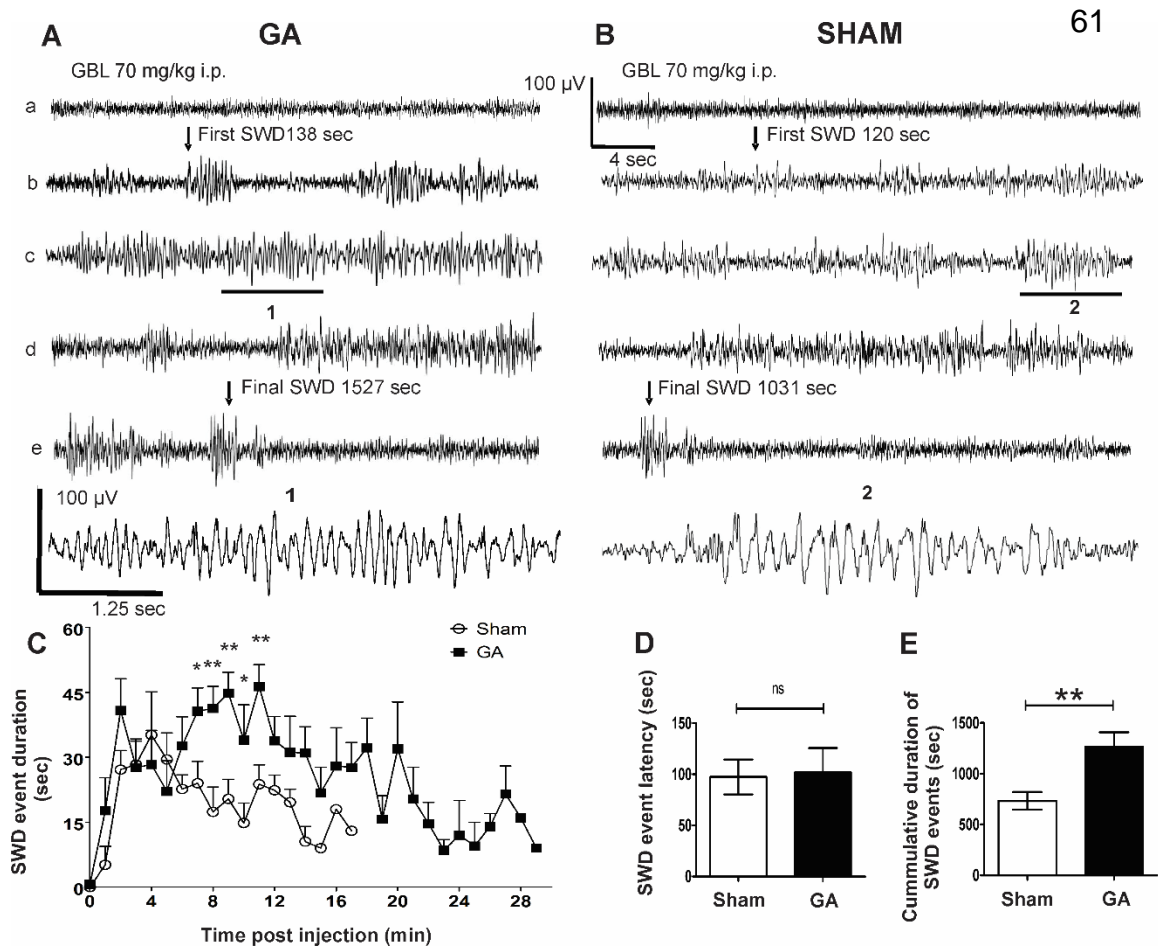


Figure 16. Rats exposed to GA at P7 display increased intensity of SWDs on EEG recordings *in vivo*. **A-B:** Original EEG recordings *in vivo* from a GA-treated rat (panel A) and a sham-treated rat (panel B). Lines a-e show progressive nonconsecutive EEG recordings following injections of 70 mg/kg i.p. GBL. Arrows indicate times of first and final SWD events following injections of GBL. Numbers next to the arrows indicate elapsed time (in seconds) from GBL injections. Calibration bars pertain to both panels. 1: The same segment of GA-treated GBL-induced SWD as labeled with a black horizontal bar in panel A is shown on an expanded time scale. 2: The same segment of sham-treated GBL-induced SWD as labeled with a black horizontal bar in panel B is shown on an expanded time scale. Black square bars indicate calibration that pertains to both panels 1 and 2. **C:** The graph shows an average time course of total SWD event duration per 1-min interval in GA- (●) and sham-treated (□) groups. There is a significant overall increase in SWD event duration per minute for the GA treated group. (n=6 rats GA and Sham, $p = 0.026$, LMM, * indicates $p < 0.05$; ** indicates $p < 0.01$, Bonferroni post hoc comparison). **D:** Quantification of the latency to the onset of first SWDs in sham (□) and GA groups (■) shows very little difference between the two groups: sham: 97 ± 17 sec; GA: 101 ± 24 sec (n=6 rats, $p > 0.05$. n.s. indicates not significant). **E:** Cumulative SWD duration during the 30 min observation period was increased significantly in the GA-treated rats by approximately 40 % (n = 6 rats, ** indicates $p < 0.01$, Student's t-test). All data presented in this figure were obtained from 6 GA-treated animals and 6 sham-treated animals and symbols and bars on panels C-E represent means from multiple animals.

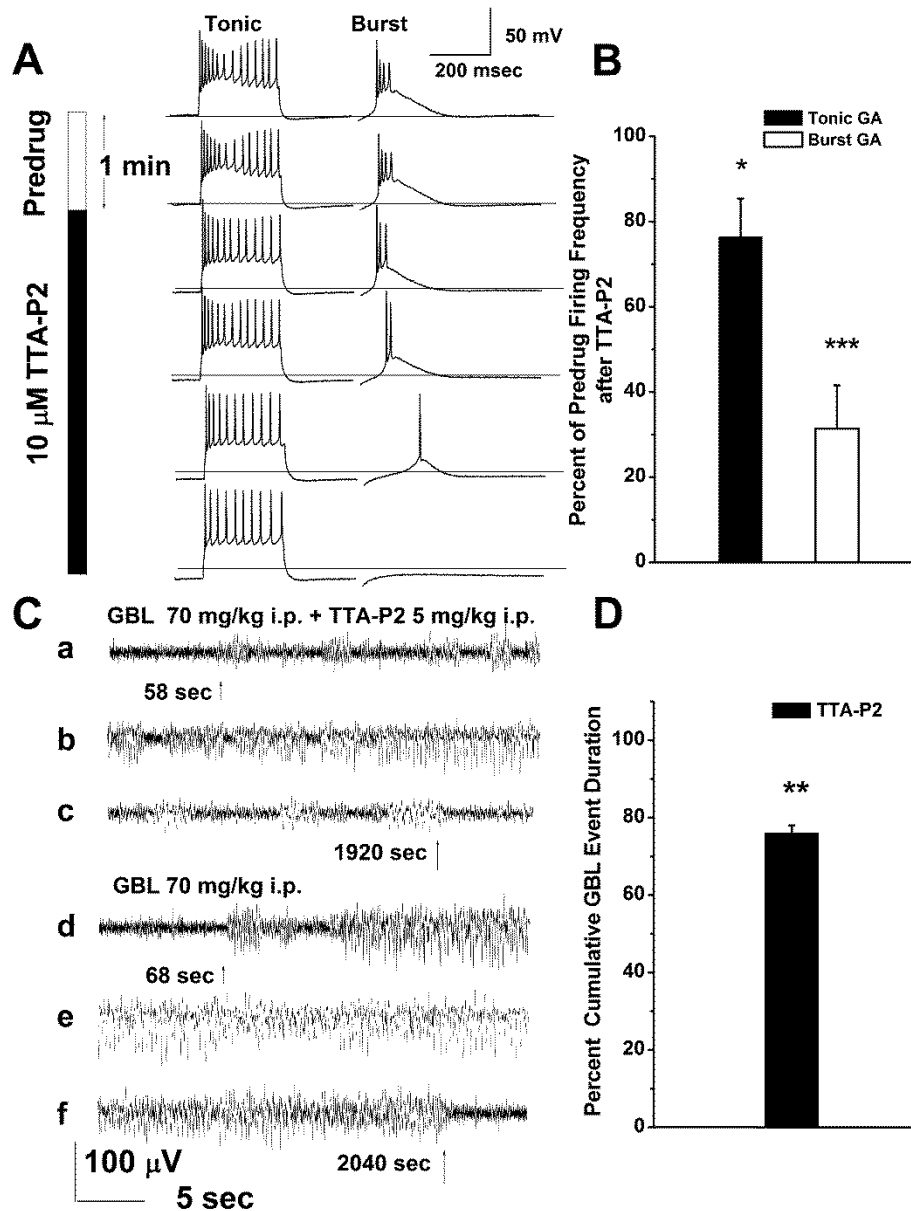


Figure 17. TTA-P2 reduces nRT neuron action potential firing *in vitro* and attenuates pharmacologically-induced SWDs of GA-exposed rats *in vivo*. **A:** Samples of original traces in GA-treated rats depict the progressive reduction in number of tonic APs from 14 to 10 mediated by bath application of 10 μ M TTA-P2; burst firing was completely inhibited in the same neurons. The dotted line represents the natural RMP of this nRT neuron of -60 mV. Tonic firing was evoked by 0.2 nA current injection for 500 msec; burst firing was evoked by a subsequent current injection of -0.2 nA for 500 msec in the same nRT neuron from GA-treated group. **B:** A graph of average data shows that 10 μ M TTA-P2 reduces the tonic AP frequencies of GA-treated rats by $24 \pm 9\%$ as compared with pre-drug values in the same neurons ($n = 12$ rats and 12 neurons; * indicates $p < 0.01$, paired T-test); burst firing was inhibited by $70 \pm 10\%$ as compared with pre-drug values ($n = 12$ rats and 12 neurons; *** indicates $p < 0.001$, paired t-test). The number of APs was measured during 500 msec-long depolarizing current injections of 0.2 nA for tonic firing, and during 1.2 sec-long period following hyperpolarized current injection of -0.2 nA for 500 msec for burst firing. All *in vitro* data presented in this figure were obtained from 9 GA-treated animals. **C:** Administration of 5 mg/kg TTA-P2 (i.p.) *in vivo* reduces the intensity of GBL-induced SWDs in GA-treated rats. Samples of representative nonconsecutive EEG traces in lines a-c depict the progression of GBL-mediated SWD events following pretreatment with i.p. TTA-P2. Samples of nonconsecutive representative EEG traces in lines d-f depict progression of control GBL-mediated SWD events in the same GA-treated rat. Bars indicate calibration. Short black arrows indicate baseline waking EEG followed by the onset of first GBL events; long black arrows indicate final SWD events and return to awake EEG pattern. Numbers next to the arrows indicate elapsed time (in seconds) from GBL injections. **D:** The bar graph summarizes the average effect of TTA-P2 on cumulative duration of SWDs following GBL injections in GA-treated group that was normalized to the effect of GBL alone in the same animals ($n=6$ rats, ** $p < 0.01$, paired t-test).

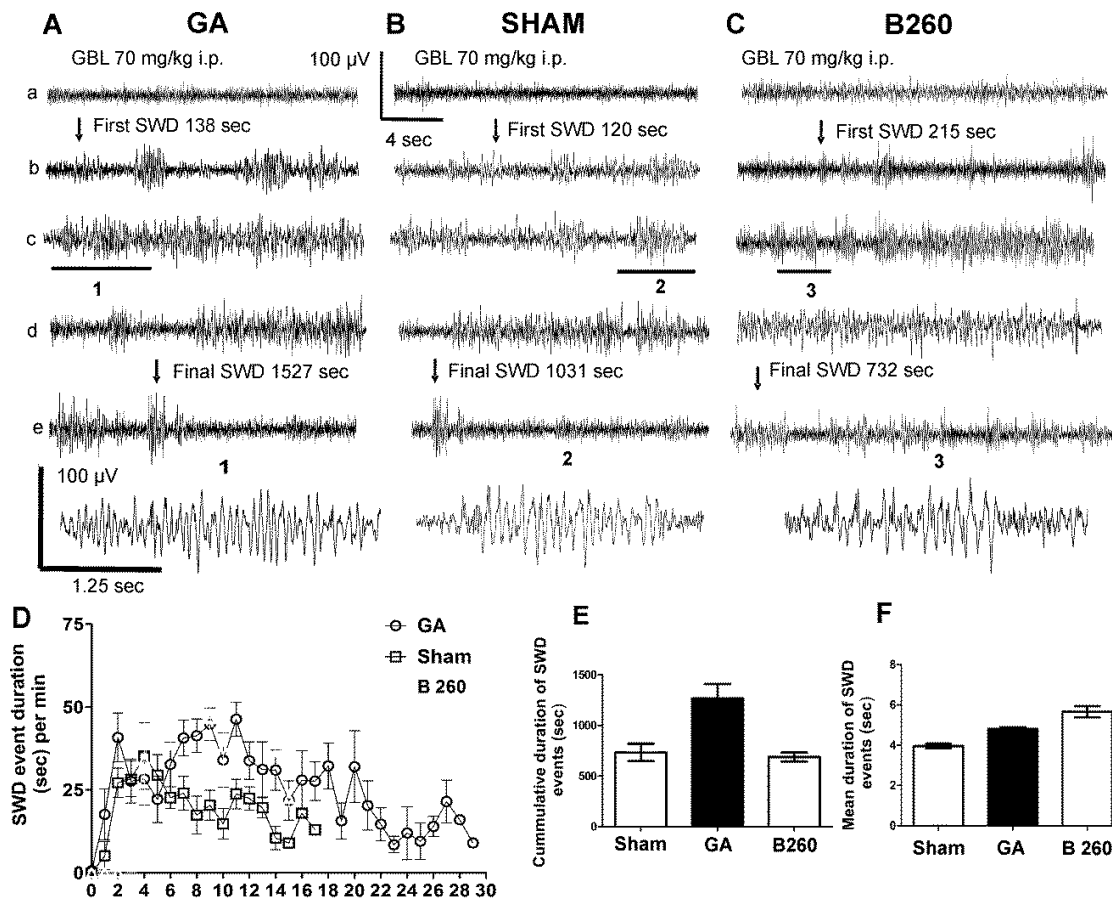


Figure 18. Rats given anesthesia with B 260 at P7 display a decreased sensitivity of SWDs on EEG recordings *in vivo* as compared to GA. **A-C:** Original EEG recordings *in vivo* from a GA-treated rat (panel A) a sham-treated rat (panel B) and a rat treated with B 260 (panel C). Lines **a-e** show progressive nonconsecutive EEG recordings following injections of 70 mg/kg i.p. GBL. Arrows indicate times of first and final SWD events following injections of GBL. Numbers next to the arrows indicate elapsed time (in seconds) from GBL injections. Calibration bars pertain to both panels. **1:** The same segment of GA-treated GBL-induced SWD as labeled with a gray bar in panel A is shown on an expanded time scale. **2:** The same segment of sham-treated GBL-induced SWD as labeled with a gray bar in panel B is shown on an expanded time scale. Black bars indicate calibration that pertain to both panels 1 and 2. **D:** Graph shows an average time course of total SWD event duration per 1-min interval in GA- (●), sham-treated (□), and B 260 treated (Δ) groups) **E:** Cumulative SWD duration during the observation period was significantly increased in the GA-treated rats by approximately 40 % The cumulative duration for the B260 group is similar to that of the sham group **F:** The bar graph shows an average single SWD event duration in sham (□), GA (■) groups and B 260 (Δ) group. The mean duration of each SWD event was increased significantly in the GA group by about 20 %. The mean duration of SWD events was also increased approximately 30% as compared to sham for the B 260 group.

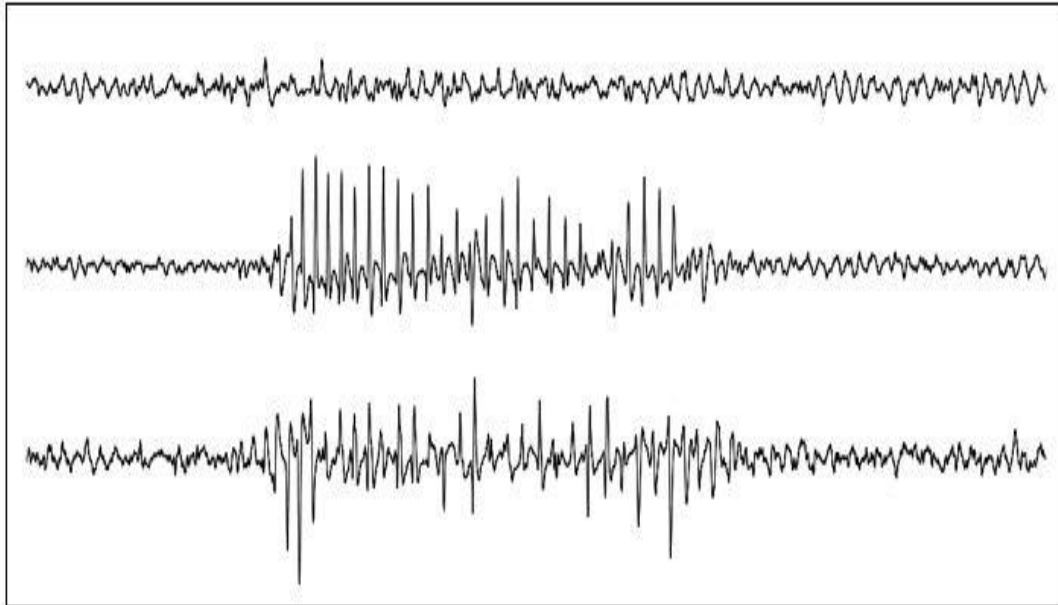


Figure 19. EEG recordings of spike-wave discharges (SWD) from WAG/Rij rats a well characterized animal model of absence epilepsy. Top trace: recordings are from the ventral hippocampus, middle trace: recordings are from the prefrontal cortex, bottom trace recordings are from the frontal cortex. Hallmark 3Hz spike and wave discharges occur in the cortex but not from the hippocampus. Figure courtesy of Dr. Howard Goodkin.

E. Discussion

Both human and animal studies have pointed to the potential role of GABA_A receptor dysfunction and/or hyperactivity of thalamic T-channels in absence seizures (reviewed in Beenhakker and Huguenard, 2009; Crunelli *et al.*, 2012). It is of particular interest for this study that intra-nRT connections mediated by long-lasting eIPSCs are critical for regulating inhibitory output and phasic bursting activity. Thus, during thalamocortical oscillations, GABA_A-mediated inhibition of nRT neurons may prevent the pathological hypersynchrony of absence epilepsy, although intracortical mechanisms also may contribute (Steriade *et al.*, 1990). Based on findings that exposure of young rats to common GAs caused lasting loss of inhibitory function of nRT, as well as up-regulation of T-currents and AMPA-mediated excitatory transmission, it was proposed that these animals may display increased propensity for absence seizures. The *in vivo* measurements of GBL-induced SWD prove this idea. This is first report that exposure to GAs can facilitate SWDs on EEGs in animals. However, another recent study found that exposure of P4-6 rat pups to ISO or SEV, also is associated with seizure-like cortical EEG patterns and behavioral developmental deficits later in life (Seubert *et al.*, 2013). It was reported that another CNS depressant and neurotoxic agent, ethanol, induces chronic neuronal hyperexcitability in cultured sensory neurons in parallel with a decrease in neuronal survival (Scott and Edwards, 1981). This data strongly suggests that exposure to GAs early in life may cause lasting dysfunction of thalamocortical circuitry later in life that possibly contributes to persisting cognitive changes. In a recent retrospective birth cohort study, Wilder and colleagues (2009) screened a large population of children exposed to GAs before the age 4 and found that they were at significant risk for the development of reading, written language, and

math learning disabilities. Definitive clinical data on potential neurotoxic effects of GAs in humans still are lacking and very little is known about possible long-term effects of GAs on thalamic signaling; but the question arises as to whether thalamocortical dysfunction after GAs may contribute to the cognitive disturbances in humans. It is well documented that thalamic hyperexcitability in humans may underlie disorders of cognition, sleep and wakefulness disorders, tinnitus, neurogenic pain, as well as absence epilepsy -collectively termed “thalamocortical dysrhythmias” (Llinas *et al.*, 2005). New clinical studies are needed to establish whether “thalamocortical dysrhythmias” are more prevalent in patients exposed to GAs during critical periods of brain development. In this thesis it is shown that alterations in the properties of T-channels in concert with alterations in inhibitory and excitatory synaptic transmission contribute to the observed hyperexcitability of nRT neurons, and that selective T-channel blockade may be used perioperatively to reverse nRT neuron hyperexcitability following exposure to GAs early in life. Hence, this study may provide the rationale for new therapeutic strategies targeting thalamic ion channels in order to prevent or improve cognitive and other persisting dysfunctions after GA exposure.

In GA exposed rats, the observed alterations in GBL induced EEG reflects hyperexcitability of thalamocortical networks. Further analysis of GA rat EEG recordings may reveal an increased occurrence of EEG events in the low frequency range of 3-5 Hz and possibly more SWDs. Animals displaying absence seizure behavior should have an increased occurrence of SWDs especially during waking (figure 19). In terms of sleep patterns alterations in low frequency EEG patterns associated with sleep patterns in the lower frequency range such as stages 1-4 may also be observed. It may also be wise to consider that there might be alterations of durations and transitions between the stages of sleep in GA exposed rats, since T-channels are crucial for sleep patterning. Ca_v 3.1 KO mice have severely impaired burst firing in thalamic neurons (Lee *et al.* 2004), and both global and regional thalamic knockout of Ca_v 3.1 and Ca_v 3.3 mice

have sleep pattern alterations, such as less non-REM sleep and decreased δ waveforms (Lee et al. 2004, Astori et al. 2011). In terms of rats exposed to GA during brain development, an increase in δ waveforms and an increase in the propensity to sleep would possibly be observed. In order to ameliorate any GA-mediated alterations, treatment with T-channel antagonists, such as ethosuximide and TTA-P2, should arrest prototypical absence seizure SWDs and behaviors, and possibly restore altered sleep patterns. This type of drug treatment could apply to a clinical setting as well.

Finally, the T-channel specific neuroactive steroid B260 was used as an alternative anesthetic and its ability to preserve thalamocortical function was assessed in EEG experiments. Although the mechanism of T-channel mediated anesthesia has yet to be elucidated, preliminary data suggests that T-channel blockade may alter nRT excitatory and possibly inhibitory synapse properties (see section III) leading to hypnosis. These findings also suggest that within the central nervous system, T channels may prove safe for use during mammalian brain development and be a viable target for next generation anesthetics.

V. Early exposure to GA alters subiculum neuron firing patterns

A. Introduction

Previous behavioral studies indicate major changes in subiculum dependent spatial learning and memory tasks that are caused by early exposure to GAs. These changes may be mediated by alterations in subicular neuron structure and function. Observed alterations in subicular neuron structure include neuropil scarcity and disarray and an overall decrease in the number of synaptic boutons (Lunardi et al., 2010). In terms of hippocampal neuron synaptic function, the known GA mediated changes include reduced long-term potentiation within the CA1 region of the hippocampus (Jetovic–Todorovic et al., 2003). It is important to note that GA mediated alterations within the subiculum are not only due to structural changes in synapse structure, for they also include widespread neuron loss due to activation of apoptotic pathways (Jetovic–Todorovic et al., 2003). In this thesis it is proposed that the functional changes in the remaining subicular neurons induced by GAs may be maladaptive and contribute to alterations in memory acquisition later in life.

Here it is hypothesized that alterations in subicular neuron action potential firing patterns contribute to the observed spatial learning and memory deficits observed in GA exposed rats. In this section, the long-term and lasting effects of an early exposure to a clinically relevant anesthetic triple cocktail consisting of 9 mg/kg midazolam, 80% N₂O and 0.75% ISO during brain development upon the action potential firing patterns of subiculum neurons are determined. In order to thoroughly elucidate subicular neuron action potential firing patterns, both tonic and hyperpolarization-induced rebound action potential firing properties of subicular neurons were characterized in combination with a single unit extracellular or loose patch protocol.

Anesthetics are known mediators of free radical production either by producing ROS directly (Orestes et al., 2011) or by altering the function of

mitochondrial complexes (Sanchez et al., 2011). Many neurotransmitter systems are sensitive to ROS. Hydrogen peroxide (H_2O_2), the superoxide anion (O_2^-) and the hydroxyl radical (OH^\cdot) are generated as byproducts of oxidative metabolism in neurons (Bao et al., 2009). The creation of ROS is part of normal neuron metabolism. There are many mechanisms such as superoxide dismutase, catalase and peroxiredoxins that are dedicated to the regulation of neuronal ROS levels (Bao et al., 2009; Drechsel et al., 2010). Physiological ROS levels can vary between mid nanomolar to low micromolar (Lei et al., 1998). However, neurological damage may result from generation of excess free radicals (Ikonomidou et al., 2011). In this thesis, the effects of free radicals upon membrane excitability in areas of the brain critical for learning, memory and object recognition such as the subiculum was evaluated.

Alterations in neuron activity level by free radicals may interfere with faithful transfer of neuronal signals during waking, and possibly induce irreversible damage to neurons during development if levels become elevated. Anesthetics are known mediators of ROS production. Previous studies identified that N_2O utilizes a free radical based mechanism of action for interaction with T-type calcium channels (Orestes et al., 2011). Furthermore, ROS levels are elevated after exposure to anesthesia (figure 20) and anesthetics interact directly with mitochondrial complexes that are responsible for maintaining normal physiological ROS levels (Sanchez et al., 2011). Here, the ability of a superoxide dismutase and catalase mimetic EUK-134 to reverse or diminish GA-mediated hyperexcitability within the subiculum was investigated.

To date, subicular neurons are known to have distinct modes of action potential firing distinct from the adjacent CA1 region of the hippocampus. Pyramidal subicular neurons will burst fire, however it is noteworthy that the active membrane properties are seemingly delineated, and pyramidal subicular neurons are divided into populations that either fire tonic action potentials, display weak bursting or those that are capable of firing high frequency action potential bursts (Staff et al., 2000). Subiculum burst firing events have been

associated with Ca^{2+} tail currents (Jung et al., 2001). However, the exact contributions of voltage activated Ca^{2+} channels to this current have yet to be determined. T-channels may play a role owing to expression of all isoforms in this brain region (Talley et al., 1999). To date, a functional characterization of T-channels within the subiculum proper has yet to be performed. Here, T-current biophysical properties from Sham and GA treated subiculum pyramidal neurons are compared.

B. Experimental design

Anesthesia At postnatal day 7 (P7) both male and female Sprague Dawley rats were exposed to 6 hours of a clinically relevant triple anesthetic cocktail consisting of 9 mg/kg midazolam, 80% N_2O , and 0.75% ISO. For experiments utilizing the catalase superoxide dismutase mimetic EUK-134, rats were pretreated with a 10 mg/kg i.p. injection. Sham controls were exposed to 6 hours of mock anesthesia consisting of a vehicle injection of 0.1 % DMSO H_2O and separation from their mother. Midazolam (Sigma) was dissolved in 0.1% DMSO and was given via an IP injection prior to exposure to volatile anesthetics. EUK-134 (Caymen) was dissolved at 1 mg/ml in sterile H_2O and administered i.p. at a dose of 10 mg/ml. Exposure involving N_2O , O_2 and ISO utilized a dedicated pre mixer of N_2O and O_2 followed by an agent-specific ISO vaporizer that delivered a set percentage of ISO anesthetic into a temperature controlled chamber preset to maintain 33-34 °C. The composition of the gas chamber was analyzed by real time feedback (Datex Capnomac Ultima) for N_2O , ISO, CO_2 , and O_2 percentages. All gas flows were adjusted manually during the exposure in order to maintain 80% N_2O , and 0.75% ISO during the duration of the procedure.

Electrophysiology Patch clamp recordings in live adolescent (P14-45) horizontal 300 μM rat brain slices were used in order to study the alterations in action potential firing patterns induced by early GA exposure. Utilizing a multi-step protocol both tonic and burst firing properties of nRT neurons were also

characterized. Subicular neurons were patched in whole cell configuration and resting membrane potentials were recorded for 100 ms. After this, neurons were injected with a single depolarizing step 0.2 nA for 400 ms, and allowed to rest for 400 ms. Then, hyperpolarizing currents in 0.2 nA intervals stepping from -0.28 to -2.08 nA were injected.

Cell-attach The properties of subicular neuron action potential properties were investigated by using a single unit extracellular “loose patch” protocol. (Nunemaker et al ., 2003). Low resistance (<50 mΩ) seals were maintained between the pipette and the subicular neuron. Both extracellular and intracellular recording solutions were ionically balanced in order to invoke an overall depolarization of the neuron membrane. The internal recording pipette solution (3-7 mΩ) consisted of the following in mM NaCl 150, Glucose 10, HEPES 10, CaCl₂ 2.5, MgCl₂ 1.3, KCl 5 whereas the external solution was in mM: NaCl 125, Glucose 10, NaH₂PO₄ 1.25, NaHCO₃ 26, KCl 5, MgCl .25, CaCl .25. All recordings were made in voltage clamp mode utilizing a holding potential of 0 mV and filtered at 10 kHz.

C. Results

1. Early GA exposure leads to hyper excitable pyramidal subicular neurons

Exposure of rat pups at age P7 to a triple anesthetic cocktail leads to a lasting increase in intrinsic cellular excitability in subicular neurons. GA mediated alterations in subicular neuron action potential firing patterns were characterized utilizing experiments designed to illicit both tonic and hyperpolarization induced “burst” or “oscillatory” neuron firing.

In terms of tonic action potential firing frequencies, average tonic firing frequency was increased in the GA-treated group (21.2 ± 5.7 Hz n=6) versus that of Sham controls (13.5 ± 0.4 Hz n=14 t-test p=0.06) (figure 21). Next, it was asked whether hyperpolarization induced rebound AP firing frequencies in GA-

treated vs. control groups were different. In figure 22 panel C the same amplitudes of hyperpolarizing current injections induced about 4 fold more APs in the GA-treated group versus that of the Sham group. For example, during current injections of -0.68 nA, the average rebound firing frequency was only 1.4 ± 0.4 Hz in the Sham group versus 4.4 ± 1.5 Hz in the GA-treated group. Resting membrane potentials and input resistances were also analyzed in order to elicit the mechanisms responsible for GA mediated subicular neuron hyperexcitability. Overall there was no significant difference in resting membrane potential between the GA (-53.1 ± 1.3 mV) and Sham (-57.37 ± 1.3 mV) groups (figure 21 panel D). There was also no significant difference in the average input resistances between the GA and Sham groups (figure 22 panel B). In pyramidal subicular neurons that displayed burst action potentials, the number of action potentials during the first current injection (-0.28 nA) was significantly increased in the GA group (figure 22 panel E).

2. In vivo co-administration of catalase super oxide dismutase mimetic EUK-134 prior to early GA triple cocktail preserves pyramidal subicular neuron function

In order to further elucidate and minimally affect the intrinsic properties of subicular neurons in action potential firing between GA exposed and Sham, subicular neurons were subjected to a single unit extracellular (loose) or cell attach protocol (Nunemaker et al., 2003). Regarding cell attach experiments; a significant increase for the GA treated group 3.9 ± 0.9 Hz as compared to Sham 0.9 ± 1.0 Hz controls (figure 23 panel B) was observed.

Using this same experimental paradigm the hypothesis that subicular neuron hyperexcitability in rats exposed to GA can be reversed by *in vivo* pre-administration of EUK-134 prior to anesthetic cocktail exposure was also investigated. When P7 rats were pretreated with the EUK-134 and then subjected to 6 hours of triple cocktail anesthesia, a reduction to 1.7 ± 0.6 Hz was

observed figure 23 panel B, a frequency very similar to that of the Shams. A frequency of 1.0 ± 0.6 Hz was observed for the Sham EUK control group. This is particularly investigation worthy because administrations of EUK-134 prior to the exposure of P7 rats to GA reversed GA mediated memory deficits observed in adolescent rats (Boscolo et al., 2012). However, it is important to note that the mechanisms underlying the protective effects of EUK-134 are not well characterized. Based on the results depicted in figure 23 it is assumed that EUK is diminishing the GA-mediated levels of ROS.

3. T channels contribute to subicular neuron AP firing

In order to investigate the contribution that T-channels make to subiculum pyramidal neuron firing a selective and potent T-channel inhibitor TTA-P2 was used. In our study, bath application of $10 \mu\text{M}$ TTA-P2 resulted in significant reductions in both tonic and rebound action potential firing. In the presence of TTA-P2 an overall decrease in the tonic action potential firing of subiculum neurons was observed; the average frequency value before bath application was 20.3 ± 1.0 Hz versus $15.4 \pm$ Hz after at least 5 minutes of bath incubation. Regarding the ability of subicular pyramidal neurons to fire hyperpolarization-induced rebound action potentials in the presence of $10 \mu\text{M}$ TTA-P2, a near complete rebound action potential blockade across most current injections (figure 24 panels B and F) was observed. This would be consistent with observations in thalamic neurons where elimination of the T-channel currents after neuron hyperpolarization results in the elimination of rebound burst action potential firing.

Next, the changes in membrane properties in the presence of TTA-P2 were investigated. In terms of resting membrane potential, an overall hyperpolarization of the membrane in the presence of $10 \mu\text{M}$ TTA-P2 was determined. This is consistent with a depolarizing T-channel window current that is well characterized within thalamic neurons (Dreyfus et al., 2010). The average membrane potential values were -63.7 ± 0.18 mV for the control and -68.3 ± 0.4

mV post TTA-P2. In the presence of 10 μ M TTA-P2 a trend towards an increase in the overall input resistance as calculated from each hyperpolarizing pulse was observed. This would be consistent with the apparent blockade of the T-channel population. In conclusion, our results prove that T-channels modulate action potential firing in pyramidal subiculum neurons.

4. Subiculum T-channel biophysical properties are altered after exposure to GA

To date, the T-channel contribution to subicular neuron firing patterns is not well understood. Here, the biophysical properties of the voltage dependence of activation, inactivation and T-current densities are characterized in both Sham and GA treated rats.

T-current waveforms in representative subiculum neurons from the Sham and GA groups are depicted in figure 25 panel A and B, respectively. On average, the peak T-current densities, as calculated from the voltage dependence of activation utilizing I-V relationships, were equivalent in the GA (■) and Sham (○) groups over the range of conditioning potentials. In figure 25 panel D, the V_{50} for the voltage-dependence of activation in the GA group demonstrated a significant depolarizing shift of about 8 mV (■, -49 ± 2 mV, $n=17$ neurons) as compared to Shams (○, -57 ± 2 mV $p<0.01$, t-test, $n=14$ neurons). In order to assess the voltage dependence of inactivation and to further compare current densities between the GA and Sham groups, an independent voltage dependence of inactivation test was used. Average data points presented in figure 25 panel E demonstrate that current densities were increased about 25% in the GA group (■) as compared with those in the Sham group (○) over the range of membrane potentials. The voltage-dependence of inactivation was also calculated. Similar to the voltage dependence of activation, figure 25 panel F shows that V_{50} for the voltage dependence of inactivation in the GA group also demonstrated a small and non-significant depolarizing shift of about 3 mV (■, -87

± 1 mV, n=20 neurons) in comparison with the Shams (\circ , -90 ± 2 mV, n=20 neurons). Thus, there is a depolarizing shift in T-channel window currents observed in the GA treated group (figure 26). T-current inactivation time constants were also assessed by fitting the inactivating portions of the I-V current waveforms with a single exponential function. There was no significant difference found between the GA (41.8 ± 4 ms, n=17 neurons) and Sham (48.5 ± 4 ms, n=23 neurons) groups.

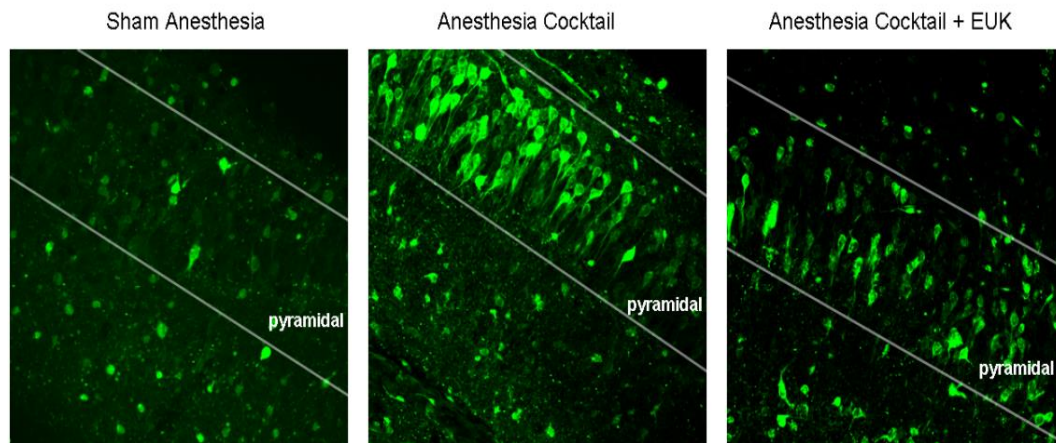


Figure 20. Co-administration of EUK-134 prior to GA reduces the level of ROS as detected by DGF-DA, a free radical sensitive dye, within subicular pyramidal neurons. Data courtesy of Dr. Victoria Sanchez

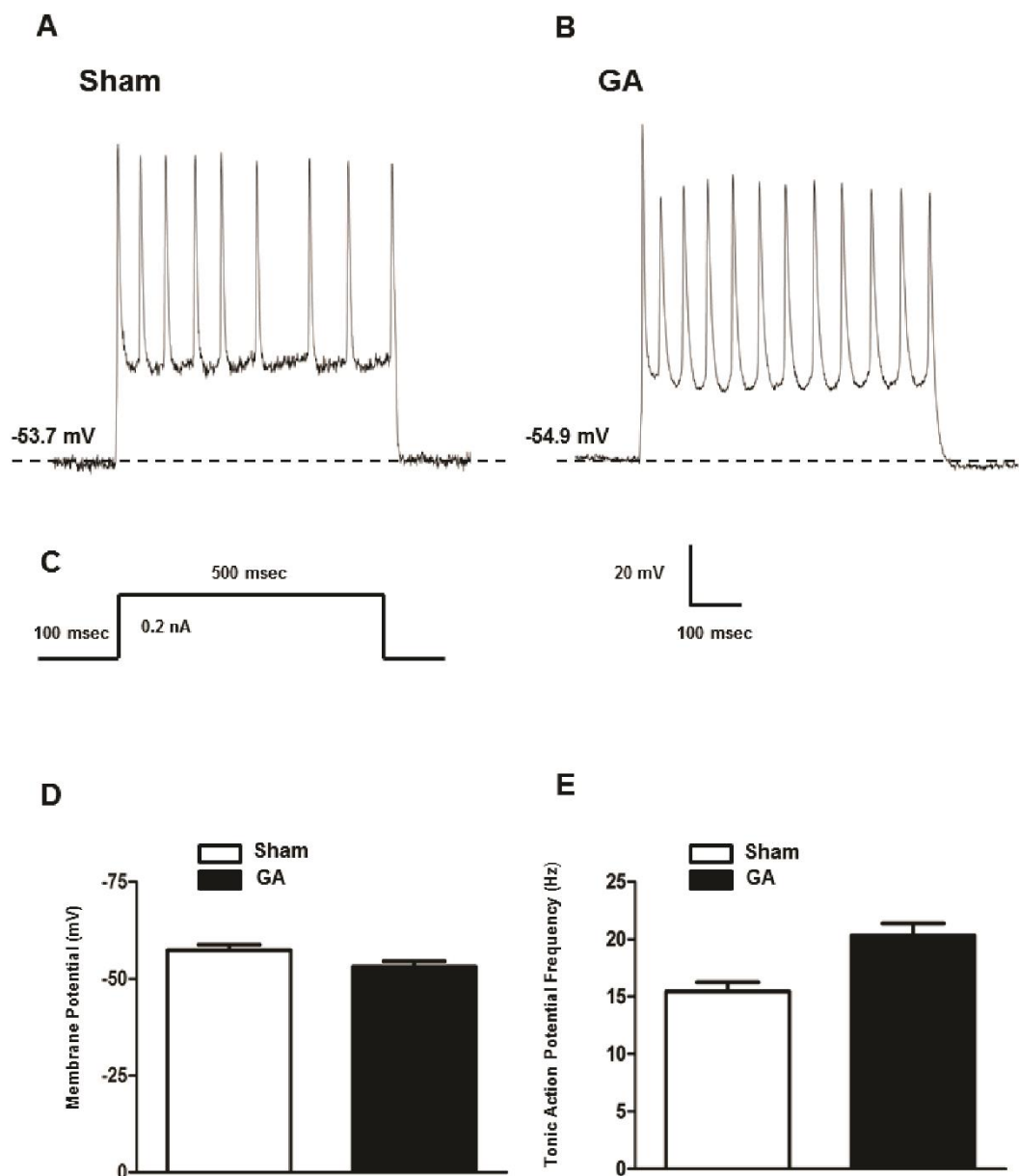


Figure 21. Tonic action potential firing frequency is increased in GA versus Sham treated pyramidal subicular neurons. **A:** Action potential trace from a representative Sham treated subicular pyramidal neuron. Dashed line indicates the resting membrane potential of the neuron. **B:** Representative action potential trace from a GA treated pyramidal subicular neuron. Note the increase in the action potential frequency. Dashed line represents the neuron resting membrane potential. **C:** Current injection protocol used to illicit tonic action potential firing in both GA and Sham treated rats. **D:** There is no significant difference between GA and Sham treated rat pyramidal subicular neuron resting membrane potentials. **E:** Quantification of the average pyramidal subicular neuron tonic action potential frequencies in GA (n=6 neurons) versus Sham (n=14 neurons) treated rats.

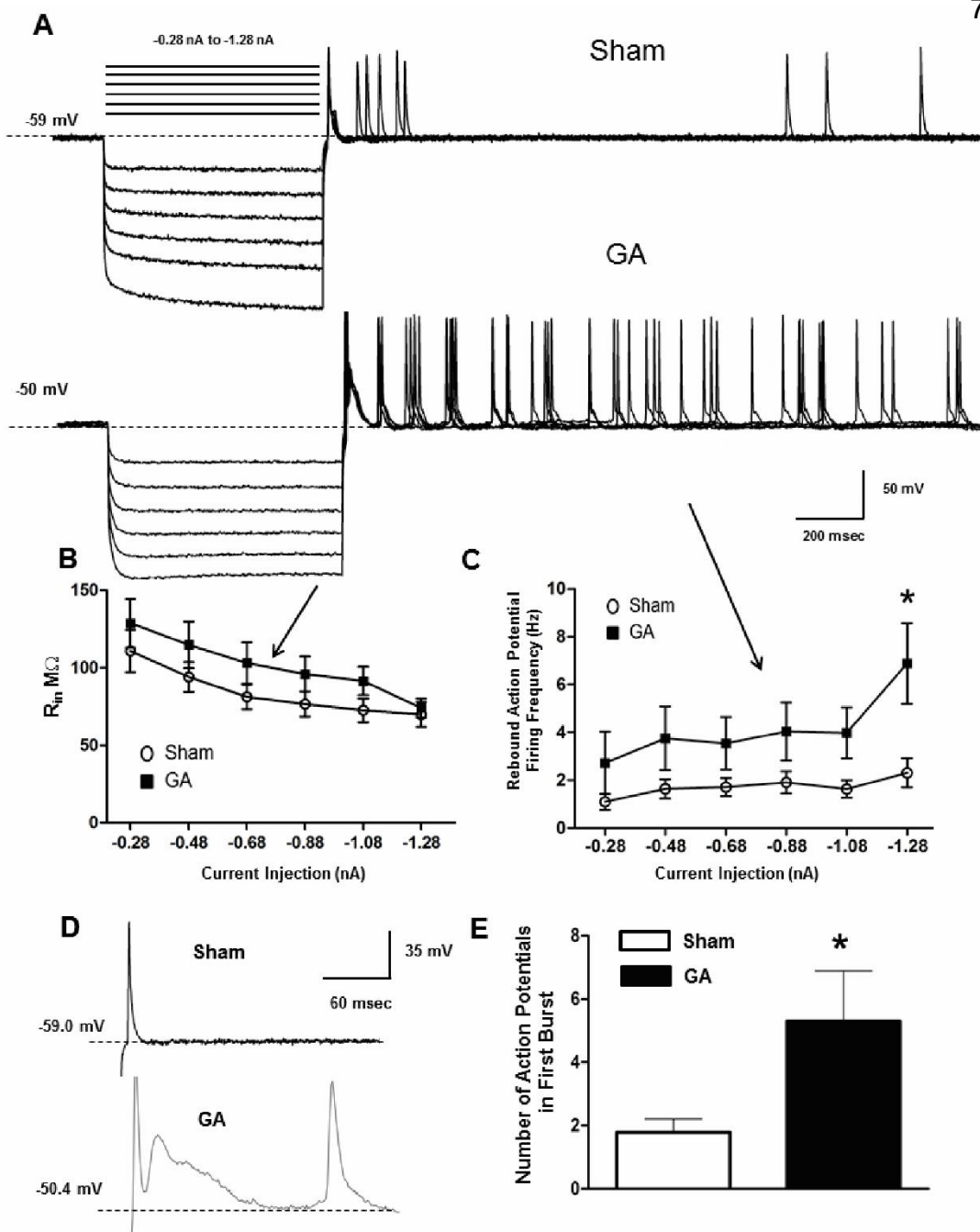


Figure 22. Rebound action potential firing is increased in GA versus Sham subicular neurons. **A:** Sample traces from a Sham control and GA subicular neurons with all rebound action potentials elicited from current injections ranging from -0.28 nA –1.28 nA. The dashed line is represents the resting membrane potentials. Note the increased action potential frequency of the GA treated neuron. **B:** There is a slight increase in the average input resistance values for the GA treated group as calculated from the hyperpolarizing current injections. **C:** The GA treated group, there is a strong trend towards an overall increase in the rebound action potential frequency verse that of the Sham treated group (* denotes $p < 0.05$ SNK $n = 17$ neurons for GA and $n = 14$ neurons for Sham, data analyzed is from at least 3 separate animals for each group). **D:** Representative action potential traces form Sham and GA treated animals. Traces depict a depolarizing membrane response that may be a HVA or LVA calcium channel mediated event. **E:** The number of first burst action potentials is increased in GA versus Sham treated rats (* denotes $p < 0.05$ T test $n = 17$ neurons for GA and $n = 14$ neurons for Sham. Data analyzed is from at least 3 separate animals for each group).

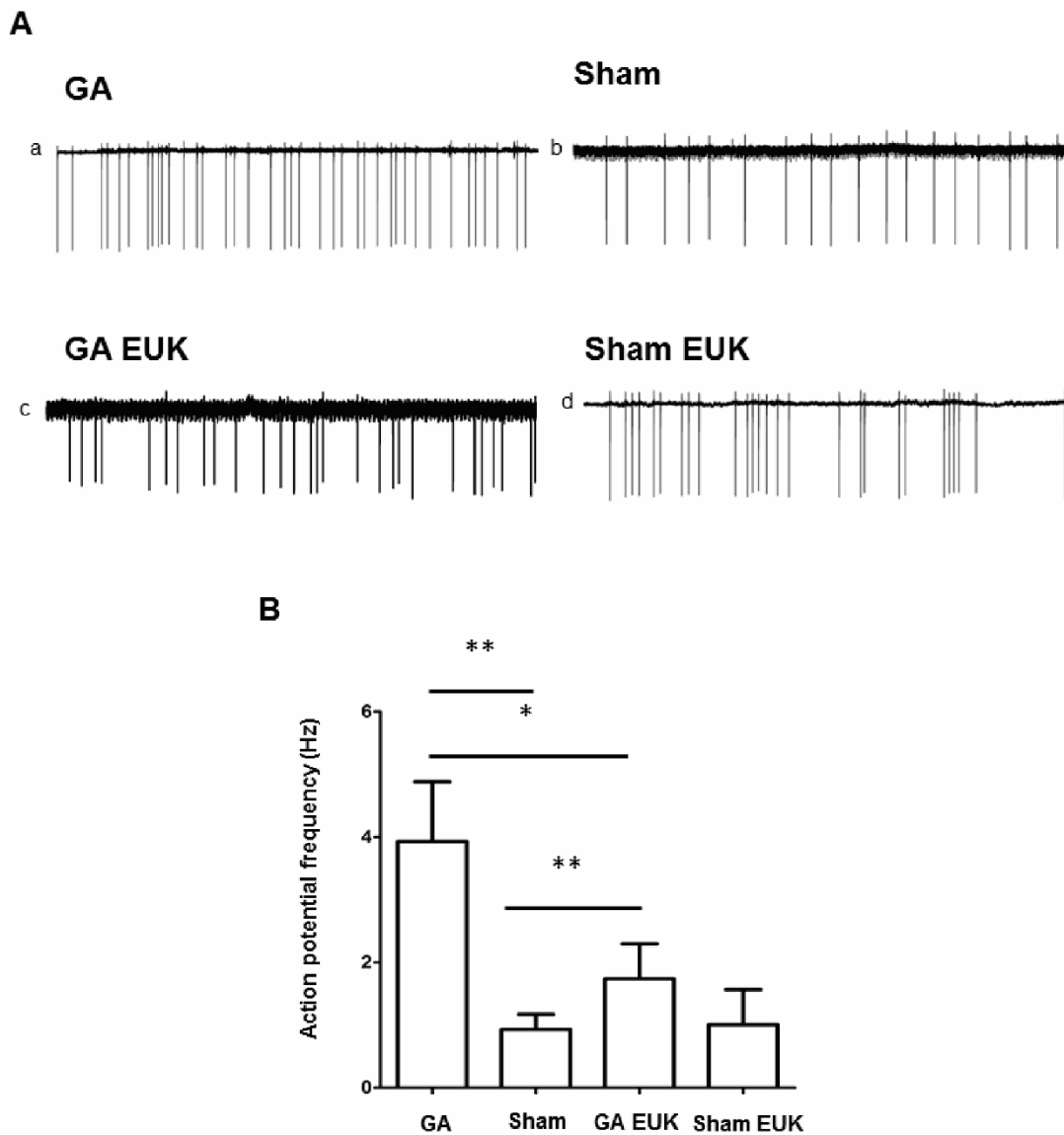


Figure 23. Pretreatment with EUK-134 rescues subicular pyramidal neurons from a GA mediated increased average firing frequency **A:** a-d sample traces from cell attach recordings from GA, Sham GA EUK and Sham treated pyramidal subicular neurons. **B:** Quantification of action potential frequencies from all groups (* $p < 0.05$, ** $p < 0.005$ SNK, GA $n=6$, Sham $n=10$, GA EUK $n=10$, Sham EUK $n=10$).

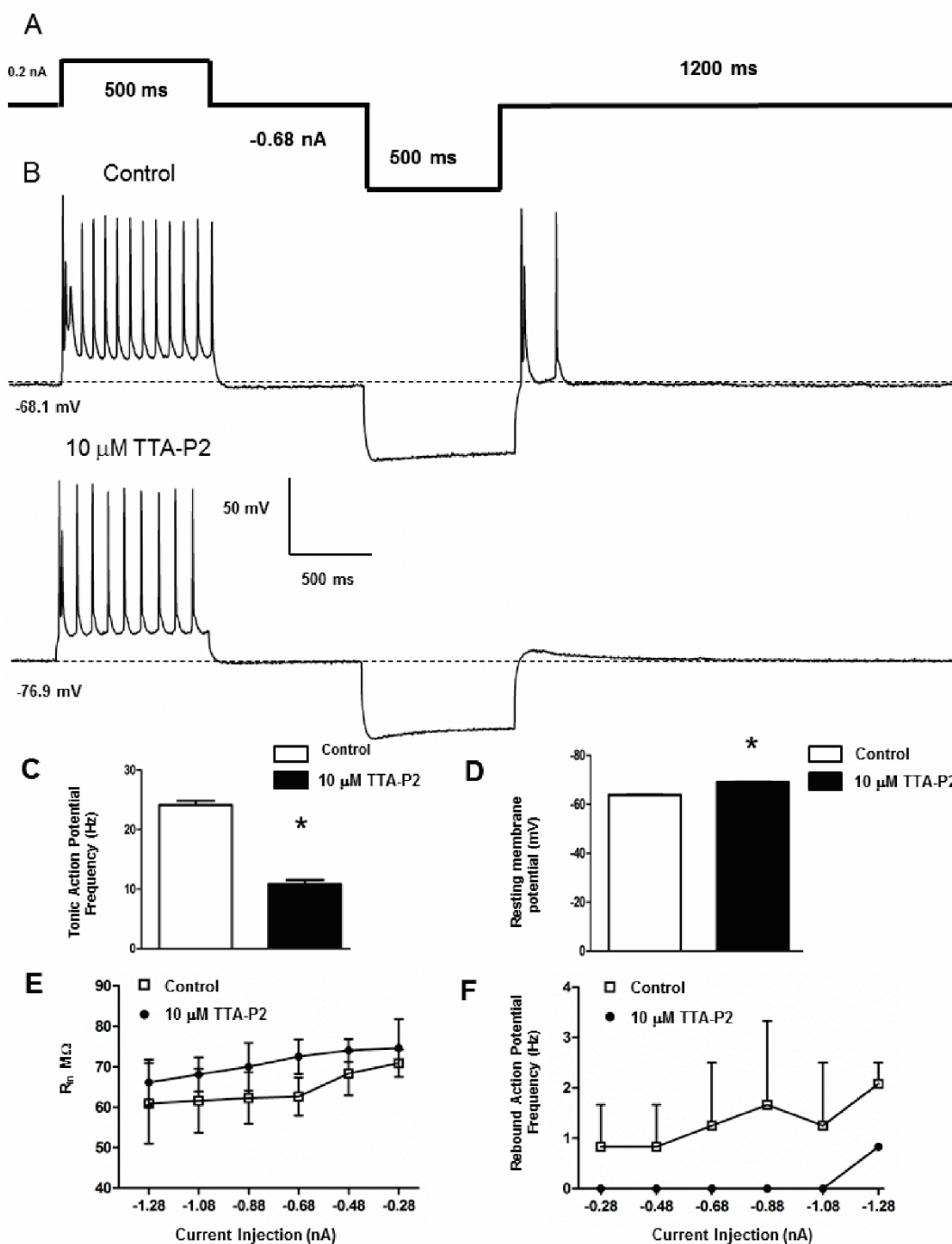


Figure 24. Application of the selective T-channel antagonist reduces both tonic and hyperpolarization induced rebound action potential firing in pyramidal subiculum neurons. **A:** Current injection protocol used to evoke both tonic and hyperpolarization induced action potentials **B:** Representative traces of the response of a control subicular pyramidal neuron to both depolarizing and hyperpolarizing current injections pre and post application of 10 μ M TTA-P2. **C:** Quantification of the TTA-P2 mediated reduction in tonic action potential frequencies. **D:** Resting membrane potentials are hyperpolarized post application of 10 μ M TTA-P2 the mean value for control was -63.7 ± 0.2 mV for control versus -68.9 ± 0.2 mV for 10 μ M TTA-P2 ($p < 0.05$ paired T-test $n = 2$ neurons). **E:** Preliminary data indicates that application of 10 μ M TTA-P2 results in a trend towards a decrease in input resistance. **F:** Quantification of hyperpolarizing rebound action potentials, 10 μ M TTA-P2 reduces action potential frequency across all current injection amplitudes.

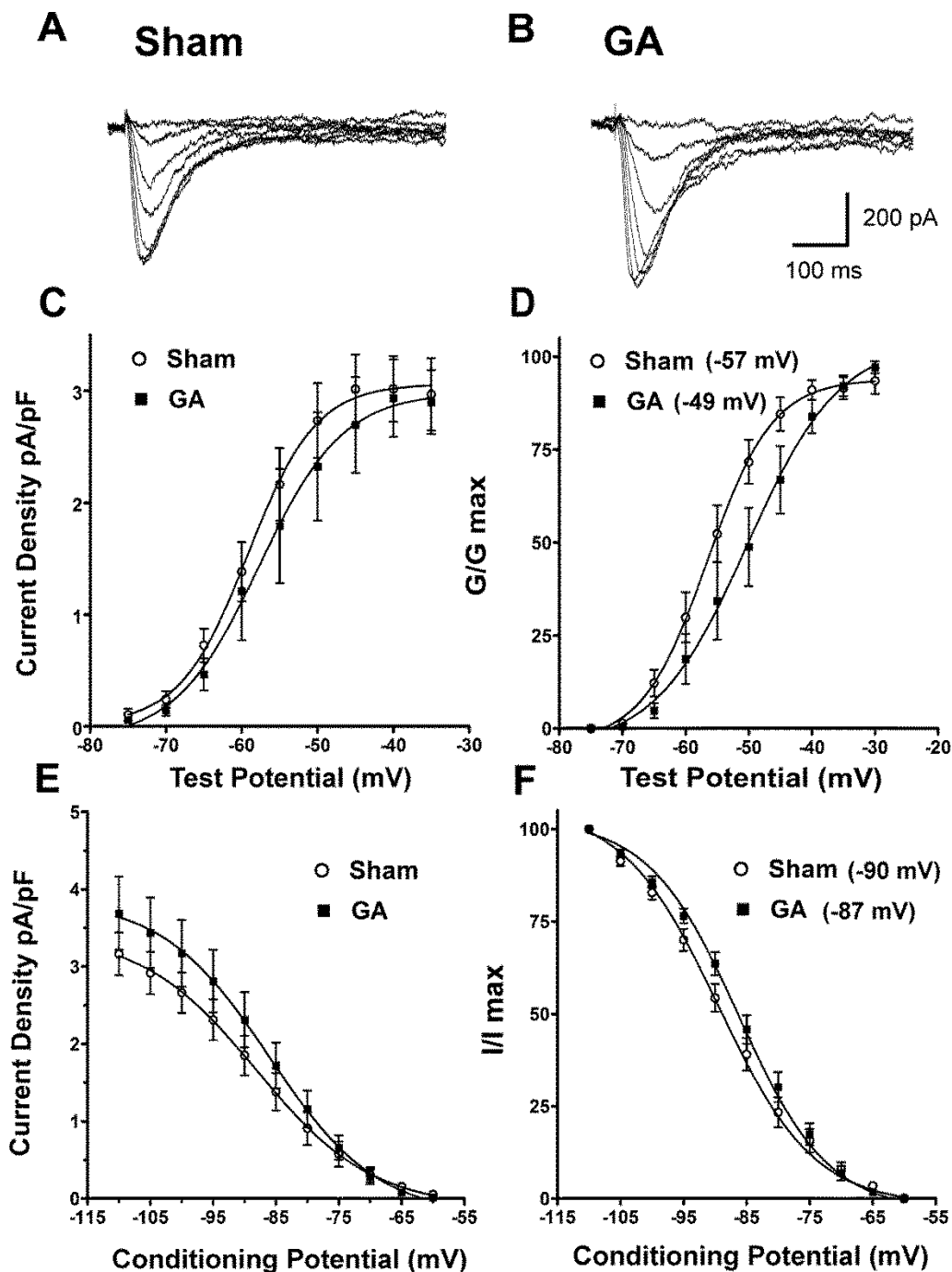


Figure 25. Exposure to GA causes a depolarizing shift in pyramidal subiculum neuron T-currents. **A-B:** Representative original T-current traces from both Sham (A) and GA (B) subiculum neurons in the range of V_t from -80 to -35 mV from V_h of -90 mV. Bars indicate calibration. **C:** T-channel current density as calculated from the voltage-dependence of activation is approximately equivalent across a broad range of test potentials in the GA-treated group when compared to the Sham group. **D:** The V_{50} for the voltage-dependence of activation (noted in parentheses) for the GA (■) group demonstrated a significant depolarizing shift of 8 mV as compared with that in the Sham (○) group. **E:** T-channel current density as calculated from the voltage-dependence of inactivation is increased in the GA group (■) when compared to the Sham group (○) across a broad range of conditioning potentials ($p > 0.05$). **F:** The V_{50} of the voltage-dependence of inactivation of the GA group (■) also demonstrated a small but non-significant depolarizing shift (as noted in parentheses) when compared with the Sham group (○).

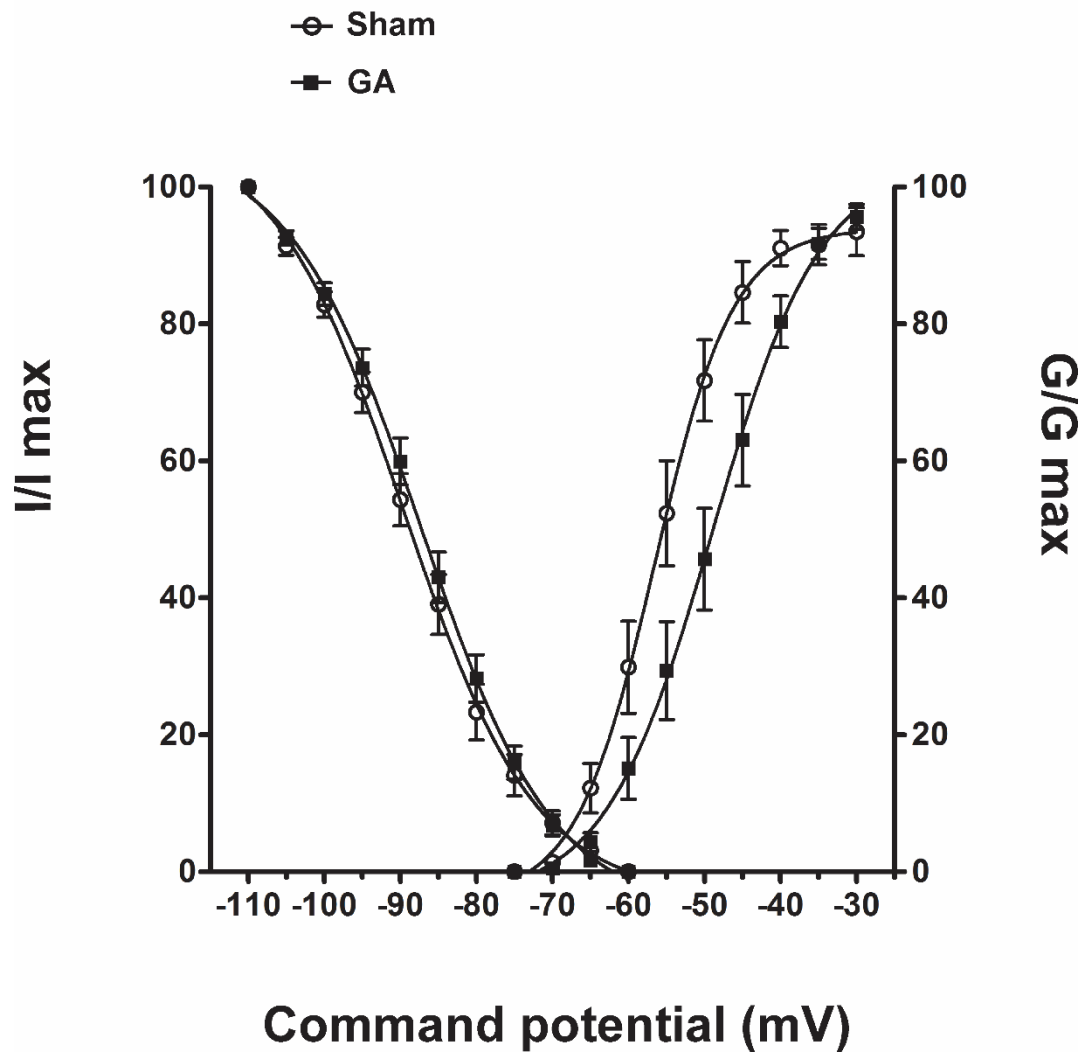


Figure 26. Subiculum pyramidal neuron T-channel window currents are altered in GA exposed rats. Graphs of the voltage dependence of inactivation and activation comprise the I_t window for the GA and Sham groups. Note the depolarizing shift in the GA group voltage dependence of activation.

E. Discussion

In this section, our data suggests that GA exposure during brain development leads to hyperexcitable pyramidal subicular neurons. The concept that *in vivo* co-administration of catalase and super-oxide dismutase mimetic EUK-134 prior to early GA triple cocktail preserves pyramidal subicular neuron function has also been explored. In terms of learning and memory tasks, there is some debate regarding the contribution of the subiculum (Omara et al., 2005). In humans, MRI studies have shown that this region is correlated with learning and memory (Gabrielli et al., 1997). In rodents, the consensus view is that subiculum specific lesions produce impairments in the learning of visual spatial tasks, however these impairments are not as severe as compared to those made within CA1 (Morris et al., 1990). It is important to note that GA mediated alterations in hippocampal formation neuron structure and function are not subiculum selective and that alterations in spatial learning acquisition are most likely due to the sum of alterations changes within CA1 and other hippocampal regions as well.

In this study the biophysical properties of T-channels are described for the first time in both Sham control and GA exposed rats. It was also shown that T-channels contribute to subicular neuron AP firing and that T-channel biophysical properties are altered after exposure to GA. Similar to the effects of GA upon nRT T-current properties, it is proposed that alterations in T-channel window current properties may also allow for T-channel participation in tonic subiculum neuron firing. Taken together, these shifts in gating kinetics would cause a more depolarized 'window current' or voltage range where channels are available to open but do not inactivate completely. The observed depolarized shift in T-channel window current promotes hyperexcitability and or increased neuron firing. In future studies a faster recovery from inactivation in pyramidal subiculum neurons from GA as compared to Sham controls may also be anticipated. A faster recovery from inactivation would allow the channels to cycle through the open→closed→inactive cycle, thus returning them to become available to open

and pass more current. Correct operation of T-channels is important for the modulation of burst firing whereas aberrant activity may contribute to pathological conditions of hyperexcitable neurons such as epilepsy and GA mediated alterations in learning and memory. Furthermore, depolarizing shifts of T-current activation and inactivation in GA group allows T-channels to participate in tonic firing of subiculum neurons as well. In conclusion, it is now established that the observed alterations in T-channel properties contribute to GA mediated hyperexcitability of subiculum neurons.

It is very plausible that subicular neuron firing properties are T-channel and HCN dependent, for Cav3.2 and HCN1 have been shown to co-localize at select hippocampal formation synapses (Huang Z et al., 2011). T-channels are known to interact with oxidation and reduction agents, and may be sensitive to elevated levels of ROS, particularly the Cav3.2 isoform (Joksovic et al., 2006; Orestes et al., 2011). In contrast, little is known regarding the interaction of HCN channels and ROS.

The I_h current is typically observed as a slowly developing inward current that is activated upon membrane hyperpolarization and is typically selective for Na^+ and K^+ conductances (Pape et al., 1996). These currents in thalamocortical neurons may have a strong influence upon rhythmic rebound bursting by limiting the duration of IPSPs within reciprocally connected GABAergic neurons (McCormic et al., 1990). Subicular neuron subtypes are known to display oscillatory and/or burst firing properties (Staff et al., 2000). I_h also has a strong influence upon hippocampal formation neuron firing patterns (Maccaferri et al., 1996), and it is known that these currents regulate resting membrane potential and input resistance (Surges et al., 2004). Previous studies have shown that NMDA receptors are ROS sensitive and possess a well-defined REDOX modulatory site (Aizenman et al., 1990; 1995). Thus, it is entirely plausible that subicular neurons are set for a state of hyperactivity post triple anesthetic exposure.

The functional role of T-channels within subiculum neurons are only beginning to be understood. Within the thalamus, T-channels play a crucial role regarding the formation of action potential patterns and the timing of eEPSC events. These AP firing events are in turn crucial for the correct encoding and transmission of somatosensory events and maintenance of sleep and wake patterns. The role of T-channels in the hippocampus may also be critical for the maintenance of action potential patterns that are critical for learning and memory. Our preliminary data suggests that T channels may play a prominent role in the burst firing characteristics of subiculum neurons. This data may also suggest that exposure to GAs during brain development may cause lasting dysfunction of hippocampus circuitry that possibly contributes to persisting cognitive changes. Definitive clinical data on potential neurotoxic effects of GAs in humans still are lacking and very little is known about possible long-term effects.

Post mortem studies of the subiculum pyramidal neurons from subjects with schizophrenia have detected smaller pyramidal cell bodies and structurally altered dendrites (Rosoklija et al., 2000). The subiculum also has an important role in the initiation and maintenance of epileptic discharges in temporal lobe epilepsy (Strafstrom et al., 2005). It is well documented that hippocampal neuron hyperexcitability in humans may underlie disorders of cognition (Bragin et al., 1999). New clinical studies are needed to establish whether “Hippocampal dysrhythmias” are more prevalent in patients exposed to GAs during critical periods of brain development. Functionally, *in vivo* subicular neurons are correlated with both theta and gamma EEG oscillations and CA1 sharp waves (Chorbak et al., 1996) and it may be prudent in future EEG experiments to compare these waveforms in GA and Sham treated rodents. Alterations in T-channels properties in concert with alterations in inhibitory and excitatory synaptic transmission may contribute to the observed hyperexcitability of subicular neurons. Thus, it would be logical to propose and that selective T-channel blockade may be used in a perioperative manner to reverse subiculum neuron hyperexcitability following exposure to GAs early in life.

VI Concluding Remarks

The novel concept presented in this thesis is that exposure to GAs during brain development results in extensive long term alterations in neuron function in thalamic and hippocampal neurons. Regarding thalamic nRT neuron synapse properties, diminished inhibitory synaptic strength coupled with an increase in excitatory synapse drive partially accounts for the observed GA mediated hyper excitability of this brain structure. Permanent alterations in T-channel biophysical properties contribute to the observed hyperexcitability of nRT neurons as well. The idea that T-channel antagonists may be used to ameliorate thalamocortical hyperexcitability has also been explored and proven. Studies of subicular neurons indicated that exposure to GAs during brain development also render these neurons in a permanent hyperexcitable state. The biophysical properties of T-channels are elucidated for the first time in pyramidal subicular neurons. Furthermore, GA exposure was shown to permanently alter T-channel gating properties in pyramidal subicular neurons as well. Experiments utilizing a pretreatment of EUK 134 prior to exposure to the GA triple cocktail proved that attenuation of ROS production during GA may provide a protective effects in terms of sparing normal brain development/function and that anesthetic mediated ROS production is in part a contributor to GA neural toxicity. Finally, the alternative and novel anesthetic B260 was compared to the GA triple cocktail. The results indicated, when used as an alternative to volatile anesthetics, that neuroactive steroids preserve thalamocortical neuron function and that they show promise as an alternative to the anesthetics currently used in children.

Although anesthetics have been used for centuries the mechanisms of action are now just beginning to be understood (Franks and Leib 1994; Franks 2008) and further studies aimed at how the current arsenal actually worked are necessary. Regarding the mechanism of GA action the basic hypothesis involves principally the blockade of glutamatergic excitatory ion channels controlling neuronal transmission and the potentiation of inhibitory GABAergic ion channels

responsible for inhibitory neurotransmission. A robust body of literature now demonstrates that alterations in the balance between excitatory and inhibitory neuron activity during brain development may lead to permanent changes in brain structure and function. There remains the question as to what the exact mechanism of GA mediated neurotoxicity is. Further studies may suggest a link between the activity of the anesthetized brain and what is causing the permanent long term changes.

Although anesthesia is generally thought as a sleep like state owing to the state of hypnosis, the science proves otherwise. In fact, general anesthesia is quite stressful and completely alters normal homeostasis. The EEG patterns resulting from GA are very different from the normal physiological stages of sleep. Muscle tone is lost and alterations in organ perfusion also occur. The restorative properties of sleep are not present, and overall GA is a catabolic process. A literature search yields little information regarding hypothalamus pituitary adrenal (HPA) axis activation during anesthesia. Elevated blood glucose along with co concomitant ACTH and glucocorticoid levels during and after surgery in healthy patients could be a hallmark event regarding HPA axis activation. Studies assessing elevated blood glucose, ACTH and Glucocorticoids may be also warranted. Taken together GA exposure may produce an allostasis that is favorable towards neurotoxicity.

Clinically, anesthetics are a necessary and vital tool that must be used in children during surgical procedures in order to ensure a positive outcome. Regarding surgical procedures and children, to date the retrospective data suggests that short duration and single exposures are safe but steps can be taken to further reduce the risk of diminished cognition. To date, there are few alternatives to midazolam, ketamine, ISO /SEV, and N₂O that can be used for general anesthesia. However, there are a number of options that may be employed as alternatives to the well-established anesthetic arsenal mentioned above. The α 2 adrenergic receptor agonist Dexmedetomidine, used in combination with opioids or benzodiazepines, may be a viable alternative to

inhalational based anesthetics such as SEV. Furthermore, it may also prove to be an effective alternative to ketamine when long term sedation is called for. Another alternative is to perform fewer surgical procedures. Surgeries that are of a cosmetic nature may be delayed until after the 4th year of life. Low yield brain imaging studies that require GA can be delayed or eliminated and tests that verbally assess cognitive function can be substituted. It is also not unrealistic to consider using these drugs when sedation is required for imaging studies and intubations. Lastly, regional anesthesia in combination with sedation can be adopted and used in more surgical procedures as an alternative to GAs; however, the limitations with this approach are that it is not part of the standard medical curriculum, it is not taught during residency, and the training requires a fellowship post residency. Clinical trials may also be used in order to determine two critical points. The first may involve basic scientists working in conjunction with clinicians in order to fully understand the mechanism of action of volatile anesthetics such as ISO and SEV. The second are clinical trials designed to reduce the risk of altered cognition by changing the way that GAs are used in children.

There are also options concerning the continued use of the current anesthetic arsenal in children. Total intravenous anesthesia (TIVA) is a general anesthesia technique that uses a combination of drugs administered intravenously (IV) thus eliminating the need for inhalational drugs such as, ISO, SEV, and N₂O. Newer IV drugs such as propofol combined with opioid derivatives, allow reliable anesthesia to be produced entirely with IV anesthetics allowing for rapid recovery even after long infusions. As a side note, using the standards of today, drugs such as ISO and SEV would not meet FDA approval standards of the day owing to lack of knowledge of the mechanism of action.

Co-administration of another drug that blocks anesthetic mediated neural degeneration is also a viable but complicated option. Drugs such as EUK -134 that are catalase and super oxide dismutase mimetic may in part lower anesthetic free radical production thereby blockading the toxic effects anesthetic

exposure thus preserving the normal course of brain development. Preliminary data involving the function of subiculum pyramidal neurons suggests that GA exposure also leads to hyperexcitability and that administration of the catalase and super oxide dismutase inhibitor mimetic EUK-134 prior to triple cocktail administration may spare thalamocortical neuron function. However, careful interpretation and classification of the signaling pathways involved must be taken in order to avoid unwanted effects caused by the co administered drug; for the introduction of a drug that lowers free radical concentration may inadvertently alter brain development as well. Experiments involving transgenic mice expressing multiple copies of super oxide dismutase (SOD) genes may be considered as well. Multiple copies of the SOD gene may be more effective at neutralizing elevated free radicals produced by the anesthetic triple cocktail. When exposed to the triple anesthetic cocktail during brain development, SOD transgenic mice may possess an inherent resistance to long GA induced alterations in brain structure and function.

After careful consideration of the data presented in this thesis, development of novel anesthetics is also another route to be considered. The neuroactive steroid B260, although initially developed as an analgesic, may have clinical potential as another alternative to the current clinical inhalational arsenal. In Section IV, when dosed as an anesthetic, the in vivo data shows that B260 has neuron sparing effects when used during rodent brain development.

The link between anesthetic modulation of ion channels and how prolonged activation of inhibitory GABA and antagonism of glutamate can cause the functional and structural changes observed in GA treated animals must be determined. Further studies designed to investigate if anesthetics can directly activate apoptosis pathways or if it is the activity patterns of neurons that is induced by anesthetics themselves that is causative of alteration in structure and function. In order to further validate the role of T channels in thalamocortical hyperexcitability, experiments with T-channel KO animals may prove fruitful. Experiments utilizing Cav3.1 and Cav3.2 KO mice affirm the hypothesis that a

reduction in nRT neuron T-channel expression may prove protective against triple anesthetic cocktail induced hyperexcitability. Calcium is a well know mediator of transcription and a general anesthetic mediated alteration in normal Ca^{2+} homeostasis may also contribute to the observed structural and functional alterations observed in GA treated mammals. In depth studies regarding how early exposure to GAs alters Ca^{2+} entry into the neuron particularly through dendrites and nerve terminals may help explain how permanent alterations in neuron excitability occur. Investigations aimed at understanding how GA mediated T-channel plasticity effects long term brain function are necessary. Other studies aimed at how GA acutely alters Ca^{2+} entry at dendrites are of value as well. Furthermore, studies aimed at how GA's may also affect endoplasmic reticular Ca^{2+} release also warrant investigation.

In conclusion, this thesis provides the rationale for retrospective studies in humans that involve pathological thalamocortical functions such as learning disability and epilepsy caused by early GA exposure. Furthermore, a new emphasis must be placed upon developing new standards regarding the use of anesthetics in children and the development of novel anesthetics that preserve the normal course of the developing human brain.

VII. References

- Astori S, Lüthi A (2013) Synaptic plasticity at intrathalamic connections via CaV3.3 T-type Ca²⁺ channels and GluN2B-containing NMDA receptors. *J Neurosci.* Jan 9;33(2):624-30
- Astori S, Wimmer RD, Prosser HM, Corti C, Corsi M, Liaudet N, Volterra A, Franken P, Adelman JP, Lüthi A (2011) The Ca(V)3.3 calcium channel is the major sleep spindle pacemaker in thalamus. *Proc Natl Acad Sci U S A.* Aug 16;108(33):13823-8.
- Agmon A, Yang LT, O'Dowd DK, Jones EG (1993) Organized growth of thalamocortical axons from the deep tier of terminations into layer IV of developing mouse barrel cortex. *J. Neurosci.* 13, 5365–5382.
- Aizenman E (1995) Modulation of N-methyl-D-aspartate receptors by hydroxyl radicals in rat cortical neurons in vitro. *Neurosci Lett.* Apr 7;189(1):57-9.
- Aizenman E Hartnett KA, Reynolds IJ (1990) Oxygen free radicals regulate NMDA receptor function via a redox modulatory site. *Neuron* Dec;5(6):841-6.
- Bao L, Avshalumov MV, Patel JC, Lee CR, Miller EW, Chang CJ, Rice ME (2009) Mitochondria are the source of hydrogen peroxide for dynamic brain-cell signaling. *J Neurosci* Jul 15;29(28):9002-10.

- Beenhakker MP and Huguenard JR (2009) Neurons that fire together also conspire together: Is normal sleep circuitry hijacked to generate epilepsy? *Neuron* 62:612-632.
- Belelli D, Lambert JJ (2005) Neurosteroids: endogenous regulators of the GABA(A) receptor. *Nat Rev Neurosci.* Jul;6(7):565-75.
- Bernardo KL, Woolsey TA (1987) Axonal trajectories between mouse somatosensory thalamus and cortex. *J. Comp. Neurol.* 258, 542–564.
- Bessaïh T, Bourgeois L, Badiu CI, Carter DA, Toth TI, Ruano D, Lambolez B, Crunelli V, Leresche N (2006) Nucleus-specific abnormalities of GABAergic synaptic transmission in a genetic model of absence seizures. *J Neurophysiol* 96:3074-3081.
- Beyer B, Deleuze C, Letts VA, Mahaffey CL, Boumil RM, Lew TA, Huguenard JR, Frankel WN (2008) Absence seizures in C3H/HeJ and knockout mice caused by mutation of the AMPA receptor subunit Gria4. *Hum Mol Genet* 17(12):1738-49.
- Boscolo A, Starr JA, Sanchez V, Lunardi N, DiGrucchio MR, Ori C, Erisir A, Trimmer P, Bennett J, Jevtovic-Todorovic V (2012) The abolishment of anesthesia-induced cognitive impairment by timely protection of mitochondria in the developing rat brain: the importance of free oxygen radicals and mitochondrial integrity. *Neurobiol Dis* 45(3):1031-41.
- Bessaïh T, Bourgeois L, Badiu CI, Carter DA, Toth TI, Ruano D, Lambolez B, Crunelli V, Leresche N. (2006) Nucleus-specific abnormalities of GABAergic synaptic

- transmission in a genetic model of absence seizures. *J Neurophysiol.* Dec;96(6):3074-81.
- Bragin A, Engel J Jr, Wilson CL, Fried I, Mathern GW (1999) Hippocampal and entorhinal cortex high-frequency oscillations (100--500 Hz) in human epileptic brain and in kainic acid-treated rats with chronic seizures. *Epilepsia.* Feb;40(2):127-37.
- Brambrink AM, Evers AS, Avidan MS, Farber NB, Smith DJ, Zhang X, Dissen GA, Creeley CE, Olney JW (2010) Isoflurane-induced neuroapoptosis in the neonatal rhesus macaque brain. *Anesthesiology* 112(4):834-41.
- Coulter DA, Huguenard JR, Prince DA (1990) Differential effects of petit mal anticonvulsants and convulsants on thalamic neurones: calcium current reduction. *Br J Pharmacol.* August; 100(4): 800–806.
- Choe W, Messinger RB, Leach E, Eckle VS, Obradovic A, Salajegheh R, Jevtovic-Todorovic V, Todorovic SM. TTA-P2 is a potent and selective blocker of T-type calcium channels in rat sensory neurons and a novel antinociceptive agent (2011) *Mol Pharmacol.* Nov;80(5):900-10.
- Chen Y, Lu J, Pan H, Zhang Y, Wu H, Xu K, Liu X, Jiang Y, Bao X, Yao Z, Ding K, Lo WH, Qiang B, Chan P, Shen Y, Wu X (2003) Association between genetic variation of CACNA1H and childhood absence epilepsy. *Ann Neurol.* 54:239–243
- Chrobak JJ, Buzsáki G. High-frequency oscillations in the output networks of the hippocampal-entorhinal axis of the freely behaving rat (1996) *J Neurosci.* May 1;16(9):3056-66.

- Cruikshank, S.J., Urabe, H., Nurmikko, A.V. & Connors, B.W (2010) Pathway-specific feedforward circuits between thalamus and neocortex revealed by selective optical stimulation of axons. *Neuron* 65, 230–245.
- Crunelli V, Leresche N (2002) Childhood absence epilepsy: genes, channels, neurons and networks. *Nat Rev Neurosci.* May;3(5):371-82.
- Crunelli V, Leresche N, Cope DW (2012) GABA-A Receptor Function in Typical Absence Seizures. In: Noebels JL, Avoli M, Rogawski MA, Olsen RW, Delgado-Escueta AV, editors. *Jasper's Basic Mechanisms of the Epilepsies* [Internet]. 4th edition. Bethesda (MD): National Center for Biotechnology Information (US).
- Crubtree JW, Lodge D, Bashir ZI, Isaac TR (2013) GABAA, NMDA and mGlu2 receptors tonically regulate inhibition and excitation in the thalamic reticular nucleus. *Eur J Neurosci* 37:850-859.
- Dobbing J, Sands J(1979) The brain growth spurt in various mammalian species. *Early Hum Dev* 3:79–84.
- Dittgen, T. Nimmerjahn A, Komai S, Licznanski P, Waters J, Margrie TW, Helmchen F, Denk W, Brecht M, Osten P (2004) Lentivirus-based genetic manipulations of cortical neurons and their optical and electrophysiological monitoring in vivo. *Proc. Natl. Acad. Sci. USA* 101, 18206–18211.
- Drechsel DA, Patel M (2010) Respiration-dependent H₂O₂ removal in brain mitochondria via the thioredoxin/peroxiredoxin system. *J Biol Chem.* Sep 3;285(36):27850-8.

Dreyfus FM, Tscherter A, Errington AC, Renger JJ, Shin HS, Uebele VN, Crunelli V, Lambert RC, Leresche N (2010) Selective T-Type calcium channel block in thalamic neurons reveals channel redundancy and physiological impact of IT window. *J Neurosci* 30(1):99-109.

Eckle VS, Digruccio MR, Uebele VN, Renger JJ, Todorovic SM (2012) Inhibition of T-type calcium current in rat thalamocortical neurons by isoflurane. *Neuropharmacology*. Aug;63(2):266-73.

Franks NP (2008) General anesthesia: from molecular targets to neuronal pathways of sleep and arousal. *Nat Rev Neurosci*. May;9(5):370-86

Fredriksson A, Pontén E, Gordh T, Eriksson P (2007) Neonatal exposure to a combination of N-methyl-D-aspartate and gamma-aminobutyric acid type A receptor anesthetic agents potentiates apoptotic neurodegeneration and persistent behavioral deficits. *Anesthesiology* Sep;107(3):427-36.

Gabrieli JD, Brewer JB, Desmond JE, Glover GH (1997) Separate neural bases of two fundamental memory processes in the human medial temporal lobe. *Science*. Apr 11;276(5310):264-6.

Galbraith S, Daniel JA, Vissel B (2010) A study of clustered data and approaches to its analysis. *J Neurosci* 30(32):10601-10608.

- Gentet LJ and Ulrich D (2004) Electrophysiological characterization of synaptic connections between layer VI cortical cells and neurons of the nucleus reticularis thalami in juvenile rats. *Eur J Neurosci* 19:625-633.
- Herd MB, Brown AR, Lambert JJ, Belelli D (2013) Extrasynaptic GABA_A receptors couple presynaptic activity to postsynaptic inhibition in the somatosensory thalamus. *J Neurosci* 33(37):14850-14868
- Heron SE, Khosravani H, Varela D, Bladen C, Williams TC, Newman MR, Scheffer IE, Berkovic SF, Mulley JC, Zamponi GW (2007) Extended spectrum of idiopathic generalized epilepsies associated with CACNA1H functional variants. *Ann Neurol*. 62:560–568.
- Huang Z, Lujan R, Kadurin I, Uebele VN, Renger JJ, Dolphin AC, Shah MM. (2011) Presynaptic HCN1 channels regulate Cav3.2 activity and neurotransmission at select cortical synapses. *Nat Neurosci*. Apr;14(4):478-86.
- Huguenard JR, Prince DA (1992) A novel T-type current underlies prolonged Ca(2+)-dependent burst firing in GABAergic neurons of rat thalamic reticular nucleus. *J Neurosci*. Oct;12(10):3804-17.
- Huguenard JR, McCormick DA (1992) Simulation of the currents involved in rhythmic oscillations in thalamic relay neurons. *J Neurophysiol*. Oct;68(4):1373-83.
- Huguenard JR, Prince DA (1994) Intrathalamic rhythmicity studied in vitro: nominal T-current modulation causes robust antioscillatory effects. *J Neurosci*. Sep;14(9):5485-5502.

- Huntsman MM, Porcello DM, Homanics GE, DeLorey TM, Huguenard JR. (1999) Reciprocal inhibitory connections and network synchrony in the mammalian thalamus. *Science* 283: 541–543.
- Ikeda H, Heinke B, Ruscheweyh R, Sandkühler J (2003) Synaptic plasticity in spinal lamina I projection neurons that mediate hyperalgesia. *Science*. Feb 21;299(5610):1237-40.
- Ikonomidou C, Kaindl AM. Neuronal death and oxidative stress in the developing brain (2011) *Antioxid Redox Signal*. Apr 15;14(8):1535-50.
- Ito Y, Izumi H, Sato M, Karita K, Iwatsuki N. Suppression of parasympathetic reflex vasodilatation in the lower lip of the cat by isoflurane, propofol, ketamine and pentobarbital: implications for mechanisms underlying the production of anaesthesia. *Br J Anaesth*. 1998;81:563–568.
- Jacus MO, Uebele VN, Renger JJ, Todorovic SM (2012) Presynaptic Cav3.2 channels regulate excitatory neurotransmission in nociceptive dorsal horn neurons. *J Neurosci*. 2012 Jul 4;32(27):9374-82.
- Joksovic PM, Weiergraber M, Lee WY, Struck H, Schneider T, Todorovic SM (2009) isoflurane-sensitive presynaptic R-type calcium channels contribute to inhibitory synaptic transmission in the rat thalamus. *J Neurosci* 29(5):1434-1445.
- Joksovic PM, Nelson MT, Jevtovic-Todorovic V, Patel MK, Perez-Reyes E, Kevin P Campbell, Chen CC, Todorovic SM (2006) CaV3.2 is the major molecular substrate for redox regulation of T-type Ca²⁺ channels in the rat and mouse thalamus *J Physiol*. July 15; 574(Pt 2): 415–430.

Jevtovic-Todorovic V, Hartman RE, Izumi Y, Benshoff ND, Dikranian K, Zorumski CF, Olney JW, Wozniak DF (2003) Early exposure to common anesthetic agents causes widespread neurodegeneration in the developing rat brain and persistent learning deficits. *J Neurosci* 23(3):876-882.

Jevtovic-Todorovic V, Hartman RE, Izumi Y, Benshoff ND, Dikranian K, Zorumski CF, Olney JW, Wozniak DF (2003) Early exposure to common anesthetic agents causes widespread neurodegeneration in the developing rat brain and persistent learning deficits. *J Neurosci*. Feb 1;23(3):876-82.

Jevtovic-Todorovic V and Olney JW (2008) PRO: Anesthesia-induced developmental neuroapoptosis: status of the evidence. *Anest Analg* 106(6):1659-63.

Jung HY, Staff NP, Spruston N (2001) Action potential bursting in subicular pyramidal neurons is driven by a calcium tail current. *J Neurosci*. May 15;21(10):3312-21.

Kann O, Kovács R. Mitochondria and neuronal activity (2007) *Am J Physiol Cell Physiol* Feb;292(2):C641-57.

Kim D, Song I, Keum S, Lee T, Jeong MJ, Kim SS, McEnery MW, Shin HS (2001) Lack of the burst firing of thalamocortical relay neurons and resistance to absence seizures in mice lacking alpha(1G) T-type Ca(2+) channels. *Neuron*. Jul 19;31(1):35-45.]

Kleinman-Weiner M, Beenhakker MP, Segal WA, Huguenard JR (2009) Synergistic roles of GABAA receptors and SK channels in regulating thalamocortical oscillations. *J Neurophysiol* 102: 203–213.

- Komuro H, Rakic P (1993) Modulation of neuronal migration by NMDA receptors. *Science*. Apr 2;260(5104):95-7.
- Kress HG (1997) Mechanisms of action of ketamine. *Anesthetist* 46:8–19.
- Latham JR, Pathirathna S, Jagodic MM, Choe WJ, Levin ME, Nelson MT, Lee WY, Krishnan K, Covey DF, Todorovic SM, Jevtovic-Todorovic V (2009) Selective T-type calcium channel blockade alleviates hyperalgesia in ob/ob mice. *Diabetes*. Nov;58(11):2656-65.
- Lacey CJ, Bryant A, Brill J, Huguenard JR (2012) Enhanced NMDA receptor-dependent thalamic excitation and network oscillations in stargazer mice. *J Neurosci* 32(32):11067-81.
- Lazarenko RM, Willcox SC, Shu S, Berg AP, Jevtovic-Todorovic V, Talley EM, Chen X, Bayliss DA (2010). Motoneuronal TASK channels contribute to immobilizing effects of inhalational general anesthetics. *J Neurosci*. Jun 2;30(22):7691-704.
- Lee J, Kim D, Shin HS. Lack of delta waves and sleep disturbances during non-rapid eye movement sleep in mice lacking alpha1G-subunit of T-type calcium channels (2004) *Proc Natl Acad Sci U S A* Dec 28;101(52):18195-9
- Lee JH, Gomora JC, Cribbs LL, Perez-Reyes E. Nickel block of three cloned T-type calcium channels: low concentrations selectively block alpha1H (1999) *Biophys J*. Dec;77(6):3034-42.
- Lee JH, Durand R, Gradinaru V, Zhang F, Goshen I, Kim DS, Fenno LE, Ramakrishnan C, Deisseroth K (2010) Global and local fMRI signals driven by neurons defined optogenetically by type and wiring. *Nature* 465, 788–792.

- Lei B, Adachi N, Arai T. Measurement of the extracellular H₂O₂ in the brain by microdialysis. (1998) *Brain Res Brain Res Protoc*. Sep;3(1):33-6.
- Lemkuil BP, Head BP, Pearn ML, Patel HH, Drummond JC, Patel PM (2011) Isoflurane neurotoxicity is mediated by p75NTR-RhoA activation and actin depolymerization. *Anesthesiology* Jan;114(1):49-57.
- Lin SF, Quan X, Zou L, Ye TH. *Zhongguo Yi Xue Ke Xue Yuan Xue Bao* (2012) Effects of propofol on brain activation in respond to mechanical stimuli. Jun;34(3):222-7.
- Liang J, Zhang Y, Chen Y, Wang J, Pan H, Wu H, Xu K, Liu X, Jiang Y, Shen Y, Wu X (2007) Common polymorphisms in the CACNA1H gene associated with childhood absence epilepsy in Chinese Han population. *Ann Hum Genet*. 71:325–335.
- Loepke AW, Istaphanous GK, McAuliffe JJ 3rd, Miles L, Hughes EA, McCann JC, Harlow KE, Kurth CD, Williams MT, Vorhees CV, Danzer SC (2009) The effects of neonatal isoflurane exposure in mice on brain cell viability, adult behavior, learning, and memory. *Anesth Analg* 108(1):90-104.
- Llinas R, Urbano FJ, Leznik E, Ramirez RR, van Merle HJ (2005) Rhythmic and dysrhythmic thalamocortical dynamics: GABA systems and the edge effect. *Trends Neurosci* 28(6):325-33.
- Lu LX, Yon JH, Carter LB, Jevtovic-Todorovic V (2006) General anesthesia activates BDNF-dependent neuroapoptosis in the developing rat brain. *Apoptosis* 11(9):1603-15.

- Lunardi N, Ori C, Erisir A, Jevtovic-Todorovic V (2010) General anesthesia causes long-lasting disturbances in the ultrastructural properties of developing synapses in young rats. *Neurotox Res.* Feb;17(2):179-88.
- Maccaferri G, McBain CJ (1996) The hyperpolarization-activated current (I_h) and its contribution to pacemaker activity in rat CA1 hippocampal stratum oriens-alveus interneurons. *J Physiol.* Nov 15;497 (Pt 1):119-30.
- McCormick DA, Pape HC. Properties of a hyperpolarization-activated cation current and its role in rhythmic oscillation in thalamic relay neurones. (1990) *J Physiol.* Dec;431:291-318.
- McCormick DA (2002) Cortical and subcortical generators of normal and abnormal rhythmicity. *Int Rev Neurobiol* 49: 99–114.
- Messinger RB, Naik AK, Jagodic MM, Nelson MT, Lee WY, Choe WJ, Orestes P, Latham JR, Todorovic SM, Jevtovic-Todorovic V. (2009) *In vivo* silencing of the Ca_v3.2 T-type calcium channels in sensory neurons alleviates hyperalgesia in rats with streptozocin-induced diabetic neuropathy. *Pain.* Sep. 145(1-2):184-95.
- Mody I (2005) Aspect of the homeostatic plasticity of GABA_A receptor-mediated inhibition. *J Physiol* 562.1: 37-46.
- Morris RG, Schenk F, Tweedie F, Jarrard LE (1990) Dissociating Components of Allocentric Spatial Learning. *Eur J Neurosci.*;2(12):1016-1028

- Nagel, G. Szellas T, Huhn W, Kateriya S, Adeishvili N, Berthold P, Ollig D, Hegemann P, Bamberg E (2003) Channelrhodopsin-2, a directly light-gated cation-selective membrane channel. *Proc. Natl. Acad. Sci. USA* 100, 13940–13945.
- O'Mara S (2005) The subiculum: what it does, what it might do, and what neuroanatomy has yet to tell us. *J Anat. Sep*;207(3):271-82.
- Orestes P, Bojadzic D, Lee J, Leach E, Salajegheh R, Digruccio MR, Nelson MT, Todorovic SM (2011) Free radical signalling underlies inhibition of CaV3.2 T-type calcium channels by nitrous oxide in the pain pathway. *J Physiol. Jan 1*;589(Pt 1):135-48
- Panayiotopoulos CP (2008) Typical absence seizures and related epileptic syndromes: assessment of current state and directions for future research. Department of Clinical Neurophysiology and Epilepsies, St. Thomas' Hospital, London, UK. *Epilepsia. Dec*;49(12):2131-9.
- Pape HC (1996) Queer current and pacemaker: the hyperpolarization-activated cation current in neurons. *Annu Rev Physiol.* 58:299-327.
- Paule MG, Li M, Allen RR, Liu F, Zou X, Hotchkiss C, Hanig JP, Patterson TA, Slikker W Jr, Wang C (2011) Ketamine anesthesia during the first week of life can cause long-lasting cognitive deficits in rhesus monkeys. *Neurotoxicol Teratol. Mar-Apr*;33(2):220-30
- Paz JT, Astra s, Peng K, Fenno L, Yizhar O, Frankel FN, Deisseroth K, Huguenard JR (2011) A new mode of corticothalamic transmission revealed in the Gria4^{-/-} model of absence epilepsy. *Nat Neurosci* 14(9): 1167–1173.

- Paz JT, Christian CA, Parada I, Prince DA, Huguenard JR (2010) Focal cortical infarcts alter intrinsic excitability and synaptic excitation in the reticular thalamic nucleus. *J Neurosci.* Apr 14;30(15):5465-79.
- Pinault D, Bourassa J, Deschênes M (1995) The axonal arborization of single thalamic reticular neurons in the somatosensory thalamus of the rat. *Eur. J. Neurosci.* 7, 31–40.
- Pontén E, Fredriksson A, Gordh T, Eriksson P, Viberg H (2011) Neonatal exposure to propofol affects BDNF but not CaMKII, GAP-43, synaptophysin and tau in the neonatal brain and causes an altered behavioural response to diazepam in the adult mouse brain. *Behav Brain Res.* Sep 30;223(1):75-80.
- de la Prida LM, Totterdell S, Gigg J, Miles R. (2006) The subiculum comes of age. *Hippocampus.*16(11):916-23.
- Reiprich P, Kilb W, Luhmann HJ (2005) Neonatal NMDA receptor blockade disturbs neuronal migration in rat somatosensory cortex in vivo. *Cereb Cortex.* Mar;15(3):349-58.
- Rizzi S, Carter LB, Ori C, Jevtovic-Todorovic V (2008) Clinical anesthesia causes permanent damage to the fetal guinea pig brain. *Brain Pathol* 18(2):198-210.
- Rosoklija G, Toomayan G, Ellis SP, Keilp J, Mann JJ, Latov N, Hays AP, Dwork AJ. (2000) Structural abnormalities of subicular dendrites in subjects with schizophrenia and mood disorders: preliminary findings. *Arch Gen Psychiatry.* 2000 Apr;57(4):349-56.

- Sanchez V, Feinstein SD, Lunardi N, Joksovic PM, Boscolo A, Todorovic SM, Jevtovic-Todorovic V (2011) Long-term impairment of mitochondrial morphogenesis and synaptic transmission in developing rat brain. *Anesthesiology* 115(5):992-1002.
- Satomoto M, Satoh Y, Terui K, Miyao H, Takishima K, Ito M, Imaki J (2009) Neonatal exposure to sevoflurane induces abnormal social behaviors and deficits in fear conditioning in mice. *Anesthesiology* Mar;110(3):628-37.
- Scott BS and Edwards BA (1981) Effect of ***chronic ethanol*** exposure on the electric membrane properties of DRG neurons in cell culture. *J Neurobiol* 12(4):379-90.
- Sherman SM (2005) The role of the thalamus in cortical function: not just a simple relay. *Thalamus & Related Systems* 3: 205-216.
- Seubert CN, Zhu W, Pavlinec C, Gravenstein N, Martyniuk AE (2013) Developmental effects of neonatal isoflurane and sevoflurane exposure in rats. *Anesthesiology* 119(2):358-64.
- Sirois JE, Lei Q, Talley EM, Lynch C 3rd, Bayliss DA (2000) The TASK-1 two-pore domain K⁺ channel is a molecular substrate for neuronal effects of inhalation anesthetics. *J Neurosci*. Sep 1;20(17):6347-54.
- Snead OC 3rd (1988) Gamma-Hydroxybutyrate model of generalized absence seizures: further characterization and comparison with other absence models. *Epilepsia* 29:361-368.
- Snead OC (1991) The gamma-hydroxybutyrate model of absence seizures: correlation of regional brain levels of gamma-hydroxybutyric acid and gamma-butyrolactone with spike wave discharges. *Neuropharmacology*. Feb;30(2):161-7.

- Sohal VS, Huntsman MM, Huguenard JR. (2000) Reciprocal inhibitory connections regulate the spatiotemporal properties of intrathalamic oscillations. *J Neurosci* 20: 1735–1745.
- Staff NP, Jung HY, Thiagarajan T, Yao M, Spruston N (2000) Resting and active properties of pyramidal neurons in subiculum and CA1 of rat hippocampus. *J Neurophysiol.* Nov;84(5):2398-408
- Steriade M, Jones EG, and Llinas RR (1990) *Thalamic oscillations and signaling*. New York: Wiley.
- Strafstrom C (2005) The Role of the Subiculum in Epilepsy and Epileptogenesis. *Epilepsy Curr.* Jul 5(4): 121–129.
- Squire LR, Zolamorgan S (1991) The Medial Temporal-Lobe Memory System. *Science* 253:1380-1386 .
- Surges R, Freiman TM, Feuerstein TJ (2004) Input resistance is voltage dependent due to activation of Ih channels in rat CA1 pyramidal cells. *J Neurosci Res.* May 15;76(4):475-80.
- Surges R, Brewster AL, Bender RA, Beck H, Feuerstein TJ, Baram TZ (2006) Regulated expression of HCN channels and cAMP levels shape the properties of the h current in developing rat hippocampus. *Eur J Neurosci.* July; 24(1): 94–104.
- Talley EM, Solórzano G, Depaulis A, Perez-Reyes E, Bayliss DA (2000) Low-voltage-activated calcium channel subunit expression in a genetic model of absence epilepsy in the rat. *Brain Res Mol Brain Res.* Jan 10;75(1):159-65.

- Todorovic SM, Pathirathna S, Brimelow BC, Jagodic MM, Ko SH, Jiang X, Nilsson KR, Zorumski CF, Covey DF, Jevtovic-Todorovic V. (2004) 5 β -reduced neuroactive steroids are novel voltage-dependent blockers of T-type Ca²⁺ channels in rat sensory neurons in vitro and potent peripheral analgesics in vivo. *Mol Pharmacol.* Nov;66(5):1223-35
- Tokuda K, O'Dell KA, Izumi Y, Zorumski CF (2010) Midazolam inhibits hippocampal long-term potentiation and learning through dual central and peripheral benzodiazepine receptor activation and neurosteroidogenesis. *J Neurosci* Dec 15;30(50):16788-95.
- Viberg H, Pontén E, Eriksson P, Gordh T, Fredriksson A (2008) Neonatal ketamine exposure results in changes in biochemical substrates of neuronal growth and synaptogenesis, and alters adult behavior irreversibly. *Toxicology.* Jul 30;249(2-3):153-9.
- Vitko I, Chen Y, Arias JM, Shen Y, Wu XR, Perez-Reyes E (2005) Functional characterization and neuronal modeling of the effects of childhood absence epilepsy variants of CACNA1H, a T-type calcium channel. *J Neurosci.* 25:4844–4855.]
- Vitko I, Bidaud I, Arias JM, Mezghrani A, Lory P, Perez-Reyes E (2007) The I-II loop controls plasma membrane expression and gating of Cav3.2 T-type Ca²⁺ channels: a paradigm for childhood absence epilepsy mutations. *J Neurosci.* 27:322–330.

- Von Krosigk M, Bal T, McCormick DA (1993) Cellular mechanisms of a synchronized oscillation in the thalamus. *Science* 261: 361–364.
- Wang W, Fang H, Groom L, Cheng A, Zhang W, Liu J, Wang X, Li K, Han P, Zheng M, Yin J, Wang W, Mattson MP, Kao JP, Lakatta EG, Sheu SS, Ouyang K, Chen J, Dirksen RT, Cheng H(2008) Superoxide flashes in single mitochondria *Cell*. Jul 25;134(2):279-90.
- Weinberger DR. (1999) Cell biology of the hippocampal formation in schizophrenia. *Biol Psychiatry*. Feb 15;45(4):395-402.
- Wilder RT, Flick RP, Sprung J, Katusic SK, Barbaresi WJ, Mickelson C, Gleich SJ, Schroeder DR, Weaver AL, Warner DO (2009) Early exposure to anesthesia and learning disabilities in a population-based birth cohort. *Anesthesiology* 110(4):796-804.
- Witter MP (2006) Connections of the subiculum of the rat: Topography in relation to columnar and laminar organization. *Behavioural Brain Research* 174:251-264,
- Witter MP, Groenewegen HJ (1990) The Subiculum - Cytoarchitectonically A Simple Structure, But Hodologically Complex. *Progress in Brain Research* 83:47-58.
- Ying SW, Tibbs GR, Picollo A, Abbas SY, Sanford RL, Accardi A, Hofmann F, Ludwig A, Goldstein PA (2011) PIP2-mediated HCN3 channel gating is crucial for rhythmic burst firing in thalamic intergeniculate leaflet neurons. *J Neurosci*. Jul 13;31(28):10412-23.

- Yon J-H, Daniel-Johnson J, Carter LB, Jevtovic-Todorovic V (2005) Anesthesia induces neuronal cell death in the developing rat brain via the intrinsic and extrinsic apoptotic pathways. *Neuroscience* 135:815-827.
- Zaman T, Lee K, Park C, Paydar A, Choi JH, Cheong E, Lee CJ, Shin H-S (2011) CaV2.3 channels are critical for oscillatory burst discharges in the reticular thalamus and absence epilepsy. *Neuron* 70: 95-108.
- Zorumski CF, Paul SM, Izumi Y, Covey DF, Mennerick S (2013) *Neurosci Biobehav Rev.* 2013 Jan; Neurosteroids, stress and depression: potential therapeutic opportunities *Neurosci Biobehav Rev.* Jan;37(1):109-22.
- Zou X, Liu F, Zhang X, Patterson TA, Callicott R, Liu S, Hanig JP, Paule MG, Slikker W Jr, Wang C (2011) Inhalation anesthetic-induced neuronal damage in the developing rhesus
- Zhao Y, Liang G, Chen Q, Joseph DJ, Meng Q, Eckenhoff RG, Eckenhoff MF, Wei H. (2010) Anesthetic-Induced Neurodegeneration Mediated via Inositol 1,4,5-Trisphosphate Receptors *J Pharmacol Exp Ther.* April; 333(1): 14–22.
- Zhang Y, Llinas RR, Lisman JE (2009) Inhibition of NMDARs in the Nucleus Reticularis of the Thalamus Produces Delta Frequency Bursting. *Front Neural Circuits.* Nov 10;3:20.
- Zucker RS, Regehr WG. Short-term synaptic plasticity (2002) *Annu Rev Physiol.* 64:355-405.